國 立 交 通 大 學

應用化學研究所

博 士 論 文

活性聚合具有環境刺激響應共聚高分子與分析其組裝結構與環境敏感智能行為

Facile Synthsis of Well-defined Environment Stimuli-responsives Coploymers and Investigation of its Assembly Architecture and “Smart” Behaviors

研 究 生：黃 承 鈞

指導教授：張 豐 志 教授

中 華 民 國 九 十 九 年 七 月

活性聚合具有刺激響應共聚高分子與分析其組裝結構與環境敏感智能行為

Facile Synthsis of Well-defined Stimuli-responsives Coploymers and Investigation of its Assembly Architecture and "Smart" Behaviors

研 究 生：黃承鈞　　Student：Cheng-Jyun Huang

指導教授：張豐志　　Advisor：Feng-Chih Chang

國 立 交 通 大 學

應 用 化 學 研 究 所

博 士 論 文

A Dissertation

Submitted to Department of Applied Chemistry

College of Science

National Chiao Tung University

in partial Fulfillment of the Requirements

for the Degree of

Doctor of Philosophy

In

Applied Chemistry

July 2010

Hsinchu, Taiwan, Republic of China

中華民國九十九年七月

活性聚合具有刺激響應共聚高分子
與分析其自組裝結構與環境敏感智能行為

學生：黃承鈞　　指導教授：張豐志

國立交通大學應用化學研究所 博士班

摘　　要

隨著奈米科技的發展以及對能源與能源應用上的需求，具有精確結構設計的功能性軟物質材料已被廣泛的研究。近年來，活性高分子聚合技術的發展，使得我們可以得到具有可控制分子量分佈、複雜結構與控制組成比例的高分子材料。自然界生物為了維持生命與生理機能，生物體內的高分子與細胞必須隨著外在環境的變化來改變其化學性質與結構。由此概念所發展出具有刺激響應的仿生高分子材料已運用在許多生醫方面的應用。自然界生物為了維持生命與生理機能，生物體內的高分子與細胞必須隨著外在環境的變化來改變其化學性質與結構。由此概念所發展出具有刺激響應的仿生高分子材料已廣泛運用在生醫材料

本研究中，我們利用活性聚合出具有刺激響應共聚高分子，並且加以研究這些高分子在固態或液態中的自組裝結構:

(1) 活性聚合聚胜肽嵌段式共聚高分子 poly(*N*-isopropylacrylamide)-*b*-poly(Z-L-lysine) (PNIPAm-*b*-PZLys) 及其性質研究:

聚胜肽(polypeptide)嵌段共聚高分子是利用具有雙官能基起始劑，一端進行原子轉移自由基聚合(atom transfer reversible polymerization)具有溫度響應的軟鏈段聚異丙基丙烯醯

胺poly(*N*-isopropylacrylamide)，另一端則進行開環反應聚合硬鏈段聚胜肽polylysine高分子。藉由此種雙親性嵌段式共聚高分子的親疏水鏈段在極性上的差異，我們發現可以藉由改變共聚高分子的組成以及共溶劑極性，在形成各種型態熱力學穩定的高分子微胞。利用小角度(SAXS)、廣角度X光繞射儀(WAXS)與穿透式電子顯微鏡(TEM)觀察此種嵌段共聚物的微相自組裝相分離結構。在移除胺基保護基苄氧羰基後，我們利用核磁共振儀觀察此共聚物在改變環境溫度與pH值的刺激響應行為。

(2) 利用逐層組裝與點擊化學製備共價鍵穩定超薄殼層溫度敏感微膠囊中空球

本研究中，我們利用原子轉移自由基聚合聚合出具有疊氮以及炔基官能基的熱敏感聚異丙基丙烯醯胺共聚物，接著利用表面改質疊氮官能基的二氧化矽微米球當作基板進行逐層組裝並同時進行1,3-偶極環加成點擊化學反應形成共價鍵穩定的多層薄膜結構。利用稀釋氫氟酸水溶液移除模板，我們可得到一個穩定型態具有可逆溫度響應的高分子中空囊球。進一步藉由控制多層薄膜的交聯度以及反應溫度可以得到不同厚度及表面粗糙度的高分子膠囊中空球。

(3) 利用逐層組裝與點擊化學製備共價鍵穩定雙刺激響應超薄高分子液胞

傳統上高分子液胞(polymer vesicles)是利用兩性嵌段共聚物在水溶液下相分離所產生的自組裝結構。我們以第二部分研究作為基礎，進一步導入酸鹼敏感聚丙烯醯丙氨酸共聚物，與熱敏感聚異丙基丙烯醯胺共聚物交替進行交替逐層組裝反應。我們藉由此技巧制備出具有類似高分子液泡結構，並可控制尺度大小與殼-核層薄膜厚度。利用共軛焦顯微鏡(CLSM)、TEM與原子力顯微鏡(AFM)可觀察此高分子液泡對溫度與酸鹼值之刺激響應行為。

Facile Synthsis of Well-defined Stimuli-Responsives Coploymers and Investigation of ts Self-Assembly Architecture and “Smart” Behaviors

Studenet：Cheng-Jyun Huang　　Advisors：Dr. Feng-Chih Chang

Institute of Applied Chemistry
National Chiao Tung University

ABSTRACT

Applications for advanced functional soft materials that possess precisely engineered properties and functional groups have been expanding significantly with the development of nanotechnology and the growing need to address resource, health, and energy issues. Recent advances in living/controlled polymerization techniques have facilitated access to (co)polymers with controlled molecular weights, complex architectures, and precisely positioned functional groups. To sustain life and maintain biological function, nature requires selectively tailored molecular assemblies and interfaces that provide a specific chemical function and structure, and which change in their environment. Synthetic materials that change properties in response to local environmental stimuli with very similar attributes are often prepared for a broad range of biomedical applications.

In this study, we synthesized well-defined stimuli-responsive copolymers by controlled/living polymerization and investigated their assembled nanostructures in the

solid-state or in solution:

(1) Polypeptide diblock copolymers: syntheses and properties of poly(*N*-isopropylacrylamide)-*b*-polylysine:

A hydrolysis-resistant amide-linkage hetero-functional initiator was synthesized and used successfully for polymerization of well-defined rod-coil block copolymers poly(*N*-isopropylacrylamide)-*b*-poly(Z-L-lysine) (PNIPAm-*b*-PZLys) by combination of atom transfer radical polymerization (ATRP) and amine hydrochloride mediated ring-opening polymerization (ROP). These amphiphilic block copolymers are able to form universal micelle morphologies of spherical micelles, wormlike micelles, and vesicles by varying the polymer compositions and the helicogenic common solvents. From synchrotron SAXS, WAXS, and TEM results, the PNIPAm-*b*-PZLys microphase self-assembly morphology in solid state is a hierarchical lamellar-in-hexagonal structure. After removing the protective ε-benzyloxycarbonyl group, the dual stimuli-responsive behaviors of the PNIPAm-*b*-PLys investigated by nuclear magnetic resonance spectroscopy in aqueous solution resulted in either coil-to-helix or coil-to-globule transition by changing the environmental condition of elevating the temperature or increasing the pH value.

(2) Using click chemistry to fabricate ultrathin thermoresponsive microcapsules through direct covalent layer-by-layer (LbL) assembly

We report the syntheses of azido- and acetylene-functionalized PNIPAm copolymers and their use in the fabrication of ultrathin thermoresponsive microcapsules through direct covalent LbL assembly using click chemistry. These clickable copolymers were prepared through ATRP at 0 °C using a synthesized dansyl-labeled initiator and the CuBr/Me_6TREN catalyst complex in 2-propanol. These clickable PNIPAm copolymers assemble alternately onto azido-modified silica particles in aqueous media through click reactions catalyzed by copper sulfate and sodium ascorbate. After removing the template, the microcapsules

remained stable because of the presence of the covalently bonded triazole units; the microcapsules exhibited thermoresponsive and thermo-reversible swelling/de-swelling behaviors upon changing the temperature of the medium. Adjusting the number of clickable functionalities resulted in changes to the degree of cross-linking, thereby allowing control over the surface morphology and thickness of the covalently stabilized PNIPAm multilayer thin films. The microcapsules fabricated close to the lower critical solution temperature of PNIPAm exhibited extremely low surface roughnesses and thick multilayer films as a result of their compact chain conformation in aqueous solution, leading to tighter packing of the PNIPAm structure.

(3) Fabrication of vesicle-like dual-responsive click capsules by direct covalent LbL assembly

We report a click chemistry approach for the consecutive LbL assembly of thermo and pH-sensitive clickable copolymers on silica particles and the subsequent formation of a vesicle-like dual-responsive click capsules. This click capsules exhibit both thermo and pH-responsive behaviors by elevating the solution temperature and incubating in acidic or basic solutions respectively. These stimuli-responsive behaviors were examined by using confocal laser scanning microscopy (CLSM), TEM, and atomic force microscopy (AFM). This approach provides potential applications in preparing well-defined vesicle-like capsules with covalent stabilization and flexibility in introducing a range of new materials including different functional polymers.

誌　謝

終於到了寫致謝詞的這一刻，這意味著研究所生涯即將正式的畫上句點。大學四年級上學期甄試上交大應化研究所後，非常幸運的能進入張豐志老師的實驗室進行研究，開啟了我對高分子研究的興趣。在研究所求學時期，非常感謝張豐志老師提供我們學生良好的研究環境與實驗室互助合作的氣氛讓我能在研究上全力以赴，老師不但培養了我具備邏輯與獨立思考的能力與自動自發的精神，讓我的研究成果能一點一滴的堆砌出今日的成果。老師的耐心與愛心著實令學生備感溫馨，不僅讓學生在研究上得到豐富的知識，亦是促使整體研究動力的來源，在此，學生要向您說聲謝謝。

論文口試期間，感謝口試委員：謝國煌教授、段葉芳教授、吳震裕教授、黃華宗教授與陳志勇教授在學生的論文上提供了非常寶貴的建議，讓學生的論文的內容更加詳實與嚴謹，在此致上最誠摯的謝意。

在研究的過程中，首先要感謝的是小呆學姐帶我走入高分子合成與高分子自組裝的領域，讓我能順利的找到我博士班的研究主題，讓我的研究順利步上軌道。還有跟我同梯一起堅持到最後的小堅，高分子物理的疑難雜症通通全部都幫我解決。還要感謝實驗室許多的學長姐，所謂前人種樹，後人乘涼，實驗室能有今天的良好的研究氣氛以及研究設備也都是各位學長姐的心血結晶，希望我在畢業後也能對實驗室繼續有貢獻讓這傳統能夠持續的維持下去，讓實驗室更加茁壯。也感謝小叮噹學妹在實驗上的幫助，以及實驗室學長與學弟妹大家共同維持實驗室的運作以及整潔，讓這我們這團隊彼此能相互合作，可以互相扶持，讓我能順利的度過豐富及多采多姿的研究生生涯。也要感謝各個學校裡的貴重儀器技術人員，幫助我各式各樣的實驗，讓我有豐富的實驗數據來完成我的實驗與論文寫作。

還要感謝陪我一起走過博士班四個年頭的女友曉詩，有了妳，讓我有更明確奮鬥的目標，有妳的陪伴讓我有了奮發向上的精神，而妳也總是支持著我，給我最大的鼓勵。希望未來我們也能在人生的路上繼續相互扶持當對方的心靈支柱。最後，要感謝的是我的爸爸、媽媽與姊姊在學業與生活上對我全力的支持，讓我能順順利利的完成我的學業，感謝我的爸爸、媽媽給了正確的人生態度，這是我最大的資產。

僅以這份論文，獻給在這一路上關心與照顧我的各位，謝謝大家。

Table of Contents

Pages

List of Schemes

Pages

List of Tables

Pages

List of Figure

Pages

Chapter 1

Introduction

1-1 Recent advances in the design of functional polymers from controlled/living radical polymerization

To sustain life and maintain biological function, nature requires selectively tailored molecular assemblies and interfaces that provide a specific chemical function and structure, and which change in their environment. Synthetic materials that change properties in response to local environmental stimuli with very similar attributes are often prepared for a broad range of biomedical applications. For example, physical or chemical hydrogels loaded with drug molecules may release their payload, only when and where required, in response to changes in the local environmental conditions, such as pH, temperature, presence of small molecules or enzymes, and oxidizing/reducing environment, among others.

Although Mother Nature provides many inspirations for designing and developing new materials, creating synthetic systems capable of responding to stimuli in a controllable and predictable fashion represents significant challenges. Particular challenges lie in mimicking biological systems where structural and compositional gradients at various length scales are necessary for orchestrated and orderly responsive behaviors.

Applications for these advanced stimuli-responsive soft materials that possess precisely engineered properties and functional groups have been expanding significantly with the development of nanotechnology and the growing need to address resource, health, and energy issues. Demand in a range of industrial and research settings are increasing the necessity to construct soft material systems with precise control over architecture, domain size, functionality, polarity, solubility, and reactivity. In addition to these materials and structural

requirements, researchers have also sought to prepare these systems via high yielding, simple covalent chemistry. Much of the inspiration for constructing such complex, multifunctional materials can be found in a combination of fundamental organic chemistry, biology, and bioconjugation chemistry; these motivations in tandem with the recent advances in controlled/living radical polymerization techniques have created a growing research area with concentration on robust, efficient, and orthogonal approaches for new soft material preparation.

1-2 Controlled/living radical polymerization (CLRP)

CLRP techniques have emerged as simple routes for preparing well-defined polymers of predetermined molecular weight (MW) and narrow molecular weight distribution (MWD), as well as various block copolymers and a wide range of complex macromolecular architectures.[1] Prior to the development of CLRP, all these features were hardly achievable. Indeed, only with living ionic polymerization[2] could such a degree of structural uniformity be reached but under very drastic polymerization conditions and with a limited choice of monomers.

In contrast to conventional free-radical polymerization where propagating radicals exhibit a very short lifetime (~1 s) that hampers the conception of well-defined architectures, the concept of CLRP is to increase this lifetime up to the timescale of the polymerization reaction, via the establishment of a reversible equilibrium between active species, which can propagate, and dormant/capped species, which cannot propagate. CLRP then proceeds in such a manner that all polymer chains grow at the same rate and the detrimental impact of irreversible termination events over the MW and the MWD are made almost negligible.[3] An ideal living polymerization system should exhibit the following features: (i) a linear evolution of the logarithmic conversion (ln [1/(1 − conversion)]) with time, accounting for a constant

propagating radicals concentration; (ii) a linear increase in the number-average molar mass, M_n, with monomer conversion, where the degree of polymerization, DP_n, is predetermined by the consumed monomer to initially introduced initiator molar ratio; (iii) low polydispersity indexes, M_w/M_n, close to a Poisson distribution ($M_w/M_n \sim 1 + 1/DP_n$); (iv) a quantitative α- and ω-functionalization and (v) the possibility for polymer chains, after monomer consumption, to further grow when additional monomer is introduced which allows block copolymer synthesis to be performed by sequential monomer addition.[3]

A plethora of well-established CLRP methods offers the polymer chemist an impressive toolbox for making advanced macromolecular architectures of increasing complexity. Among them, nitroxide-mediated polymerization (NMP),[1a] atom transfer radical polymerization (ATRP)[1b,1c,1f,1h] and reversible addition-fragmentation chain transfer (RAFT),[1d,1e,1j,1k] the latter including macromolecular design via the interchange of xanthates (MADIX), represent the three most well-known CLRP techniques. In addition to these famous approaches, one can find the iniferter[4] system and cyanoxyl-mediated polymerization[5] as well as recently emerged CLRP techniques, such as iodine transfer polymerization (ITP),[6] single electron transfer-living radical polymerization (SET-LRP),[7] organotellurium-mediated polymerization (TERP),[1k] organostibine-mediated polymerization (SBRP)[1k] and cobalt-mediated polymerization (CMRP).[8]

1-2.1 Atom transfer radical polymerization (ATRP)

ATRP was discovered independently by Sawamoto[9] and Matyjaszewski.[10] The ATRP process is based on a rapid exchange of a halide atom (especially Cl or Br) between a growing radical and a dormant species, *via* a redox process involving a transition metal complex as shown in Figure 1-1.

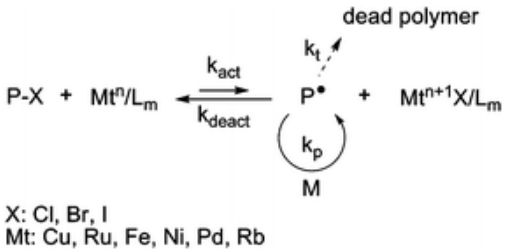

Figure 1-1: The activation–deactivation equilibrium in atom transfer radical polymerization.

Various transition metals can be employed in ATRP (Cu, Ru, Fe, Ni, *etc.*). In the first ATRP process, called direct ATRP, the transition metal complex in a lower oxidation state (Mt^n/L_m, where Mt is the metal and L is the ligand) is directly added to the reaction as an activator and reacts reversibly with the dormant species (P-X, with X a halogen atom) to form a deactivator ($Mt^{n+1}X/L_m$) and the active species $P^•$. In contrast, when the polymerization is initiated by a conventional initiator and a metal complex at the higher oxidation state, the process is called reverse ATRP. The simultaneous reverse and normal initiation (SR&NI) process takes advantage of both normal and reverse ATRP as Cu(II) (which is tolerant to oxygen), an alkyl halide and a radical initiator are initially present in the reaction medium.[11] It provides a way to reduce the amount of copper complex and to prepare more complex macromolecular architectures.

Recently, new ATRP processes have been developed, namely activators generated by electron transfer (AGET)[12] and activators regenerated by electron transfer (ARGET).[13] The AGET process employs a reducing agent (*e.g.* ascorbic acid or tin(II) 2-ethylhexanoate) which reacts with $Mt^{n+1}X/L_m$ to generate the active catalyst (Mt^n/L_m). The process then follows a direct ATRP process. AGET ATRP allows the preparation of pure block copolymers with no homopolymer of the second monomer. The ARGET process uses an excess of reducing agent which allows a significant reduction of the amount of metal in the media.

This powerful and versatile technique can be used under mild experimental conditions and in various polymerization media with a wide range of monomers including styrenics, alkyl (meth)acrylates, acrylonitrile, (meth)acrylamides as well as water-soluble monomers to give tailor-made polymers. An additional flexibility is provided by the possibility of using commercially available functionalized initiators and to functionalize chain ends. However, if ATRP can be used with a large range of monomers, the polymerization of functional monomers bearing acid or amine function remains hardly achievable.

1-2.2 Reversible addition fragmentation chain transfer (RAFT)

RAFT polymerization is governed by a reversible transfer reaction between a growing (macro)radical (active species) and a (macro)RAFT agent (dormant species).[14] RAFT agents, denoted Z–C(=S)SR, act as transfer agents by a two-step addition-fragmentation mechanism as shown in Figure 1-2.

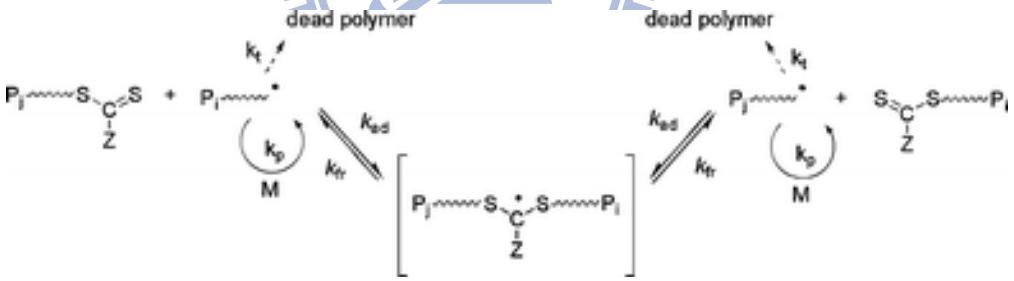

Figure 1-2: Mechanism of reversible addition fragmentation chain transfer.

The RAFT group is typically a thiocarbonylthio group such as dithioester (Z = alkyl), trithiocarbonate (Z = S-alkyl), xanthate (O-alkyl) or dithiocarbamate (Z = N(alkyl)$_2$). The RAFT process using thiocarbonylthio compounds, including dithioesters and trithiocarbonates, was reported by the CSIRO laboratory in early 1998[15] whereas a similar process using xanthates as RAFT agents (the so-called MADIX) was reported in late 1998.[16] RAFT is potentially universal and can be applied to a wide range of functional monomers (styrenics,

alkyl (meth)acrylates, acrylic acid, vinyl acetate *etc.*), which allows polymers with precisely controlled structural parameters to be prepared such as random, block, gradient, grafted and star copolymers.[1d,1j,1k]

Even though Moad, Rizzardo and co-workers recently succeeded in elaborating a switchable RAFT agent,[17] one of the major drawback of this technique was the lack of a universal RAFT agent. In particular, dithioesters or trithiocarbonates were suitable for controlling polymerization of more activated monomers such as styrene (S) and derivatives, methacrylic esters (*e.g.* methyl methacrylate MMA), methacrylic acid (MA), methacrylamide (MAM), acrylic acid (AA), acrylamide (AM) or acrylonitrile (AN). However they inhibit or retard the polymerization of less activated monomers such as vinyl acetate (VAc), *N*-vinylpyrrolidone (NVP) or *N*-vinylcarbazole (NVC), for which xanthates or dithiocarbamates are more suitable.[1d,1j,1k] The choice of R and Z groups is thus crucial to achieve a good control of the polymerization.

1-2.3 Nitroxide-mediated polymerization (NMP)

NMP is based on a reversible termination reaction between a growing radical, P・, and a free nitroxide, N・, to form a (macro)alkoxyamine, P–N (Figure 1-3).

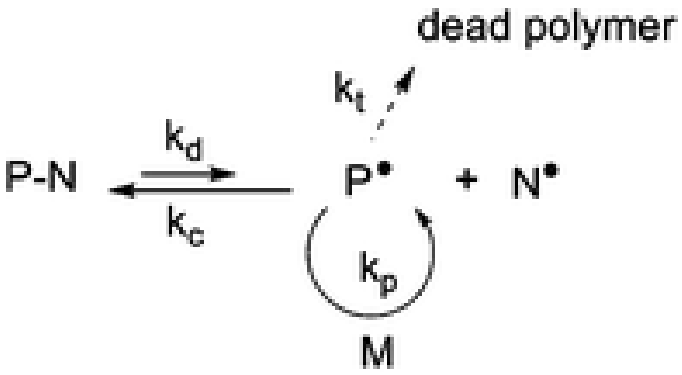

Figure 1-3: The activation–deactivation equilibrium in nitroxide-mediated polymerization.

This equilibrium between active and dormant species presents the advantage of being a purely thermal process: the (macro)alkoxyamine regenerates the propagating radical and the nitroxide by homolytic cleavage at high temperature (usually > 70 °C).

A typical NMP can be initiated following two different pathways: (i) by using a bicomponent initiating system (*i.e.* a conventional radical initiator and a free nitroxide) or (ii) *via* a monocomponent initiating system (*i.e.* a preformed alkoxyamine). Georges and co-workers first reported the controlled radical polymerization of styrene with (2,2,6,6-tetramethylpiperidinyl-1-oxy) (TEMPO, **N1**, Figure 1-4) as the mediator.[18]

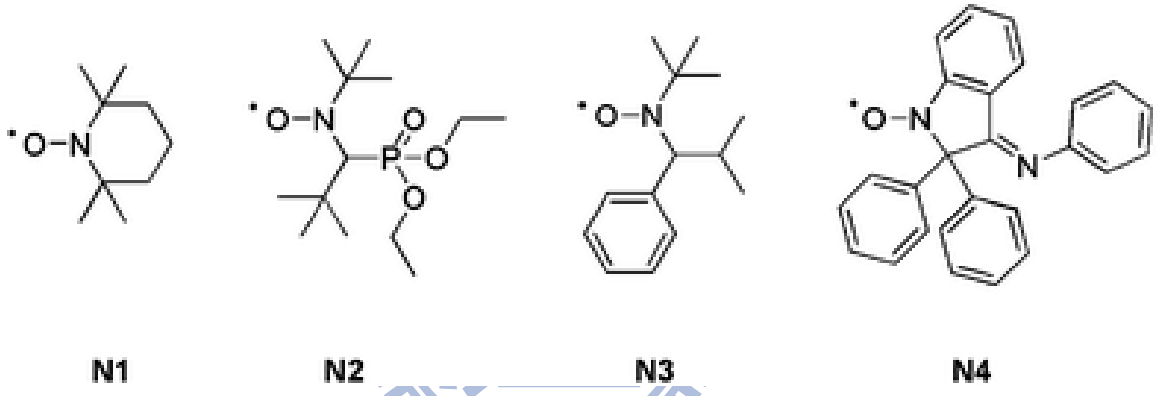

Figure 1-4: The structures of nitroxides used as mediators in NMP: TEMPO (N1), SG1 or DEPN (N2), TIPNO (N3) and DPAIO (N4).

However, as TEMPO was almost exclusively limited to styrenic monomers (only a sterically hindered TEMPO derivative allowed the control of the *n*-butyl acrylate polymerization),[19] new acyclic nitroxides have been designed to improved the range of polymerizable monomers under controlled/living conditions. More precisely, *N-tert*-butyl-*N*-[1-diethylphosphono-(2,2-dimethylpropyl)] nitroxide (SG1 or DEPN, **N2**, Figure 1-4)[20] and *N-tert*-butyl-*N*-[1-phenyl-2-(methylpropyl)]nitroxide (TIPNO, **N3**, Figure 1-4)[21] are now able to control the polymerization of styrenics, alkyl acrylates, acrylic acid, acrylamides and dienes.[20a,21a,22] The polymerization of methacrylic esters can be controlled

either: (i) by using a particular nitroxide such as 2,2-diphenyl-3-phenylimino-2,3-dihydroindol-1-yloxyl nitroxide (DPAIO, **N4**, Figure 1-4),[23] specific to methacrylates or (ii) by a copolymerization approach under SG1 control with a small amount of comonomer such as styrene[24] or acrylonitrile.[25]

1-3 Click chemistry reactions employed in polymer science

Recent advances in living/controlled polymerization techniques have facilitated access to (co)polymers with controlled molecular weights, complex architectures, and precisely positioned functional groups. However, even the most robust polymerization methods are not sufficient for the synthesis of many interesting macromolecules. Postpolymerization modification is still an essential method of incorporating functionality not compatible with polymerization, characterization, or processing conditions. Polymer−polymer conjugation is often the only viable means to prepare complex chain topologies or copolymers that contain monomer units not polymerizable by the same methods. However, transformations on polymers are often inefficient and may lead to side reactions with other groups within the polymer. Therefore, efficient and specific reactions are needed to ensure successful postpolymerization modification.

As usual, Nature provides inspiration by example, since many natural molecules of the most sophisticated function, such as proteins and nucleic acid, are made by the seemingly simple repetition of reliable bond-forming operations. In 2001, a group of chemists led by K. Barry Sharpless at The Scripps Research Institute gave the name of "click chemistry" to the very best chemical reactions.[26] They are easy to perform, give rise to their intended products in very high yields with little or no byproducts, work well under many conditions, and are unaffected by the nature of the groups being connected to each other. Click reactions share the following attributes:

(1) Many click components are derived from alkenes and alkynes, and thus ultimately from the cracking of petroleum. Carbon–carbon multiple bonds provide both energy and mechanistic pathways to be elaborated into reactive structures for click connections.

(2) Most click reactions involve the formation of carbon–heteroatom (mostly N, O, and S) bonds. This stands in contrast to the march of modern synthetic organic chemistry, which has emphasized the formation of carbon–carbon bonds.

(3) Click reactions are strongly exothermic, either by virtue of highly energetic reactants or strongly stabilized products.

(4) Click reactions are usually fusion processes (leaving no byproducts) or condensation processes (producing water as a byproduct).

(5) Many click reactions are highly tolerant often accelerated by the presence of water.

There are several highly efficient reactions meet the click criteria as shown Figure 1-5.

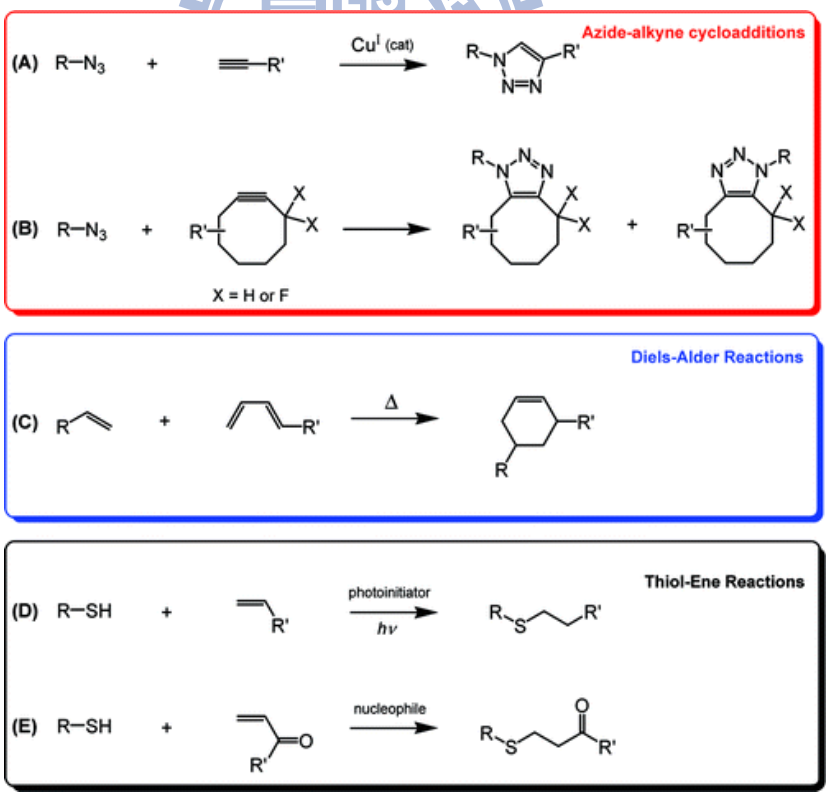

Figure 1-5: Examples of click reactions commonly employed in polymer synthesis and functionalization.

1-3.1 Copper-Catalyzed Azide−Alkyne Cycloadditions (CuAAC)

In 2002, the groups of Meldal[27] and Sharpless[28] independently reported the use of a copper(I) catalyst to allow azide−alkyne cycloadditions to be conducted at low temperatures with high rates, efficiency, and (regio)specificity (Figure 1-5A). This coupling process reaches near-quantitative conversion in both aqueous and organic media with little or no side reactions being observed. The efficiency afforded by CuAAC has influenced the field of macromolecular engineering in many ways. For example, block copolymer synthesis commonly relies on living/controlled polymerization methods to grow one block from another; however, many click reactions have proven capable of coupling preexisting homopolymers to prepare block copolymers in a modular and highly efficient manner (Figure 1-6). Several benefits arise from employing a modular method of this type. Each block can be individually characterized prior to coupling, and block copolymers can be prepared from monomers that do not polymerize by a common mechanism. Opsteen and van Hest first demonstrated it was possible to prepare a library of AB[29] or ABC[30] block copolymers by coupling various combinations of azido- or alkyne-terminated polymers by CuAAC. Barner-Kowollik and Stenzel et al.[31] successfully coupled RAFT-generated polymers by a similar approach. Macromolecular architectures of greater intricacy have been prepared in an analogous manner, with CuAAC facilitating efficient preparation of various types of graft[32] and star[33] copolymers via modular grafting-to approaches.

While the large majority of reports to date have relied on CuAAC to enhance macromolecular engineering capabilities, several other highly efficient reactions also meet the click criteria.[34] Additional cycloaddition reactions such as strain-promoted azide−alkyne coupling[35] (SPAAC) (Figure 1-5B) and Diels−Alder reactions[36] (Figure 1-5C) have allowed many new polymers to be efficiently prepared or functionalized. Thiol−ene reactions[37] (radical- or nucleophile-mediated) have proven particularly useful for polymer synthesis

under extremely mild conditions, often with no solvent and little-to-no product cleanup (Figure 1-5D,E).

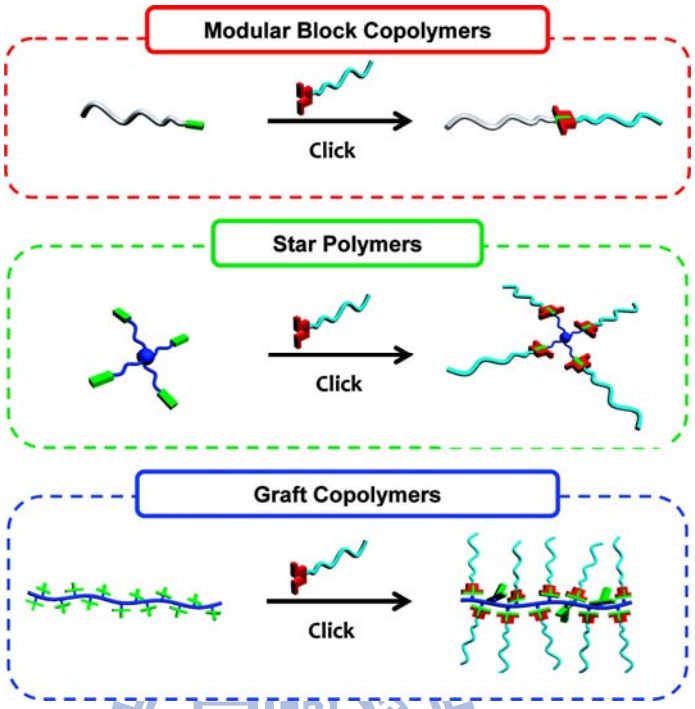

Figure 1-6: Modular approach of synthesizing block copolymers, stars, and graft copolymers by click chemistry.

1-4 Polymeric capsules

Nature serves as the model for stimuli-responsive polymers, but it remains a challenge to create materials that interact with, or respond to, biological environments.[38] A typical cell in Nature contains several types of organelles. These compartments, which are mostly surrounded by a single bilayer phospholipid membrane, each fulfill a unique role within the cellular environment. Different organelles comprise different collections of specific enzymes that catalyze requisite chemical reactions. The process of compartmentalization to ensure the integrity of catalytic pathways has inspired chemists to mimic Nature and create artificial environments for reactions to take place in.

In recent years a different type of vesicular architecture, composed of macromolecules instead of small organic compounds, has become topic of investigation. A wide variety of polymeric capsules has been developed, such as polymersomes,[39] layer-by-layer capsules,[40] and hollow microspheres,[41] or hollow microcapsules.[42] (Scheme 1-7) The use of polymers instead of organic molecules to construct the membrane makes these systems more stable and robust compared to liposomes. Additionally a vast amount of monomers as well as many different techniques to build up the polymeric structures are available; it is better possible to tune the properties of polymeric capsules for the desired purpose. Another effect of the use of polymers instead of small phospholipids for the build-up of the capsule shell is the reduced permeability of the membranes due to the higher thickness and the decreased fluidic character. This latter property however can be undesired when the capsules are applied for synthetic purposes, since the substrate has difficulty reaching the catalytic species inside the capsule.

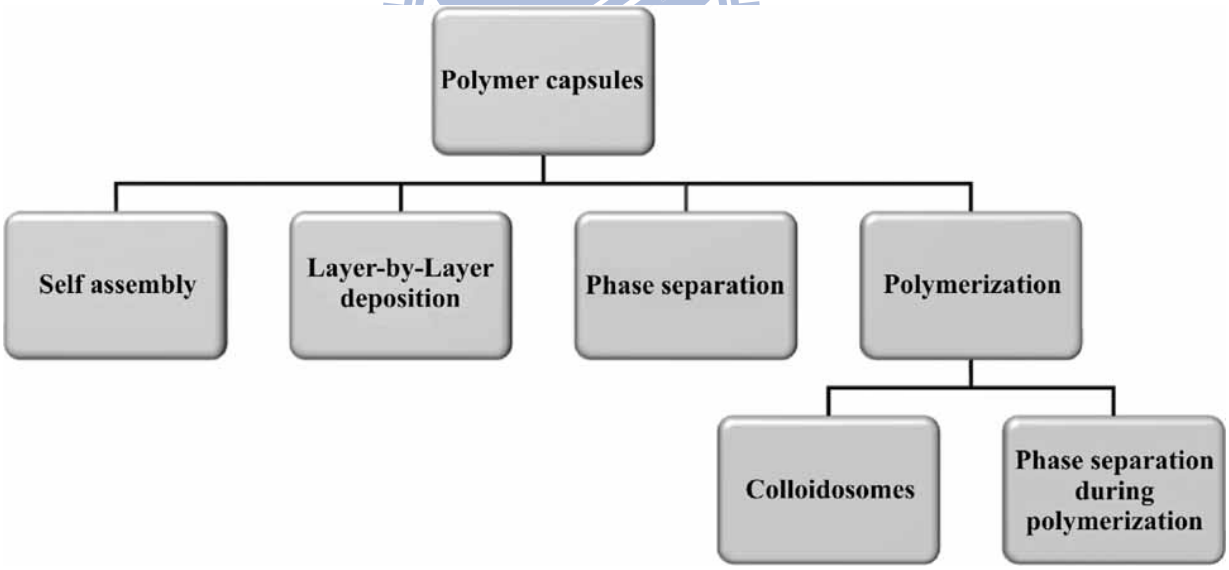

Figure 1-7: Overview of polymer capsules prepared via different methodologies.

1-4.1 Polymersomes

Polymer vesicles, commonly called polymersomes, are spherical shell structures in which an aqueous compartment is enclosed by a bilayer membrane made of amphiphilic block

copolymers. Because of the high molecular weight of these block copolymers, polymer vesicles have superior stability and greater toughness[43] than liposomes, their low molecular weight analogues. More interestingly, their membrane properties can be extensively tailored using polymer chemistry (*e.g.* variation of chemical structure[44] and length of each polymer component,[45] crosslinking,[46] conjugation with biomolecules such as membrane proteins,[47] etc).

For the aggregation of small amphiphiles such as phospholipids, Israelachvili developed a model which is based on the geometry of the molecules.[48] A packing parameter is defined in this model, which is determined by the surface area of the polar headgroup and the length and volume of the hydrophobic tails as depicted in Figure 1-7. This packing parameter can predict whether the formation of micelles, vesicles or inverted structures is expected.

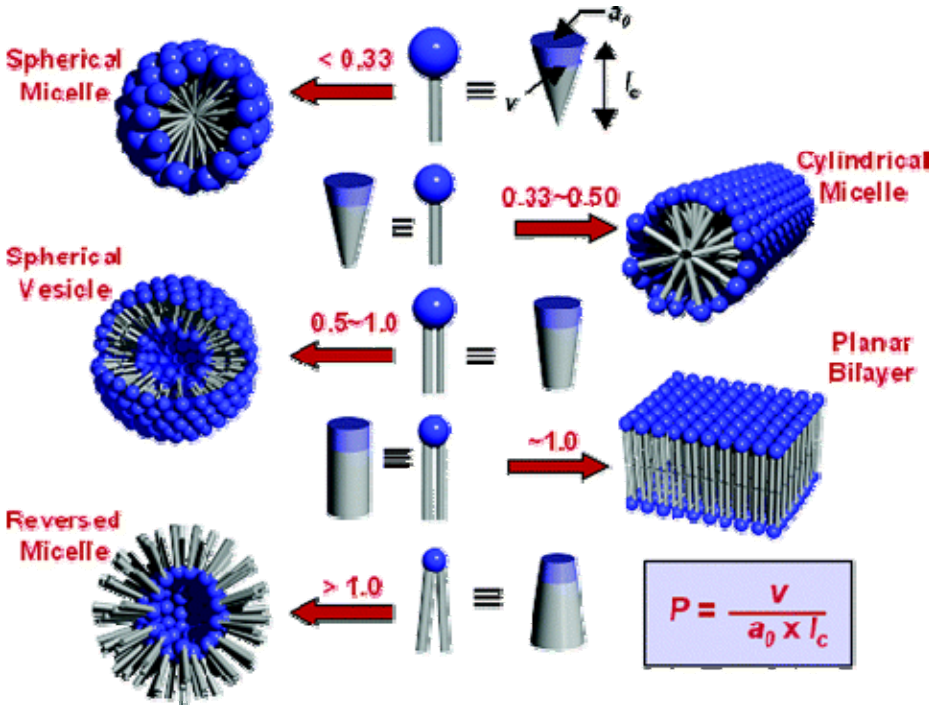

Figure 1-8: Different morphologies predicted by the packing parameter. For $p < \frac{1}{2}$ micelles are predicted, vesicles are formed when $\frac{1}{2} < p < 1$, and inverted structures are expected for $p > 1$.

This theory was adapted by Discher et al. for block copolymers with hydrophilic and hydrophobic character. They introduced a theory in which the effective interaction energy between hydrophobic blocks is the key to aggregate stability, whereas the relative mass or volume fraction of each block is the key to morphology (Figure 1-9).[49] The molecular shape of an amphiphile, whether cylinder, wedge or cone shape, dictates whether membrane, cylindrical, or spherical morphologies will respectively form. This shape is simply a reflection of the hydrophilic fraction *f*. If large hydrophilic blocks are used, $f \gg 50\%$, this leads to conically shaped amphiphiles, which give micellar structures. When a hydrophilic fraction of $40\% > f > 50\%$ is used, wedge shaped amphiphiles are self-assembled into rod-like aggregates. For vesicles it is ideal to have a hydrophilic fraction of $25\% > f > 40\%$, in which the amphiphile has a cylindrical shape and assembles into a vesicular morphology.

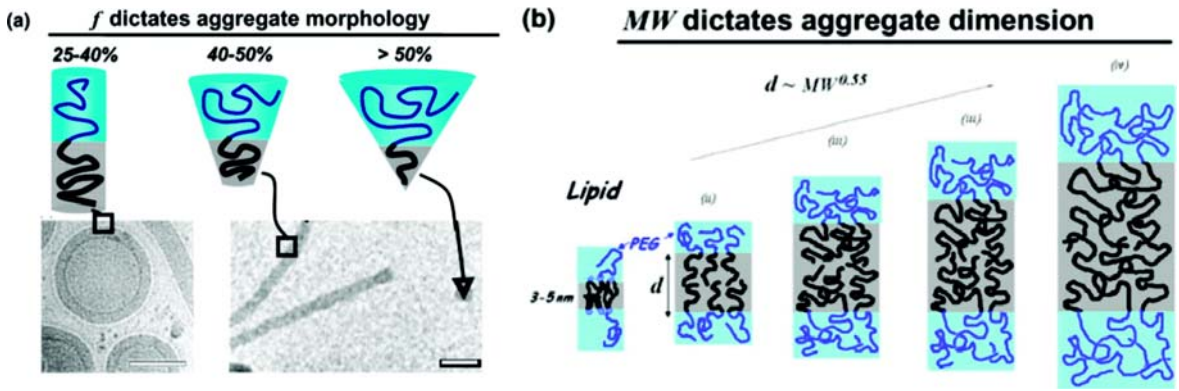

Figure 1-9: (a) Schematics of block copolymer hydrophilic fractions "*f*" with respective cryogenic transmission electron microscopy images showing vesicles or worm micelles and spherical micelles. (b) Schematic scaling of polymersome membrane thickness with copolymer molecular weight (MW).

Polymer vesicles have mostly been produced from three families of amphiphilic block copolymers-regular (coil-coil) block copolymers, block copolymers with rigid blocks (rod-coil and rod-rod) and block copolymers with intermolecular interactions (charge

interactions, ligand binding, H-bonds, dipolar interactions, etc).[50] Of these families, coil-coil block copolymers have been the most studied. In dilute solution, the shape and size of the supramolecular assemblies of coil-coil block copolymers, such as poly(acrylic acid)-*b*-polystyrene (PAA-*b*-PS)[51] and poly(ethylene oxide)-*b*-polybutadiene (PEO-*b*-PBD),[52] are typically determined by the respective lengths of the polymer blocks, their affinity for each other and for the solvents, the temperature, and also the ionic concentration in the case of charged systems.[53]

1-4.2 Polypeptide-based vesicles

Besides the well known vesicles that are composed of synthetic block copolymers, vesicles also have been prepared, which consist solely of polypeptides as the hydrophilic and hydrophobic block, or which contain one block that is comprised of a polypeptide structure. This class of peptide containing polymersomes has recently drawn much attention, since new methods have emerged in which the molecular weight of block copolypeptides can be precisely controlled and increasingly complex polypeptides can be synthesized yielding polymers having superior properties than ill-defined homopolypeptides.[54]

Deming et al. showed vesicle formation using either poly(L-lysine)-*block*-poly(L-leucine) or poly(L-glutamic acid)-*block*-poly(L-leucine) diblock copolypeptides.[55] These vesicles could be prepared with diameters ranging from 50 to 1000 nm and which retained their polar contents without leakage. Recently they reported on a polypeptide block copolymer[56] with a small variation to the previously described polypeptides. Polyarginine-*block*-poly(L-leucine), depicted in Figure 1-10, has an α-helical hydrophobic block which favors the formation of flat membranes and a highly charged hydrophilic segment, which increases membrane fluidity.

Vesicles could also be prepared from hybrid polymer-polypeptide systems. The formation of spherical micelles and large vesicles ("peptosomes") in an aqueous solution of a block

copolymer of polybutadiene-*block*-polyglutamate was described by Kukula et al.[57] Also Checot et al. reported vesicular aggregates formed by polybutadiene-*block*-polyglutamate and showed the occurrence of a transition of the hydrophilic block from an α-helical conformation to a random coil conformation.[58]

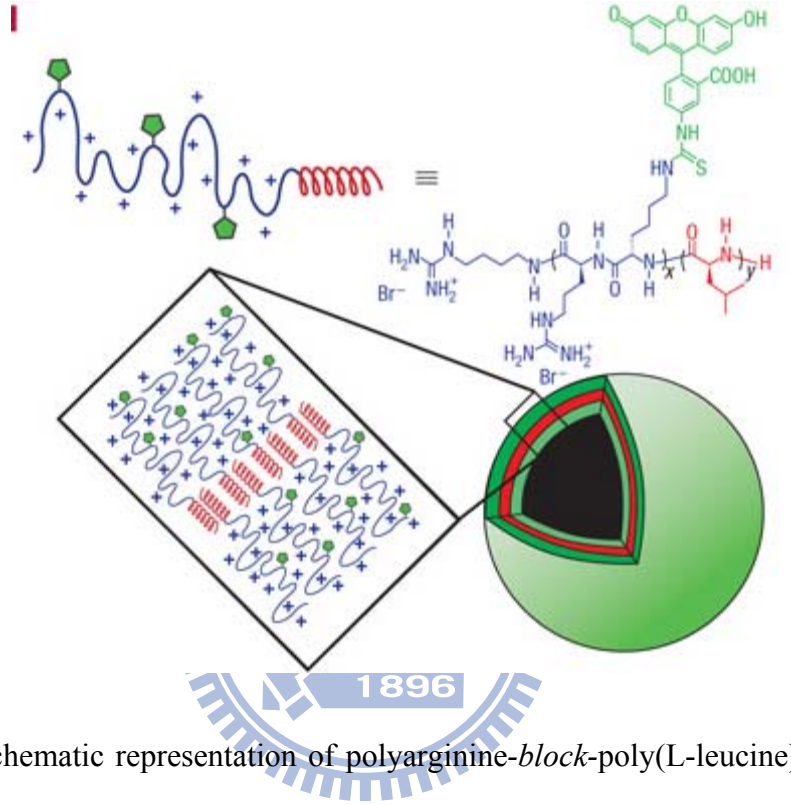

Figure 1-10: Schematic representation of polyarginine-*block*-poly(L-leucine) with 10 mol-% randomly placed lysine residues in the arginine block that allow facile attachment of fluorescein dyes.

Kataoka et al. developed a new entity of hybrid peptide based polymer vesicles with a polyion complex (PIC) membrane, so called PICsomes.[59] These PICsomes (Figure 1-11) were prepared by mixing the positively charged poly(ethylene glycol)-*block*-poly[(5-aminopentyl)-α, β-aspartamide] [PEG-P(Asp-AP)] with the negatively charged poly(ethylene glycol)-*block*-poly(α, β-aspartic acid) [PEG-P(Asp)] in a Tris-HCl buffer and subjecting them to sonication. By matching the chain length of block copolymer pairs with oppositely charged segments and compensating for the counter charge in a stoichiometric manner, semipermeable vesicles were formed.

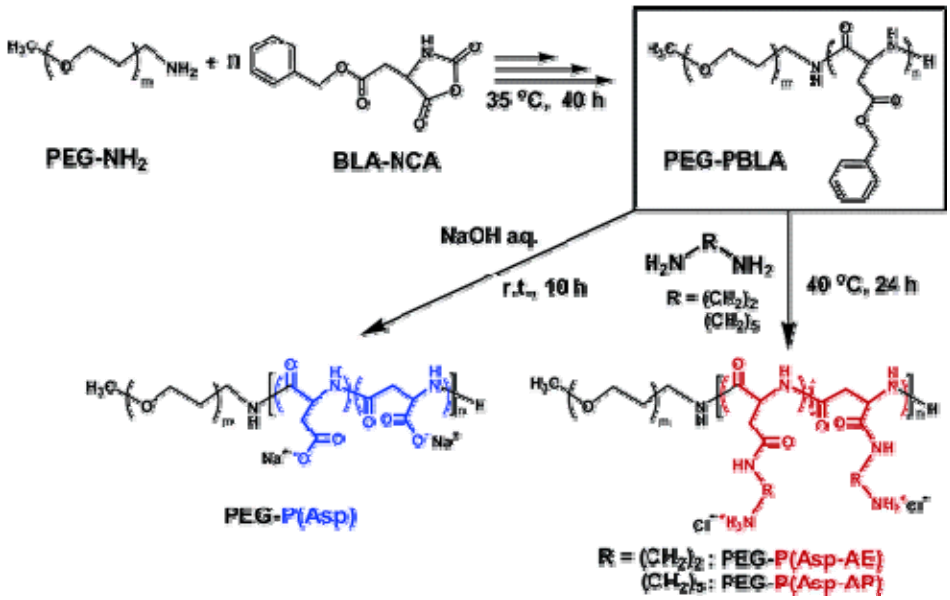

Figure 1-11: Synthesis of a pair of oppositely charged block copolymers. These double hydrophilic block copolymers can form polymersomes based on the electrostatic attraction between the oppositely charged blocks, forming polyion complexsomes, or PICsomes.

1-4.3 Layer-by-layer vesicles

In the beginning of the nineteen nineties the layer-by-layer (LbL) technique was introduced by Decher and was originally used for sequential adsorption of oppositely charged polymers, polyelectrolytes, on a charged surface.[60] When a polyelectrolyte is adsorbed on a glass surface, the charge of the polymer overcompensates, leading to a reversal of the surface charge, thereby promoting the adsorption of the next oppositely charged polyelectrolyte. This procedure is schematically illustrated in Figure 1-12.

Currently a large number of components, other than charged polymers, have been included in between the multilayers, like DNA, proteins, nanoparticles, lipids and viruses, yielding thin films with tailor made properties. Besides electrostatic interactions, other interactions such as H-bonds, covalent bonds, biospecific interactions and stereocomplex formation have also been used to build up these multilamellar systems.[40a]

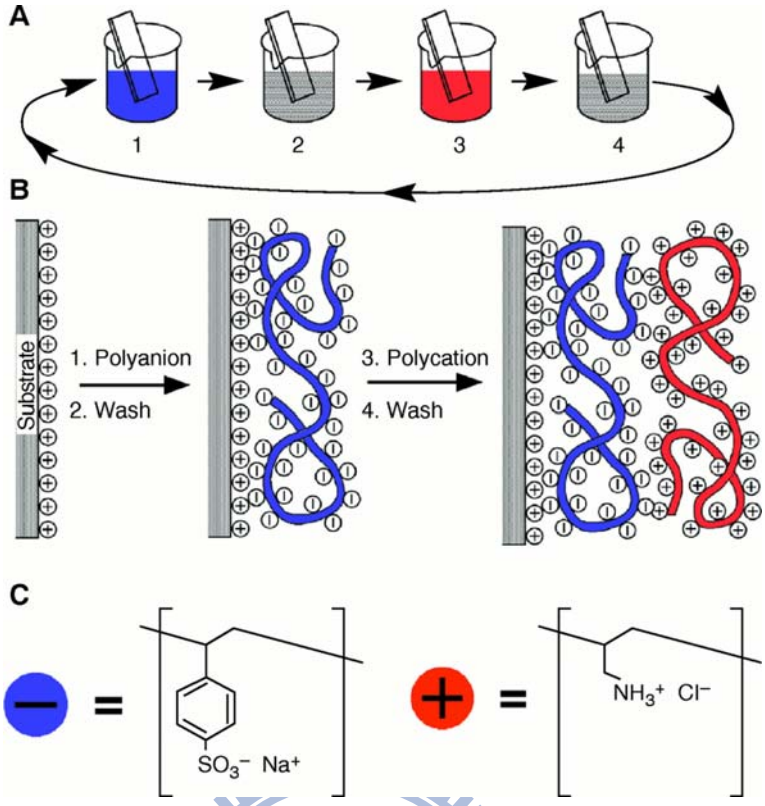

Figure 1-12: (A) Schematic representation of the deposition of oppositely charged polyelectrolytes. Steps 1 and 3 represent the adsorption of a polyanion and a polycation respectively. Steps 2 and 4 represent the washing steps. (B) Polyelectrolytes adsorbed on the surface following the steps 1-4. (C) Chemical structure of poly(styrene sulfonate) (PSS) and poly(allylamine hydrochloride) (PAH), which are often used for LbL films.

In the late 1990s Möhwald et al.[61] extended the LbL technique to polymeric capsules by depositing polyelectrolytes onto charged colloidal particles as templates. Various multilayers can be formed with a variety of constituents. The process for assembly of these multilayers is depicted in Figure 1-13. For the fabrication of hollow polyelectrolyte capsules, a template is used which can be removed later. First PS or cross-linked melamine formaldehyde (MF) microcapsules were used as core material. However, the MF capsules proved difficult to remove after the formation of the multilayer and in case of PS an osmotic pressure could be built up in the capsule due to the fast dissolution of the polymer core, which could destroy the

polymeric shell. To overcome these problems inorganic substrates such as $CaCO_3$, $MnCO_3$ and $CdCO_3$ are now used more frequently.[62] These inorganic carbonates have the advantage that upon dissolution with an ethylenediamine tetraacetate (EDTA) solution the metal ions are complexed and can pass the membrane of the polyelectrolyte shell. These capsules are known for their permeability of molecules with a molecular weight below 5 kDa and should therefore have no osmotic stress.[63]

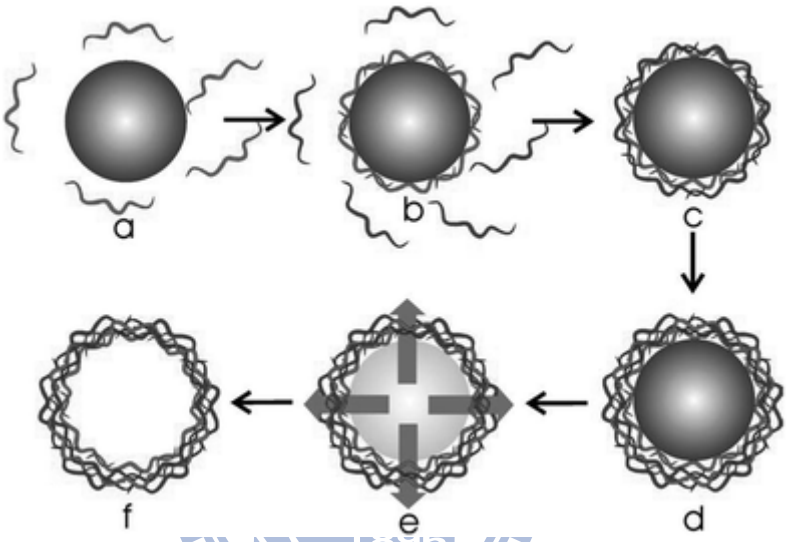

Figure 1-13: Schematic illustration showing the preparation of "hollow" polyelectrolyte capsules. The initial steps (a through d) involve stepwise film formation by repeated exposure of the colloids to polyelectrolytes of alternating charge. Between each step the excess polyelectrolytes are removed before the next layer is deposited. When the desired number of polyelectrolyte layers is obtained the core is decomposed (e) resulting in a suspension of "hollow" polyelectrolyte capsules (f).

These layer-by-layer techniques describe above using solid particles in an aqueous medium. A novel development is the layer-by-layer deposition on a liquid core. Grigoriev et al. have recently described a general method for the encapsulation of a broad range of emulsions comprised of various hydrophobic substances and oil-soluble compounds.[64] To an

emulsion of didodecyldimethylammonium bromide (DODAB), chloroform and dodecane in water was gently added a polyelectrolyte solution. After deposition of a layer, a washing step was carried out, before the next layer was deposited, resulting in microcapsules as shown in Figure 1-14.

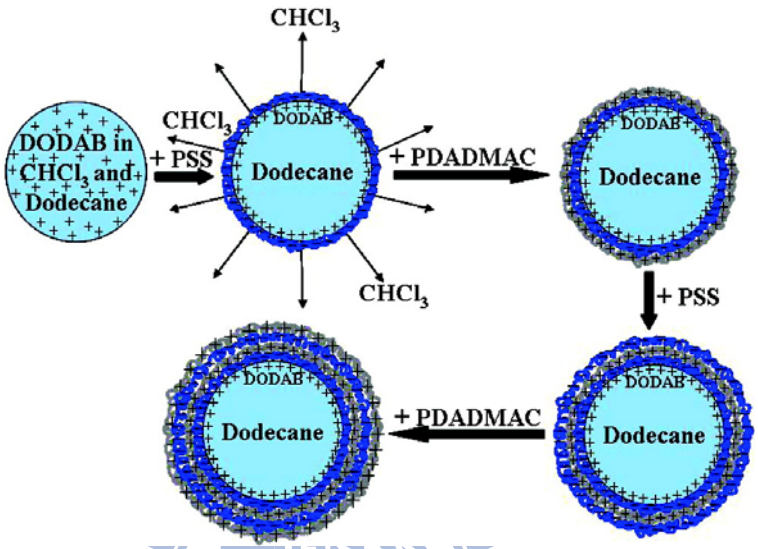

Figure 1-14: Schematic representation of several steps during LbL encapsulation of a liquid core. Explanation of abbreviations: DODAB: didodecyldimethylammonium bromide, PSS: poly(sodium 4-styrenesulfonate), PDADMAC: poly(diallyldimethylammonium chloride).

1-5 Stimuli-responsive polymer materials

The human body is fascinating for its ability to respond to its environment from the molecular to the macroscopic level. Stimuli response is crucial for maintaining normal function as well as fighting disease. At the molecular level, for example, the body releases insulin to initiate glycogen formation in response to higher glucose levels in the blood. Molecular interactions also take place at cellular surfaces to stimulate a number of events including cell signalling and endocytosis. At the macroscopic level, the body responds to external stimuli with a cascade of events, such as when nerve cells transmit signals to the brain in response to a pain-causing stimulus and subsequently cause muscle contraction. These examples have

inspired scientists to fabricate 'smart' materials that respond to light, pH, temperature, mechanical stress or molecular stimuli. Synthetic polymeric materials capable of responses to external or internal stimuli represent one of the most exciting and emerging areas of scientific interest and unexplored commercial applications. While there are many exciting challenges facing this field, there are a number of opportunities in design, synthesis, and engineering of stimuli-responsive polymeric systems and Mother Nature serves as a supplier of endless inspirations.

1-5.1 Stimuli-responsive solutions

Stimuli-responsive behavior is easily obtained in polymeric solutions as the Brownian motion of solvent molecules requires relatively low energies for macromolecular segments to displace solvent molecules. For an ideal system, the kinetic energy required for the Brownian motion at room temperature is $1.5k_BT$ (where the k_B is Boltzman constant (1.38×10^{-23} J/K), and T is the temperature). One example of these transitions in polymeric solutions is lower critical solution temperature (LCST), which is the lowest temperature of phase separation on the concentration–temperature phase diagrams. Below LCST, polymer chains and solvent molecules are in one homogenous mixing phase, and exhibit favorable free energy ($\Delta G < 0$), which is believed to be facilitated by hydrogen-bonding interactions between the two phases. Above LCST, a phase separation occurs as enthalpic (ΔH) energy overcomes the entropic (ΔS) contributions resulting in unfavorable free energy ($\Delta G > 0$) of the entire system. For the majority of polymeric solutions[65] temperature induced LCST transitions result in the particle or aggregate size decreases above LCST, and the reported size changes are substantial, typically in the range from 250 to 3000 nm below LCST, to 100 to 1000 nm above.

1-5.2 Temperature and pH responses

Energetic rearrangements are driven by molecular entities capable of responsiveness to stimuli in a given environment. For polymeric solutions to exhibit stimuli-responsiveness, it is necessary to provide suitable molecular building blocks capable of responses. Figure 1-15, A and B, illustrates several examples of temperature and pH-responsive monomeric blocks which, upon polymerization maintain stimuli-responsiveness. A well known polymer with the LCST behavior is poly(*N*-isopropylacrylamide) (PNIPAm)[65a,b,c] which exhibits coil-to-globule phase transition at 32 °C. Poly(*N*-vinylcaprolactone) (PVCL),[65d,e,f] poly(*N*-(DL)-(1-hydroxymethyl) propylmethacrylamide) (p(DL)-HMPMA),[66] and poly(N,N′-diethylacrylamide) (PDEAAm)[67] are also temperature-responsive, and their LCSTs are about 32, 37, 33 °C, respectively. Thus, molecular designs of a polymer backbone allow one to control temperature at which a given system is responsive. It is well established that the LCST phase transition is a nanometer scale event, where the particle or aggregate dimensions change.[68] However, for individual polymer chains, the coil-to-globule transitions can be thermodynamically controlled by adjusting polymer compositions,[69] as determined by atomic force microscopy (AFM). When copolymerized with hydrophilic or hydrophobic comonomers, LCST transitions may shift to higher or lower temperatures, respectively. Block copolymers of poly(ethylene oxide)–poly(propylene oxide) (PEO–PPO) also exhibit thermal responses in solutions,[70] but it is believed that the driving forces for these transitions originate from amphiphilic balance.

pH-responsive polymer solutions represent another group, in which chemical structures of pH-responsive compounds have ionizable functional groups capable of donating or accepting protons upon environmental pH changes. In this case, electrostatic repulsions between generated charges cause alternations of the hydrophobic volume along a polymer chain, which is capable of extending or collapsing. Polyacids, such as poly(acrylic acid)

(PAAc),[71] and poly(methacrylic acid) (PMAAc)[72] with pKa values in the range of 5 will release protons and swell under basic pH values. In contrast, pH-responsive polybases accept protons and extend under acidic pH conditions, where amino and amine functional groups in poly(*N*,*N*′-dimethyl aminoethyl methacrylate) (PDMAEMA)[73] and poly(vinyl pyridine) (PVP),[74] respectively, are responsible for these transitions. One of the common trends in designing stimuli-responsive polymers is to copolymerize monomers with different stimuli-responsiveness in order to achieve multiple-responsive behavior.

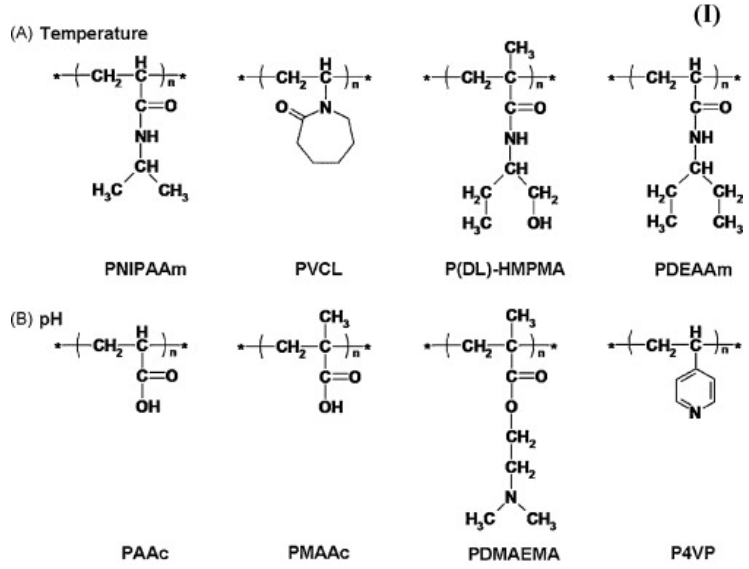

Figure 1-15: Examples of molecular structures responsive to temperature (A) and pH (B).

1-5.3 Electromagnetic-responsiveness

Incorporation of photo-chromic molecules provides opportunity to develop polymers capable of responding to electromagnetic radiation.

Figure 1-16 illustrates most common photo-sensitive molecules, which are classified into the following categories: cis–trans isomers (A), ionization monomers (B), and dimerization monomers (C). As shown in Figure 1-16A, photo-responsive azobenzene is a molecule that exhibits trans-to-cis photoisomerization with sufficiently low energy (2–3 kcal/mol) to induce

photo-chromic transitions.[75] The rearrangement mechanism for lecuo[76] and spiropyran[77] derivatives shown in Figure 1-16B is based on ionization upon exposure to electro-magnetic irradiation. When exposed to UV light, dissociated ion pairs are generated, which can be further neutralized when heated in the dark. As illustrated in Figure 1-16B′ and B″, photo-induced polymer chains of lecuo and spiropyran derivatives shrink and expand, which is attributed to the reversible exchange of the electrostatic repulsion between ionic states. This process typically requires less than 5 kcal/mol.[78] Figure 1-16C illustrates another photo-reactive molecule cinnamate[79] which is able to dimerize upon UV irradiation with the energy barrier of about 7 kcal/mol.[80] These molecular entities can be utilized as photo-reversible covalently crosslinkers in polymers, thus offering potential applications as switching segments in shape memory systems and other devices.

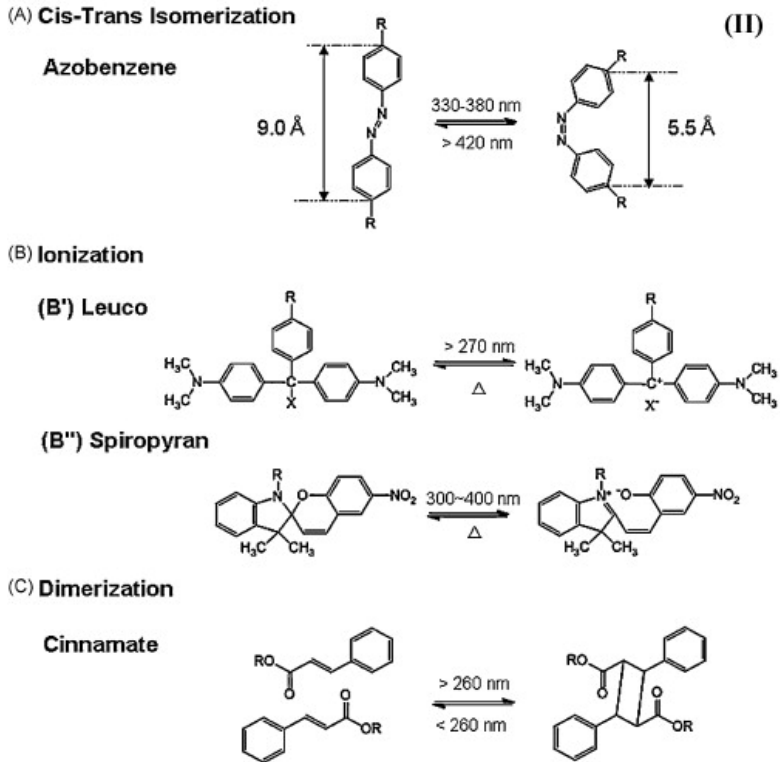

Figure 1-16: Examples of molecular structures of photo-responsive monomers: cis–trans isomer of azobenzene (A); ionization monomers (B) of leucos (B′) and spiropyran (B″); and dimerization monomer of cinnamate (C).

Liquid crystalline materials are stimuli-responsive polymers that have been known for a few decades. These are molecules with permanent dipole moments embedded in polymer matrices, which due to optical and geometrical anisotropies are able to respond to electromagnetic field by aligning their mean optic axis parallel to the external field,[81] which results in orientation changes.

As shown in Figure 1-17A, liquid crystalline molecules are freely dispersed between the two electrodes with no electric field. When an electric field is applied, the molecules align along the electric field axis and the driving force for the alignment results from the electrostatic interactions. Figre 1-17B summarizes selected examples of chemical entities capable of responsiveness, and their common feature is the permanent dipole moment, in this case generated by electron-withdrawing groups nitrile (CN) and trifluoromethyl (CF3) groups.

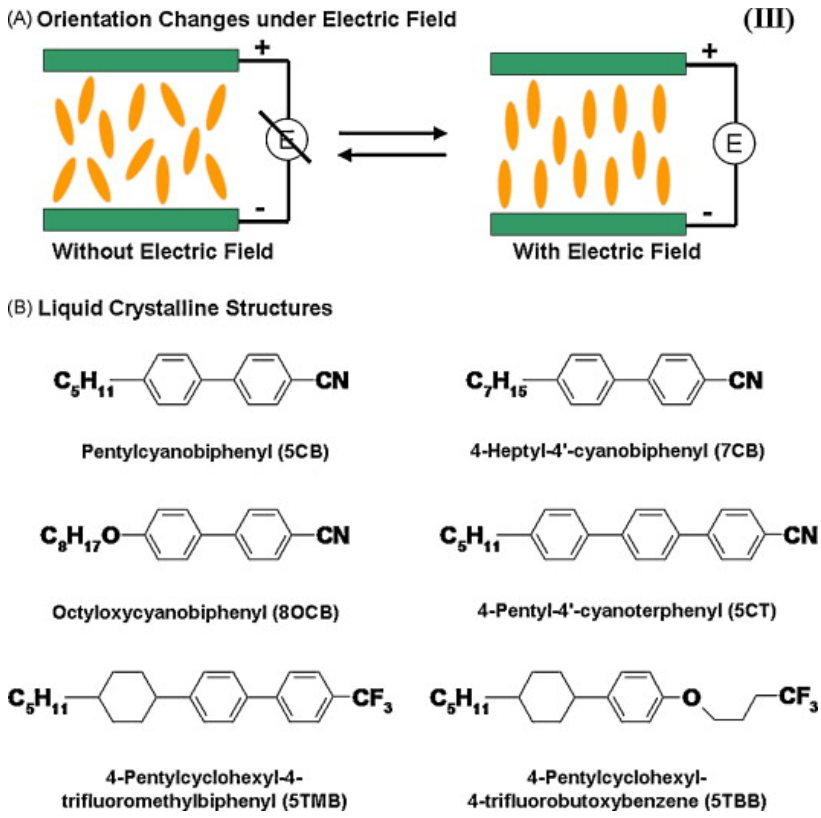

Figure 1-17: Examples of molecular structures of photo-responsive monomers: Orientation changes (A) and molecular structures (B) of liquid crystalline molecules.

1-5.4 Multiple-responsive systems

As pointed out earlier, a growing trend in designing stimuli-responsive polymeric solutions is toward creating systems with multiple-responsive components, with covalently or physically bonded segments responsive to different stimuli. One example of the multi-responsive switchable copolymer is based on temperature-responsive NIPAAm and pH- and photo-responsive spirobenzopyran which exhibits temperature, pH, and photo-responsiveness in aqueous solutions. Along the same lines, acrylic acid, NIPAAm, and cinnamoyloxyethyl acrylate have been copolymerized and exhibit four responses.[82] Acrylic acid component responds to pH and ionic strength, while the NIPAAm and cinnamoyloxyethyl acrylate species exhibit temperature and UV responses, respectively. There are many opportunities for designing multiple-responsive polymeric solutions, in particular using colloidal synthesis where surfaces of colloidal particles may serve as protein or cell adhesion sites,[83] or stabilized with bioactive materials.[84] Due to spatial restrictions significantly greater challenges exist in the development of multiple-responsive systems at surfaces and interfaces, in polymeric gels, and in thermoplastic and thermosetting polymeric networks.

References

1. (a) Hawker, C. J.; Bosman, A. W.; Harth E. *Chem. Rev.* **2001**, *101*, 3661–3688. (b) Kamigaito M.; Ando, T.; Sawamoto, M. *Chem. Rev.* **2001**, *101*, 3689–3745. (c) Matyjaszewski K.; Xia, J. *Chem. Rev.* **2001**, *101*, 2921–2990. (d) Perrier S.; Takolpuckdee P.; *J. Polym. Sci., Part A: Polym. Chem.* **2005**, *43*, 5347–5393. (e) Favier, A.; Charreyre, M. T. *Macromol. Rapid Commun.* **2006**, *27*, 653–692. (f) Ouchi, M.; Terashima, T.; Sawamoto, M. *Chem. Rev.* **2009**, *109*, 4963–5050. (g) Yamago, S. *Chem. Rev.* **2009**, *109*, 5051–5068. (h) Tsarevsky, N. V.; Matyjaszewski, K. *Chem. Rev.* **2007**, *107,* 2270–2299. (i) Braunecker, W. A.; Matyjaszewski, K. *Prog. Polym. Sci.* **2007**, *32*, 93–146. (j) Moad, G.; Rizzardo, E.; Thang, S. H. *Aust. J. Chem.* **2005**, *58*, 379–410. (k) Moad, G.; Rizzardo, E.; Thang, S. H. *Aust. J. Chem.* **2006**, *59*, 669–692.
2. Szwarc M. *Nature*, **1956**, ***178***, 1168–1169.
3. Matyjaszewski, K.; Davis, T.P. ed., *Handbook of Radical Polymerization*, John Wiley & Sons, Inc., Hoboken, **2002**.
4. (a) Otsu, T.; Yoshida, M. *Makromol. Chem. Rapid Commun.* **1982**, *3*, 127–132. (b) Otsu, T.; Yoshida, M.; Tazaki, T. *Makromol. Chem. Rapid Commun.* **1982**, *3*, 133–140. (c) Otsu, T. *J. Polym. Sci., Part A: Polym. Chem.* **2000**, *38*, 2121–2136. (d) Otsu T.; Matsumoto, A. *Adv. Polym. Sci.* **1998**, ***136***, 75–137.
5. Druliner, J. D. *Macromolecules* **1991**, ***24***, 6079–6082.
6. David, G.; Boyer, C.; Tonnar, J.; Ameduri, B.; Lacroix-Desmazes, P.; Boutevin, B. *Chem. Rev.* **2006**, *106*, 3936–3962.
7. Percec, V.; Guliashvili, T.; Ladislaw, J. S.; Wistrand, A.; Stjerndahl, A.; Sienkowska, M. J.; Monteiro, M. J.; Sahoo, S. *J. Am. Chem. Soc.* **2006**, *128*, 14156–14165.
8. (a) Debuigne, A.; Caille, J.-R.; Detrembleur C.; Jérôme, R. *Angew. Chem., Int. Ed.* **2005**, *44*, 3439–3442. (b) Debuigne, A.; Caille, J.-R.; Jérôme, R. *Angew. Chem., Int. Ed.* **2005**,

44, 1101–1104.

9. Kato, M.; Kamigaito, M.; Sawamoto, M.; Higashimura, T.; *Macromolecules* **1995**, *28*, 1721–1723.
10. (a) Wang, J.-S.; Matyjaszewski, K. *J. Am. Chem. Soc.* **1995**, *117*, 5614–5615. (b) Wang, J.-S.; Matyjaszewski, K. *Macromolecules* **1995**, *28*, 7901–7910. (c) Wang, J.-S.; Matyjaszewski, K. *Macromolecules* **1995**, *28*, 7572–7573.
11. Gromada, J.; Matyjaszewski, K. *Macromolecules* **2001**, *34*, 7664–7671.
12. Min, K.; Gao, H.; Matyjaszewski K. *J. Am. Chem. Soc.* **2005**, *127*, 3825–3830.
13. Jakubowski W.; Matyjaszewski, K. *Angew. Chem., Int. Ed.* **2006**, *45*, 4482–4486.
14. Chiefari, J.; Chong, Y. K.; Ercole, F.; Krstina, J.; Jeffery, J.; Le, T. P. T.; Mayadunne, R. T. A.; Meijs, G. F.; Moad, C. L.; Moad, G.; Rizzardo, E.; Thang, S. H. *Macromolecules* **1998**, *31*, 5559–5562.
15. Solomon, D. H.; Rizzardo, E.; Cacioli, P. *Csiro*, **1986**.
16. Corpart, P.; Charmot, D.; Biadatti, T.; Zard, S. Z.; Michelet, D. *Rhodia Chimie*, **1998**, p. 62.
17. Benaglia, M.; Chiefari, J.; Chong, Y. K.; Moad, G.; Rizzardo E.; Thang, S. H. *J. Am. Chem. Soc.* **2009**, *131*, 6914–6915.
18. Georges, M. K.; Veregin, R. P. N.; Kazmaier, P. M.; Hamer, G. K. *Macromolecules*, **1993**, *26*, 2987–2988.
19. Studer, A.; Harms, K.; Knoop, C.; Müller C.; Schulte, T. *Macromolecules*, **2004**, *37*, 27–34.
20. (a) Benoit, D.; Grimaldi, S.; Robin, S.; Finet, J.-P.; Tordo, P.; Gnanou, Y. *J. Am. Chem. Soc.* **2000**, *122*, 5929–5939. (b) Grimaldi, S.; Finet, J.-P.; Moigne, Le F.; Zeghdaoui, A.; Tordo, P.; Benoit, D.; Fontanille M.; Gnanou, Y. *Macromolecules* **2000**, *33*, 1141–1147. (c) Lacroix-Desmazes, P.; Lutz, J.-F.; Boutevin, B. *Macromol. Chem. Phys.* **2000**, *201*,

662–669. (d) Lacroix-Desmazes, P.; Lutz, J.-F.; Chauvin, F.; Severac, R.; Boutevin, B. *Macromolecules* **2001**, *34*, 8866–8871.

21. (a) Benoit, D.; Chaplinski, V.; Braslau, R.; Hawker, C. J. *J. Am. Chem. Soc.* **1999**, *121*, 3904–3920. (b) Benoit, D.; Grimaldi, S.; Finet, J. P.; Tordo, P.; Fontanille, M.; Gnanou, Y. *Polym. Prepr.* (*Am. Chem. Soc., Div. Polym. Chem.*) **1997**, *38*, 729–730. (c) Benoit, D.; Harth, E.; Fox, P.; Waymouth, R. M.; Hawker, C. J. *Macromolecules* **2000,** *33*, 363–370. (d) Benoit, D.; Hawker, C. J.; Huang, E. E.; Lin, Z.; Russell, T. P. *Macromolecules* **2000**, *33*, 1505–1507. (e) Harth, E.; Van Horn, B.; Hawker, C. J. *Chem. Commun.* **2001**, 823–824.

22. (a) Couvreur, L.; Lefay, C.; Belleney, J.; Charleux, B.; Guerret, O.; Magnet, S. *Macromolecules* **2003**, *36*, 8260–8267. (b) Diaz, T.; Fischer, A.; Jonquieres, A.; Brembilla, A.; Lochon, P. *Macromolecules* **2003**, *36*, 2235–2241. (c) Schierholz, K.; Givehchi, M.; Fabre, P.; Nallet, F.; Papon, E.; Guerret, O.; Gnanou, Y. *Macromolecules* **2003**, *36*, 5995–5999.

23. Guillaneuf, Y.; Gigmes, D.; Marque, S. R. A.; Astolfi, P.; Greci, L.; Tordo, P.; Bertin, D. *Macromolecules* **2007**, *40*, 3108–3114.

24. (a) Charleux, B.; Nicolas, J.; Guerret, O. *Macromolecules* **2005**, *38*, 5485–5492. (b) Nicolas, J.; Dire, C.; Mueller, L.; Belleney, J.; Charleux, B.; Marque, S. R. A.; Bertin, D.; Magnet, S.; Couvreur, L. *Macromolecules* **2006**, *39*, 8274–8282. (c) Nicolas, J.; Mueller, L.; Dire, C.; Matyjaszewski, K.; Charleux, B. *Macromolecules* **2009**, *42*, 4470–4478.

25. Nicolas, J.; Brusseau, S.; Charleux, B. *J. Polym. Sci., Part A: Polym. Chem.* **2010**, *48*, 34–47.

26. (a) Kolb, H. C.; Finn, M. G.; Sharpless, K. B. *Angew. Chem., Int. Ed.* **2001**, *40*, 2004–2021. (b) Kolb, H. C.; Sharpless, K. B. *Drug Discovery Today* **2003**, *8*, 1128–1137.

(c) Lewis, W. G.; Green, L. G.; Grynszpan, F.; Radic, Z.; Carlier, P. R.; Taylor, P.; Finn, M. G.; Sharpless, K. B. *Angew. Chem., Int. Ed.* **2002**, *41*, 1053–1057.

27. Tornoe, C. W.; Christensen, C.; Meldal, M. *J. Org. Chem.* **2002**, *67*, 3057–3064

28. Rostovtsev, V. V.; Green, L. G.; Fokin, V. V.; Sharpless, K. B. *Angew. Chem., Int. Ed.* **2002**, *41*, 2596–2599

29. Opsteen, J. A.; van Hest, J. C. M. *Chem. Commun.* **2005**, 57–59.

30. Opsteen, J. A.; van Hest, J. C. M. *J. Polym. Sci., Part A: Polym. Chem.* **2007**, 45, 2913–2924

31. Quemener, D.; Davis, T. P.; Barner-Kowollik, C.; Stenzel, M. H. *Chem. Commun.* **2006**, 5051–5053.

32. (a) Gao, H.; Matyjaszewski, K. *J. Am. Chem. Soc.* **2007**, 129, 6633–6639. (b) Helms, B.; Mynar, J. L.; Hawker, C. J.; Frechet, J. M. J. *J. Am. Chem. Soc.* **2004**, 126, 15020–15021.

33. (a) Gao, H.; Matyjaszewski, K. *Macromolecules* **2006**, 39, 4960–4965. (b) Gao, H.; Min, K.; Matyjaszewski, K. *Macromol. Chem. Phys.* **2007**, 208, 1370–1378.

34. Becer, C. R.; Hoogenboom, R.; Schubert, U. S. *Angew. Chem., Int. Ed.* **2009**, 48, 4900–4908.

35. Baskin, J. M.; Prescher, J. A.; Laughlin, S. T.; Agard, N. J.; Chang, P. V.; Miller, I. A.; Lo, A.; Codelli, J. A.; Bertozzi, C. R. *Proc. Natl. Acad. Sci*. U.S.A. **2007**, *104*, 16793–16797.

36. Joralemon, M. J.; O'Reilly, R. K.; Matson, J. B.; Nugent, A. K.; Hawker, C. J.; Wooley, K. L. *Macromolecules* **2005**, *38*, 5436–5443.

37. (a) Dondoni, A. *Angew. Chem., Int. Ed.* **2008**, *47*, 8995–8997. (b) Hoyle, C. E.; Lowe, A. B.; Bowman, C. N. *Chem. Soc. Rev.* **2010**, *39*, 1355–1387. (c) Lowe, A. B. *Polym. Chem.* **2010**, *1*, 17–36.

38. Alarcon, C. D. H.; Pennadam, S.; Alexander, C. *Chem. Soc. Rev.* **2005**, *34*, 276–285.

39. Van Hest, J. C. M.; Delnoye; D. A. P.; Baars, M. W. P. L.; Van Genderen, M. H. P.; Meijer, E. W. *Science* **1995**, *268*, 1592–1595.

40. (a) Geest, B. G. De; Sanders, N. N.; Sukhorukov, G. B.; Demeester, J.; Smedt, S. C. De *Chem. Soc. Rev.* **2007**, *36*, 636–649. (b) Li, J. B.; Möhwald, H.; An, Z. H.; Lu, G. *Soft Matter.* **2005**, *1*, 259–264. (c) Sukhorukov, G. B.; Möhwald, H. *Trends Biotechnol.* **2007**, 25, 93–98. (d) Wang, Y.; Angelatos, A. S.; Caruso, F. *Chem. Mater.* **2008**, *20*, 848–858.

41. (a) Basinska, T. *Macromol. Biosci.* **2005**, *5*, 1145–1168. (b) Freiberg, S.; Zhu, X. *Int. J. Pharm.* **2004**, *282*, 1–18. (c) Daamen, W. F.; Geutjes, P. J.; van Moerkerk, H. T. B.; Nillesen, S. T. M.; Wismans, R. G.; Hafmans, T.; van den Heuvel, L.; Pistorius, A. M. A.; Veerkamp, J. H.; van Hest, J. C. M.; van Kuppevelt, T. H. *Adv. Mater.* **2007**, *19*, 673–677.

42. (a) Bergman, S. D.; Wudl, F. *J. Mater. Chem.* **2008**, *18*, 41–62. (b) Yow, H. N.; Routh, A. F. *Soft Matter* **2006**, *2*, 940–949.

43. Discher, B. M.; Won, Y.-Y.; Ege, D. S.; Lee, J. C.-M.; Bates, F. S.; Discher, D. E.; Hammer, D. A. *Science* **1999**, *284*, 1143–1146.

44. Zhang, L.; Yu, K.; Einsenberg, A. *Science* **1996**, *272*, 1777–1779.

45. Azzam, T.; Eisenberg, A. *Angew. Chem. Int. Ed.* **2006**, 45, 7443–7447.

46. Discher, B. M.; Bermudez, H.; Hammer, D. A.; Discher, D. E.; Won, Y.-Y.; Bates, F. S. *J. Phys. Chem. B* **2002**, *106*, 2848–2854.

47. (a) Meier, W.; Nardin, C.; Winterhalter, M. *Angew. Chem. Int. Ed.* **2000**, *39*, 4599–4602. (b) Graff, A.; Sauer, M.; Gelder, P. V.; Meier, W. *Proc. Natl. Acad. Sci. USA* **2002**, *99*, 5064–5068.

48. (a) Israelachvili, J. N.; Marcelja, S.; Horn, R. G. *Quart. Rev. Biophys.* **1980**, 13, 121–200. (b) Israelachvili, J. N.; Mitchell, D. J.; Ninham, B. W. *J. Chem. Soc., Faraday Trans. 2* **1976**, *72*, 1525–1568.

49. Discher, D. E.; Ahmed, F. *Annu. Rev. Biomed. Eng.* 2006, *8*, 323–341.

50. Antonietti, M.; Förster, S. *Adv. Mater.* **2003**, *15*, 1323–1333.

51. Cameron, N. S.; Corbierre, M. K.; Eisenberg, A. *Can. J. Chem.* **1999**, *77*, 1311–1326.

52. Jain, S.; Bates, F. S. *Science* **2003**, *300*, 460–464.

53. Zhulina, E. B.; Adam, M.; LaRue, I.; Sheiko, S. S.; Rubinstein, M. *Macromolecules* **2005**, *38*, 5330–5351.

54. (a) Börner, H. G.; Schlaad, H. *Soft Matter* **2007**, *3*, 394–408. (b) Deming, T. J. *Adv. Mater.* **1997**, *9*, 299–311. (c) Deming, T. J. Adv. *Drug Delivery Rev.* **2002**, *54*, 1145–1155. (d) Deming, T. J. *Prog. Polym. Sci.* **2007**, *32*, 858–875.

55. Holowka, E. P.; Pochan, D. J.; Deming, T. J. *J. Am. Chem. Soc.* **2005,** *127*, 12423–12428.

56. Holowka, E. P.; Sun, V. Z.; Kamei, D. T.; Deming, T. J. *Nat. Mater.* **2007**, *6*, 52–57.

57. Kukula, H.; Schlaad, H.; Antonietti, M.; Forster, S. *J. Am. Chem. Soc.* **2002**, *124*, 1658–1663.

58. Checot, F.; Lecommandoux, S.; Gnanou, Y.; Klok, H. A. *Angew. Chem. Int. Ed.* **2002**, *41*, 1339–1343.

59. (a) Kishimura, A.; Koide, A.; Osada, K.; Yamasaki, Y.; Kataoka, K. *Angew. Chem. Int. Ed.* **2007**, *46*, 6085–6088. (b) Koide, A.; Kishimura, A.; Osada, K.; Jang, W. D.; Yamasaki, Y.; Kataoka, K. *J. Am. Chem. Soc.* **2006**, *128*, 5988–5989.

60. Decher, G. *Science* **1997**, *277*, 1232–1237.

61. Sukhorukov, G. B.; Donath, E.; Davis, S.; Lichtenfeld, H.; Caruso, F.; Popov, V. I.; Mohwald, H. *Polym. Adv. Technol.* **1998**, *9*, 759–767.

62. (a) Petrov, I.; Volodkin, D. V.; Sukhorukov, G. B. *Biotechnol. Prog.* **2005**, 21, 918–925. (b) Sukhorukov, G. B.; Volodkin, D. V.; Gunther, A. M.; Petrov, A. I.; Shenoy, D. B.; Möhwald, H. *J. Mater. Chem.* **2004**, *14*, 2073–2081. (c) Volodkin, D. V.; Larionova, N. I.; Sukhorukov, G. B. *Biomacromolecules* **2004**, *5*, 1962–1972. (d) Volodkin, D. V.; Petrov, A. I.; Prevot, M.; Sukhorukov, G. B. *Langmuir* **2004**, *20*, 3398–3406. (e) Zhu, H. G.; Stein, E. W.; Lu, Z. H.; Lvov, Y. M.; McShane, M. J. *Chem. Mater.* **2005**, *17*, 2323–2328.

63. Sukhorukov, G. B.; Brumen, M.; Donath, E.; Möhwald, H. *J. Phys. Chem. B* **1999**, *103*, 6434–6440.

64. Grigoriev, D. O.; Bukreeva, T.; Möhwald, H.; Shchukin, D. G. *Langmuir* **2008**, *24*, 999–1004.

65. (a) Fujishige, S.; Ando, K.K.I. *J Phys. Chem.* **1989**, *93*, 3311–3313. (b) Pelton, R. H.; Chibante, P. *Colloids Surf* **1986**, *20*, 247–256. (c) Baltes, T.; Garret-Flaudy, F.; Freitag, R. J *Polym. Sci. Part A: Polym. Chem.* **1999**, *37*, 2977–2989. (d) Lau, A. C. W.; Wu, C. *Macromolecules* **1999**, *32*, 581–584. (e) Makhaeva, E. E.; Tenhu, H.; Khokhlov, A. R.; *Macromolecules* **2002**, *35*, 1870–1876. (f) Maeda, Y.; Nakamura, T.; Ikeda, I. *Macromolecules* **2002**, *35*, 217–222.

66. (a) Aoki, T.; Muramatsu, M.; Torii, T.; Sanui, K.; Ogata, N. *Macromolecules*, **2001**, *34*, 3118–3119. (b) Liu, F.; Urban, M. W. *Macromolecules* **2008**, *41*, 352–360.

67. Idziak, I,; Avoce, D.; Lessard, D.; Gravel, D.; Zhu, X. X. *Macromolecules* **1999**, 32, 1260–1263.

68. Zareie, H. M.; Volga Bulmus, E.; Gunning, A. P.; Hoffman, A. S.; Piskin, E.; Morris, V. J. *Polymer* **2000**, *41*, 6723–6727.

69. Kujawa, P.; Winnik, F. M. *Macromolecules* **2001**, *34*, 4130–4135.

70. Alexandridis, P.; Holzwarth, J. F.; Hatton, T. A. *Macromolecules* **1994**, *27*, 2414–2425.

71. (a) Connal, L. A.; Li, Q.; Quinn, J. F.; Tjipto, E.; Caruso, F.;Qiao, G. G. *Macromolecules* **2008**, *41*, 2620–2626. (b) Li, G.; Song, S.; Guo, L.; Ma, S.; *J Polym. Sci. Part A: Polym. Chem.* **2008**, *46*, 5028–5035. (c) Binks, B. P.; Murakami, R.; Armes, S. P.; Fujii, S.; Schmid, A. *Langmuir* **2007**, *23*, 8691–8694.

72. (a) He, E.; Yue, C. Y.; Tam, K. C. *Langmuir* **2009**, *25*, 4892–4899. (b) Ravi, P.; Dai, S.; Tan, C. H.; Tam, K. C. *Macromolecules* **2005**, *38*, 933–939.

73. (a) Muñoz-Bonilla, A.; Fernández-García, M.; Haddleton, D. M. *Soft Matter* **2007**, *3*, 725–731. (b) Hu, L.; Chu, L. Y.; Yang, M.; Wang, H. D.; Hui, N. C. *Langmuir* **2007**, *23*, 110 – 117. (c) Liu, F.; Urban, M. W. *Macromolecules* **2008**, *41*, 6531–6539.

74. (a) Butsele, K. V.; Fustin, C. A.; Gohy, J. F.; Jérôme, R.; Jérôme, C. *Langmuir* **2009**, *25*, 107–111. (b) Li, D.; He, Q.; Cui, Y.; Li, J. *Chem Mater* **2007**, *19*, 412–417. (c) Snoswell, D. R. E.; Brill, R. K.; Vincent, B. *Adv Mater* **2007**, *19*, 1523–1527.

75. Kumar, G. S.; Neckers, D. C. *Chem. Rev.***1989**, *89*, 1915–1925.

76. (a) Ishikawa, M.; Kitamura, N.;Masuhara, H.; Irie, M. *Makromol. Chem. Rapid Commun.* **2003**, *12*, 687–690. (b) Mamada, A.; Tanaka, T.; Kungwatchakun, D.; Irie, M. *Macromolecules* **1990**, *23*, 1517–1519.

77. (a) Sakai, H.; Ebana, H.; Sakai, K.; Tsuchiya, K.; Ohkubo, T.; Abe, M. *J. Colloid Interface Sci.* **2007**, *316*, 1027–1030. (b) Fissi, A.; Pieroni, O.; Angelini, N.; Lenci, F. *Macromolecules* **1999**, *32*, 7116–7121. (c) Sumaru, K.; Kameda, M.; Kanamori, T.; Shinbo, T. *Macromolecules* **2004**, *37*, 4949–4955.

78. Lukyanov, B. S.; Ivanov, N. B.; Nivorozhkin, L. E.; Minkin, V. I.; Borodkin, G. S. *Chem. Heterocycl. Compd.* **1995**, *31*, 1096–1102.

79. (a) Nakayama, Y.; Matsuda, T. *J. Polym. Sci. Part A: Polym. Chem.* **1992**, *30*, 2451–2457. (b) Lendlein, A.; Jiang, H.; Jünger, O.; Langer, R. *Nature* **2005**, *434*, 879–882.

80. Stoddard, B. L.; Bruhnke, J.; Porter, N.; Ringe, D.; Petsko, G. A. *Biochemistry* **1990**, *29*, 4871–4879.

81. (a) Fernández-Nieves, A. *Soft Matter* **2006**, *2*, 105–108. (b) Lanzo, J.; Nicoletta, F. P.; De Filpo, G.; Chidichimo, G. *J. Appl. Phys.* **2002**, *92*, 4271–4275.

82. Szczubialka, K.; Moczek, L.; Blaszkiewicz, S.; Nowakowska, M. J. *Polym. Sci. Part A: Polym. Chem.* **2004**, *42*, 3879–3886.

83. (a) Bae, W. S.; Urban, M. W. *Biomacromolecules* **2006,** *7*, 1156–1161. (b) Bae, W. S.; Lestage, D. J.; Proia, M.; Heinhorst, S.; Urban, M. W. *Biomacromolecules* **2005**, *6*, 2615–2621.

84. Lestage, D. J.; Yu, M.; Urban, M. W. *Biomacromolecules* 2005, *6*, 1561–1572.

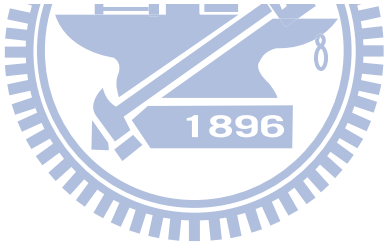

Chapter 2

Polypeptide Diblock Copolymers: Syntheses and Properties of Poly(*N*-isopropylacrylamide)-*b*-Polylysine

Abstract

A hydrolysis-resistant amide-linkage hetero-functional initiator was synthesized and used successfully for polymerization of well-defined rod-coil block copolymers poly(*N*-isopropylacrylamide)-*b*-poly(Z-L-lysine) (PNIPAm-*b*-PZLys) by combination of atom transfer radical polymerization (ATRP) and amine hydrochloride mediated ring-opening polymerization (ROP). The ATRP of NIPAm was carried out at 0 °C using CuBr/Me_6TREN complex in 2-propanol and resulted in narrow polydispersity and high monomer conversion. The amine hydrochlorides has been replaced the primary amine in PNIPAm macroinitiator resulting in a well-controlled ROP of N^{ε}-(carbobenzoxy)-L-lysine *N*-carboxyanhydride in DMF at 20 °C. These amphiphilic block copolymers are able to form universal micelle morphologies of spherical micelles, wormlike micelles, and vesicles by varying the polymer compositions and the helicogenic common solvents. From synchrotron SAXS, WAXS, and TEM results, the PNIPAm-*b*-PZLys microphase self-assembly morphology in solid state is a hierarchical lamellar-in-hexagonal structure. After removing the protective ε-benzyloxycarbonyl group, the dual stimuli-responsive behaviors of the PNIPAm-*b*-PLys investigated by nuclear magnetic resonance spectroscopy in aqueous solution resulted in either coil-to-helix or coil-globule transition by changing the environmental condition of elevating the temperature or increasing the pH value.

2-1 Introduction

Self-assembly of block copolymers, driven by the incompatibility of constituents, into ordered structures in solution and solid state in the sub-micrometer range provide a route to hierarchical nanostructure materials with a variety of potential applications.[1] Bio-mimetic stimuli-responsive block copolymers capable of self-assembly in aqueous solution are particularly interesting as their promising potential in variety of applications such as in drug delivery,[2] in biotechnology,[3] and in the development of sensors.[4] These "smart" materials can reversibly change their physicochemical properties in response to variations in temperature,[5] pH,[6] or ionic strength.[7]

Block copolymers comprised of polypeptide segments have shown significant advantages in controlling functional and supramolecular structures of bio-inspired self-assemblies in aqueous solution.[8] Peptide copolymers provide many advantages over conventional synthetic polymers due to its ability to hierarchically assemble into stable ordered conformations. With different amino acid substitutions, polypeptides can adopt well-defined stable secondary structures such as the α-helix, β-sheet, or coil depending on external environment.[9] Therefore the hybrid copolymers (also named molecular ''chimeras'')[10] combining various conventional synthetics of specific functionalities with polypeptides have been intensively investigated.[11]

To be successful in these purposes, it is important that materials can self-assemble into precisely and predictable structures. Since the late 1940s, the ring-opening polymerization (ROP) of α-amino acid *N*-carboxyanhydrides (NCAs) initiated by nucleophiles or bases have been the most common technique used for polypeptides preparation.[12] However, attempt to prepare polypeptides always results in unmatched compositions with monomer feed ratios and significant homopolymer contaminants because of the nucleophilic/basic duality of the initiator. Elimination of these side reactions has been the major synthetic challenge for this

polymerization system.[13] Several innovative approaches have been proposed for controlling NCA polymerization by different concepts. Deming reported that replacing primary amine initiators with organonickel initiators which are able to give controllable polymerization of a wide range of NCA monomers from pure enantiomers to racemic mixtures.[14] Sequential addition different NCA monomers enables preparation of block copolypeptides with defined sequence and composition. Recently, Deming *et al.* also described the first use of a macroinitiator bearing amido-amidate nickel cycle end groups to synthesize hybrid block copolymers.[15] Both Hadjichristidis and Schlaad groups reported the conventional primary amine-initiated polymerization of NCAs with distinct ideals. The former employed their high vacuum technique to create and maintain conditions necessary for the living polymerization of NCAs.[16] Their approaches of controlling the reaction conditions resolved the existing problem for more than fifty-year-old challenge presented by the NCA/nucleophile system. The latter group's strategy is to allow the reversible dissociation equilibrium between free primary amine and a proton $H^+(Cl^-)$ to exist only a very short lifetime of reactive amine, the amine chain-end group is immediately protonated and thus to prevent side reactions.[17] This approach has been applied by other groups to synthesize well-defined hybrid copolymers.[18]

In order to incorporate desired functional segments into polypeptides based copolymers, additional polymerization techniques are required. Controlled/living radical polymerization (CRP), developed in the past decade,[19] enables the facile synthesis of polymers with controlled molecular weight, low polydispersity, and well-defined architecture. Additionally, desired functionalities can be incorporated into either end group or distributed along polymer backbone. Since ROP and CRP are distinct mechanisms, a dual hetero-functional initiator[20] to combine these two routes is important to design and synthesize various hybrid block copolymers.

Few research activities have been focused on dual stimuli-responsive hybrid block copolymers consisting of pH-sensitive polypeptides and thermo-sensitive segment.[21] Poly(*N*-isopropylacrylamide) (PNIPAm), the most widely studied thermo-responsive polymer, exhibits coil-to-globule transition above the lower critical solution temperature (LCST) at 32 °C in aqueous solution. Below this critical temperature, it is in a hydrophilic state, and above this temperature it is in a hydrophobic state.[22] All the major CRP techniques, atom transfer radical polymerization (ATRP),[23] nitroxide-mediated polymerization (NMP),[24] and reversible addition-fragmentation chain transfer polymerization (RAFT)[25] have been successfully used to prepare poly(*N*-isopropylacrylamide) with low-to-moderate chain length and narrow molecular weight distribution.

In this paper, we report the synthesis of a new amide-linkage phthalimidoethyl 2-bromo-2-methylpropionamide hetero-functional initiator which allows both polymerizations to be conducted consecutively by ATRP then the amine hydrochloride mediated ROP of N^{ε}-(carbobenzoxy)-L-lysine *N*-carboxyanhydride (Z-Lys-NCA) or γ-benzyl L-glutmate *N*-carboxyanhydride (BLG-NCA) to synthesize well-defined poly(*N*-isopropylacrylamide)-*b*-polypeptides hybrid block copolymers. An investigation of these rod-coil hybrid block copolymers' hierarchical self-assembly nanostructure and dual stimuli-responsive of pH and thermo-sensitive behaviors in aqueous solution and in solid states are detail presented.

2-2 Experimental Section

2-2.1 Materials

All reagents and solvents were purchased from commercial suppliers and used as received unless otherwise noted, including L-glutamic acid 5-benzyl ester (Fluka, >99%), N^{ε}-(carbobenzoxy)-L-lysine (ACROS, 98%), triphosgene (TCI, >98%), ethanolamine (Tedia, 99%), bromoisobutyryl bromide (ACROS, 98%), diethyl azodicarboxylate solution 40% in toluene (Fluka), triphenylphosphine (Lancaster, 99%), phthalimide (ACROS, 98%), hydrazine monohydrate (Sigma-Aldrich, 98%), 2-propanol (Tedia, 99.5%), uranyl acetate dihydrate (Fluka, 98%), hydrogen bromide 33 wt. % in acetic acid (ACROS), and trifluoroacetic acid (ACROS, 99%). The monomer *N*-isopropylacrylamide (NIPAm, 99%, TCI) was recrystallized in hexane/toluene, and dried under vacuum before use. Ethyl acetate (Tedia, 99.8%) and *N*,*N*-Dimethylformamide (DMF; Tedia, 99.8%) were dried over CaH_2 (ACROS, 93%) and distilled under reduced pressure. Tetrahydrofuran (Tedia, 99.8%) was distilled over Na/benzophenone. Deioned (DI) water used in all reactions, solution preparations, and polymer isolations was purified to a resistance of 18 MΩ (Milli-Q Reagent Water System, Millipore Corporation). N^{ε}-(carbobenzoxy)-L-lysine *N*-carboxyanhydride (Z-L-lysine NCA) and γ-benzyl L-glutmate *N*-carboxyanhydride (BLG NCA) were synthesized according to the method described by Poché *et al*. (Fuchs-Farthing method).[26] Hexamethylated tris(2-(dimethylamino)ethyl)amine (Me_6TREN) was synthesized according to method of Ciampolini.[27]

2-2.2 Synthesis of 2-bromo-*N*-(2-hydroxyethyl)-2-methylpropionamide (BrPA) (1) (Scheme 1)

Ethanolamine (5.31 g, 86.9 mmol, 1.0 equiv) and TEA (8.8 g, 173.8 mmol, 2.0equiv) dissolved in THF (400mL) were fed into a 500 mL two-necked round-bottomed flask fitted

with a Ar inlet and a rubber septum and were cooled in an ice bath. The α-bromoisobutyryl bromide (20 g, 86.9 mmol, 1.0 equiv) was added into the mixture dropwise. White precipitate of triethylammonium bromide was observed and the reaction was allowed to stir at room temperature overnight. After the precipitate was filtered off, THF was removed by rotary evaporation. The residue was purified with column chromatography (silica gel, hexane/ethyl acetate: v/v: 1/1) yield product 1 (11.33 g, 62%) as a viscous oil. ^{1}H NMR ($CDCl_3$, δ, ppm) 7.13 (br, 1H, -N<u>H</u>-), 3.72 (m, 2H, HO-C<u>H</u>$_2$-), 3.42 (m, 2H, HO-CH$_2$-C<u>H</u>$_2$-), 2.32 (br, 1H, <u>H</u>O-CH$_2$-), 1.93 (s, 6H, Br(C<u>H</u>$_3$)$_2$-C-). ^{13}C NMR ($CDCl_3$, δ, ppm): 173.12 (-NH-<u>C</u>(O)-C-), 62.51 (Br(CH$_3$)$_2$-<u>C</u>-C(O)-), 61.77 (HO-<u>C</u>H$_2$-CH$_2$-), 42.97 (HO-CH$_2$-<u>C</u>H$_2$-), 32.48 (Br(<u>C</u>H$_3$)$_2$-C-).

2-2.3 Synthesis of phthalimidoethyl 2-bromo-2-methylpropionamide (PIBrPA), (2) (Scheme 1)

To a THF solution (250 mL) of a mixture of product (1) (9 g, 42.8 mmol, 1.0 equiv), triphenylphosphine (14.6 g, 55.6 mmol, 1.3 equiv), phthalimide (6.3 g, 42.8 mmol, 1.0 equiv) was added dropwise 40 % toluene solution of diethylazodicarboxylic acid (DEAD; 24.3 g, 55.6 mmol, 1.3 equiv), and the resulting mixture was stirred under argon at room temperature for 12h. The reaction mixture was then evaporated to dryness, and the residue was purified with column chromatography (silica gel, hexane/ethyl acetate: v/v: 4/1) and recrystallization with THF/hexane to yield product (2) (6.5 g, 45%) as a white needle-like crystals. ^{1}H NMR ($CDCl_3$, δ, ppm): 7.86 (m, 2H, phthalyl aromatic), 7.70 (m, 2H, phthalyl aromatic), 7.09 (br, 1H, -N<u>H</u>-), 3.87 (m, 2H, -C<u>H</u>$_2$-CH$_2$-NH-), 3.54 (m, 2H, -CH$_2$-C<u>H</u>$_2$-NH-), 1.85 (s, 6H, Br(C<u>H</u>$_3$)$_2$-C-). ^{13}C NMR ($CDCl_3$, δ, ppm): 172.44 (-NH-<u>C</u>(O)-C-), 168.43 (-C-<u>C</u>(O)-N-), 134.12, 131.86, 123.38 (aryl-<u>C</u>), 62.13 (Br(CH$_3$)$_2$-<u>C</u>-C(O)-), 39.82 (-C<u>H</u>$_2$-CH$_2$-NH-), 37.16 (-CH$_2$-<u>C</u>H$_2$-NH-), 32.23 (Br(<u>C</u>H$_3$)$_2$-C-).

2-2.4 Preparation of phthalimide end-capped poly(*N*-isopropylacrylamide) (3) by ATRP (Scheme 2)

A typical polymerization procedure of NIPAm at monomer/initiator ratio of 250 was as carried out follows. NIPAm (4.00 g, 35.40 mmol), initiator (0.048 g, 0.14 mmol), and 2-propanol (7.65 mL) were combined and deoxygenated by performing freeze-pump-thaw cycle. Upon equilibration at 20 °C after the third cycle, the flask was immersed into an water or ice bath. To allow the buildup of the complex between the metal and ligand, an oxygen free solution of 2-propanol (2.55 mL) containing CuBr or CuCl (20.5 mg or 14.16 mg, 0.1416 mmol) and Me_6TREN (32.7 mg, 38.85 μL) was prepared separately. This solution was then added to the monomer and initiator mixture via an argon-washed syringe to start polymerization. The reaction mixture was exposure to air to stop polymerization, then evaporated to dryness and the residue was dissolved in 150mL of THF, and the copper catalyst was removed by passing through a neutral alumina column. The solution was concentrated and precipitated in n-hexane to yield PNIPAm as white powder. To obtain the actual M_n calculated from the ratio of the integral of the phthalimide and methine protons peak by ^{1}H NMR, the phthalimide end-capped PNIPAm was further purify by dialysis against DI water to exclusively eliminate residual monomer and non-initiated initiator. ^{1}H NMR (500MHz, $CDCl_3$): δ 1.12 (br, $CH(C\mathbf{H}_3)_2$) 1.33 − 2.24 (br, aliphatic **H**) 3.98 (br, $C\mathbf{H}(CH_3)_2$), 6.63 (br, N**H**), 7.71 (br, phthalyl aromatic), 7.81 (br , phthalyl aromatic).

2-2.5 Hydrazinolysis of phthalimide end-capped PNIPAm to primary amine (4a) and amine hydrochloride-functionalized PNIPAm (4b) (Scheme 2)

Phthalimide end-capped PNIPAm (5 g) and 5-folds excess hydrazine monohydrate were dissolved in ethanol (25 mL) and the mixture was stirred at room temperature under argon for 12 hours. (upon the addition of the hydrazine, the solution became yellowish due to the

formation of phthalyl hydrazide.) The mixture was placed in a dialysis bag (MWCO = 3500 Da) and dialyzed against DI water for 48 hours. The DI water was changed every hour for the first five hours. Finally the water solution was freeze-dried. Isolated yield: 2.3 g (46%). To convert primary amine into amine hydrochloride, excess amount of 1 M HCl was added into the mixture solution and stirred for two hours to convert primary amine into amine hydrochloride. The mixture was dialyzed and lyophilized. The amine hydrochloride-functionalized PNIPAm isolated yield: 2.6 g (52%). ^{1}H NMR (500MHz, D_2O): δ 1.05 (br, $CH(C\mathbf{H}_3)_2$), 1.50 (br, -$CHC\mathbf{H}_2$-), 1.92 (br, -$C\mathbf{H}CH_2$-), 3.02 (br, -CH_2-$C\mathbf{H}_2$-$NH_3^+Cl^-$), 3.39 (br, -$C\mathbf{H}_2$-CH_2-$NH_3^+Cl^-$), 3.81 (br, $C\mathbf{H}(CH_3)_2$).

2-2.6 General procedure for synthesis of poly(*N*-Isopropylacrylamide-*b*-peptide) block copolymer (5, 6) by ROP polymerization (Scheme 2)

Typically, the functionalized PNIPAm macroinitiator and *N*-carboxyanhydride monomer were dried at room temperature at separated dried flask under high vacuum for one hour. Then, two separate DMF solutions were prepared and subsequently combined via transfer needle under argon to give ~9 wt% solution. The mixture was stirred at room temperature for several days under inert argon atmosphere. After polymerization, the solvent was concentrated to a minimum amount under high vacuum. The concentrated DMF solution was precipitated in ether and subsequently dried under vacuum.

2-2.7 Deprotection of the ε-benzyloxycarbonyl (Cbz-group) side chains in PNIPAm-b-PZLys (7) (Scheme 2)

A round-bottom flask was charged with a solution of the appropriate PNIPAm-*b*-PZLys in trifluoroacetic acid (100 mg/ 3 mL). Then, a 4-folds molar excess of a 33 wt% solution of HBr in acetic acid was added, and the reaction mixture was stirred for one hour at room temperature. Finally, the reaction mixture was precipitated in ether and repeatedly dialyzed

against water until the conductivity remains constant. The product was isolated via lyophilization.

2-2.8 Preparation samples of block copolymer micelles assembled in water

Dried solid block copolymer powder was dissolved in DMF or THF (1.0 mL) to give a 0.1% (w/v) solution. A stir bar was added followed by dropwise addition of DI water (0.1 mL) under constant stirring. The solution was allowed to stir for 48 hours before exhaustive dialysis (Spectra/Por CE (cellulose ester) dialysis membranes, MWCO: 2000) against DI water for another 48 hours to remove DMF or THF.

2-2.9 Preparation of polymer film

Polymer film was prepared by solvent casting 10% polymer solutions in DMF as a non-selective solvent. Liquid samples were placed on Teflon-coated aluminum foil (BYTAC) and were slowly dried within five days at 70 °C. The sample was scratched off the foil and isolated as transparent thin film.

2-2.10 Characterizations

^{1}H NMR and ^{13}C NMR measurements were carried out at room temperature on a Varian Unity inova spectrometer operating at 500 MHz using $CDCl_3$, DMSO-d_6 or D_2O as solvents. Monomer conversion was determined from the ^{1}H NMR integration ratio of the monomer double bond at 5.5 ppm to polymer peak at 3.8 ppm in DMSO-d_6. The molecular weight and molecular weight distribution were determined by gel permeation chromatography (GPC) using a HITACHI PUMP L-7100—equipped with a RI 2000 refractive Index detector, and three Ultrastyragel columns (100, 500, and 10^3 Å) connected in series in order of increasing pore size—using DMF as an eluent at a flow rate of 0.6 mL/min. The molecular weight calibration curve was obtained using polystyrene standards. Fourier Transform Infrared

Spectroscopy (FT-IR) spectra of solid samples were recorded at room temperature with a Nicolet AVATAR 320 FT-IR Spectrometer. Transmission electron microscopy (TEM) images were obtained by using a JEOL JEM-2000EXII instrument operated at 120 KV. The sample was ultra-microtomed at room temperature using a diamond knife from Leica Ultracut UCT Microtome to give 70 nm-thick sections then transferred onto carbon-coated copper grids. For a selective staining of poly(Z-L-lysine), specimens were exposed to the vapor of a freshly prepared aqueous RuO_4 solution. In micelles solution, one drop of each respective sample was placed on a 200 mesh Formvar coated copper grid and allowed to remain on the grid for 120 seconds. Filter paper was then used to remove the residual sample and liquid. One drop of 2 % (w/v) uranyl acetate (negative stain) was then placed on the grid, allowed to stain for 60 seconds, and subsequently removed by wicking away excess liquid with filter paper. The resulting samples were imaged by TEM. Wide-angle X-ray scattering (WAXS) spectrum was recorded on film sample using a Rigaku D/max-2500 type X-ray diffraction instrument. The radiation source used was Ni-filtered, Cu Kα radiation (λ = 1.54Å). The sample was mounted on a circular holder, the scanning rate was 0.6°/min from 2θ = 1 to 80. Data were collected and plotted as intensity versus scattering vector, q, where $q = (4\pi/\lambda)\sin(\theta)$ and θ is the Bragg angle (or 1/2 the scattering angle). Small-angle X-ray scattering (SAXS) measurement was conducted on a dedicated setup at the end-station of the BL17B3 beamline of the National Synchrotron Radiation Research Center (NSRRC), Taiwan. We used an X-ray beam of 0.5 mm diameter and a wavelength (λ) of 1.24 Å for the SAXS measurements.

2-3 Results and Discussion

2-3.1 Synthesis of amide linkage hetero-functional ATRP initiator

Since ester groups are good activating groups, α-haloester-based compounds are commonly used as ATRP initiators. In order to combine mechanistically incompatible initiation group into ATRP initiator compound, usage of the robust amide linkage of α-haloamide-based initiator[28] is an alternative method to build up various architecture block copolymers. There have been several examples of using 2-bromo-2-methylpropionamide-based ATRP initiators to prepare various homopolymers and block copolymers.[29] In this study, α-bromo amide-based initiator was synthesized by amidation of the amino group of ethanolamine with α-bromoisobutyryl bromide and then the hydroxyl group was substituted by Mitsunobu reaction into phthalimide group which can be converted into amino group (Scheme 2-1). Accordingly, an new hetero-functional initiator was afforded for consecutive polymerization of *N*-isopropylacrylamide by ATRP and then ROP of amino acids NCA (Scheme 2-2).

2-3.2 Preparation of phthalimide end-capped poly(*N*-isopropylacrylamide)

Stöver and co-works recently showed that ATRP of NIPAm in different alcohols, especially in 2-propanol that alleviate catalyst inactivation by hydrogen bonding between amide groups and branched alcohols, led to narrow-disperse PNIPAm with high conversion and good molecular weight control.[23] Me_6TREN, a branched tetradentate ligand, forms one of the most active catalyst complex among all the ligands has been investigated, particular success in ATRP of acrylamides with good control over polymerization in room temperature.[30] In this study, the polymerization of NIPAm was investigated under a range of reaction conditions to investigated the catalysts and reaction temperature effect on ATRP. All reactions were conducted at the ratio of NIPAm/2-propanol = 1/2 (w/w) with Me_6TREN as ligand. When the Cu(I)Br was used to form the catalyst complex, the reaction was conducted at 20 °C for 70

minutes and yielded PNIPAm in 56.19% conversion with M_n = 17747 g mol^{-1} and polydispersity (PDI) = 1.31. When the reaction was carried out with Cu(I)Cl at 20 °C, a halide exchange catalyst system,[31] polymerization for 250 minutes resulted in higher conversion of 70.25% with M_n=19 846 g mol^{-1} (PDI = 1.32). At lower polymerization temperature at 0 °C, product with significant narrow molecular weigh distribution was achieved (PDI=1.12) over 720 minutes with conversion of 63.88% and M_n=18 444 g mol^{-1}. These polymerization data are summarized in Table 1. The reaction catalyzed by Cu(I)Br at 20 °C give the fastest polymerization rate and the kinetic plot is non-linear (Figure 2-1, square). This highly active Cu(I)Br/Me_6TREN has large equilibrium constant in the ATRP and can rapidly initiate the initiators to generate high radical concentration at early stages of polymerization. Irreversible radical combination occurs continuously and initiators are consumed until a sufficient number of the Cu(II)Br_2 deactivators are established to the activation/deactivation equilibrium. As a result, high persistent radical[32] concentration of Cu(II)Br_2 decreases the polymerization rate and increases the product PDI because active catalysts are insufficient for fast exchange between active and dormant chain ends. In addition, portion of initiators produce low molecular weight polymer chains at the early stage of polymerization during the irreversible radicals combination, leading to lower initiation efficiency and higher PNIPAm molecular weight than theoretical values (Figure 2-2, square). A small number of dead chains in Figure 2-3a suggest low initiation efficiency. In order to alleviate the fast polymerization rate, the halide exchange (R-Br/Cu(I)Cl) catalyst system was performed. Slower polymerization rate and a non-linear kinetic plot were observed in this system (Figure 2-1, triangle). This is because stable terminal C-Cl bonds are formed from halide exchange during propagation step. Therefore the polymerization via R-Br/Cu(I)Cl system can achieve higher monomer conversion but gives a broad polydispersity similar to the R-Br/CuBr system (Figure 2-2, triangle).

The polydispersity of polymers prepared by ATRP, reflecting the polymerization control, depends on the efficiency of deactivation according to equation (1).[33]

$$\mathrm{PDI} = 1 + \left(\frac{k_p [\mathrm{RX}]_0}{k_{deact} [\mathrm{Cu^{II}X}]} \right) \left(\frac{2}{p} - 1 \right) \quad (1)$$

where k_p is the propagation rate constant, k_{deact} is the deactivation rate constant, p is the monomer conversion, $[RX]_0$ is the initiator concentration, and $[Cu^{II}X]$ is the deactivator concentration. In general, the values of $k_{deact}[Cu^{II}X]$ are higher for X = Br than for X = Cl. Therefore lower polydispersity is expected in systems in which alkyl bromide initiator and copper bromide-based catalysts are used.[32] Nevertheless, R-Br/Cu(I)Br system in this study produced molecular weights deviated form theoretical values because of high polymerization rate. Moreover, an improving R-Br/Cu(I)Cl system gives controllable living polymerization in contrast to R-Br/Cu(I)Br system but the initial PDI has already increased to 1.20 for 5 minutes (Figure 2-3b). This can be attributed to the relatively slower rate of initiation reaction in R-Br/Cu(I)Cl system comparing with R-Br/Cu(I)Br system, and thus, deactivators are not enough to implement fast deactivation of active species to dormant polymer chains. In order to utilize the highly active Cu(I)Br/Me_6TREN possessing high efficiency in deactivation for narrow molecular weights distribution, polymerization of NIPAm with Cu(I)Br/Me_6TREN was also conducted at 0 °C. The kinetic plot (Figure 2-1, circle) shows that the polymerization rate is significantly reduced relative to the halide exchange system. The slow polymerization rate can be attributed to lower reaction temperature, however, a narrower molecular weight distribution is achieved (Figure 2-3c). The reaction reactivity at 0 °C still has high enough equilibrium constant to maintain the reactivity of Cu(I)Br/Me_6TREN and the Cu(II)Br_2 deactivators provide effective deactivation rate to lower polydispersity according to equation (1). Although the kinetic plot is not linear, especially in the late stages of polymerization, however, the polydispersity remains narrow and the molecular weight linearly increases with

conversion, indicating negligible loss of terminal alkyl halides. From the linearity of the $M_{n,GPC}$ versus conversion plot and low polydispersity, controllable polymerization of NIPAm can be achieved by ATRP using CuBr/Me_6TREN in 2-propanol at 0 °C.

The phthalimide end-capped PNIPAm was analyzed by ^{1}H NMR spectroscopy. The characteristic α-end phthalimide signals (*e*, *f*) derived from the initiator and other signals specific for polymer main chain protons are depicted in Figure 2-4. In addition, the M_n of the polymer was also determined from the PNIPAm methine protons (-C*H*$(CH_3)_3$)/phthalimide protons intensity ratios and the obtained values agree well with that determined by GPC. These results indicate that the hetero-functional initiator gives the end-functionalized PNIPAm by ATRP.

2-3.3 Hydrazinolysis of phthalimide end-capped PNIPAm

Primary amine and amine hydrochloride-functionalized PNIPAm were employed as macroinitiators for the anionic ring-opening polymerization of NCA to synthesize the diblock copolymers of PNIPAm-*b*-PZLys and PNIPAm-*b*-PBLG. The GPC profiles show that these two macroinitiators, PNIPAm-NH_2 and PNIPAm-$NH_3^+Cl^-$, dialyzed at different temperatures against DI water after hydrazinolysis (Figure 2-5). By comparing the molecular weight distribution of these two dialysis conditions, coupling reaction in the presence of doubled molecular weight polymer arose during dialysis at ambient temperature 20 °C. The coupling reaction could be due to the nucleophilic substitution between the α-amine group and the terminal bromo-group of PNIPAm.[34] We found that the nucleophilic substitution can be inhibited by dialyzing against cold water at 5 °C with negligible trace of coupling polymers in GPC analysis. For the phthalimide initiators utilized in previous studies, isomerization to 2-hydroxyethylamides on deprotection is a significant problem. This was pointed out first by Wooley[35] and then subsequently mentioned by Davis and coworkers.[36] However, according to

the ^{1}H NMR spectra of these two α-functional macroinitiators shown in Figure 2-6, these two samples exhibit the characteristic α-end functional signals derived from the initiator after hydrazinolysis, including the amide methylene protons (*f*) and amine or amine hydrochloride methylene protons (*g*).

IR spectra for hetero-functional initiator, phthalimide end-capped PNIPAm, and PNIPAm-NH_2 are shown in Figure 2-7. The C=O characteristic peaks for the phthalimide group of initiator is at 1774 and 1706 cm^{-1} while peaks at 1644 and 1538 cm^{-1} are attributed to amide I and amide II bands. The spectrum of the phthalimide end-capped PNIPAm sample shows two phthalimide characteristic peaks, confirming that the ATRP is initiated by this initiator to form PNIPAm polymer. After hydrazinolysis of the phthalimide end-capped PNIPAm, the PNIPAm-NH_2 remains intact and only the phthalimide characteristic peaks are disappeared. In addition to NMR results, IR spectra further confirm our successful synthesis of the amine-functionalized PNIPAm macroinitiator.

2-3.4 Synthesis of Diblock Copolymer

By confirming the existence α-terminal functional groups by ^{1}H NMR, anionic ring-opening polymerization of NCA was performed by these two macroinitiators GPC signals of PNIPAm-*b*-polypeptides via primary amine-functionalized PNIPAm (PNIPAm-NH_2, DP=125, M_n=15411 g mol^{-1}) (Figure 2-8). These reactions can be completed within 24 hours but are uncontrollable due to inevitable activated monomer polymerization mechanism rather than normal amine mechanism. To eliminate the side reaction initiated by the nucleophilic/basic duality of primary amine, the primary amine-functionalized PNIPAm was replaced with amine hydrochloride-functionalized PNIPAm to prevent the activated monomer mechanism. The kinetic study of amine hydrochloride mediated ROP ($[ZLys\text{-}NCA]_0/[MI]_0 = 90$) is shown in Figure 2-9a by monitoring the GPC traces of monomer and molecular weight evolution of copolymers. Indeed, it clearly shows that the monomer signal intensity decreases and

copolymer molecular weight increases simultaneously. The polymerization rate slows down (completed in 90 hours) and the molecular weight distribution is controlled. These results demonstrate that ROP of ZLys-NCA improves the control of molecular weight distribution and elimination of side reactions by replacing primary amine with amine hydrochloride. These diblock copolymers characterized by GPC (Figure 2-9b) and ^{1}H NMR and results are summarized in Table 2-2 (expt. 1 and expt. 2). Then in a second reaction step, the Cbz protective side chains were removed by treating these block copolymers with HBr/AcOH in trifluoroacetic acid and the resulting block copolymer was characterized by ^{1}H NMR. The spectra before and after deprotection of the Cbz groups for expt.1 are shown in Figure 2-10. Comparing the peak integral ratio (Figure 2--10a) of the methine protons of PNIPAm (C*H*: δ 3.8) and the methylene protons of the Z group (C*H*$_2$C$_6$H$_5$: δ 4.9), the DP of PZLys is 71. After deprotecting of the PNIPAm-*b*-PZLys, the peak integral ratio (Figure 2-10b) of the methine protons of PNIPAm (C*H*: δ 3.8) and α-methine protons of PLys (COC*H*NH: δ 4.2) result in DP of 72. Based on ^{1}H NMR calculation, we confirmed that neither loss of the lysine repeating units by backbone scission nor cleavage of the amide group to a secondary amino group in the PNIPAm block. Therefore, we can ascertain that the polymerization of Z-Lys-NCA and deprotection of Cbz-groups are successfully accomplished by using the amine hydrochloride-functionalized PNIPAm. The polydispersity of PNIPAm$_{90}$-*b*-PZLys$_{71}$ is about 1.20 and the DP is close to the value predicted from the initial monomer/macroinitiator ratio. In a similar fashion, ROP of BLG-NCA was also performed by PNIPAm-$NH_3^+Cl^-$ and results are summarized in Table 2-2 (expt.3 and 4). However, the kinetic study gives noticeable broader molecular weight distribution (Figure 2-11). The broader polydispersity product is possibly due to higher reactivity of the BLG-NCA in comparison with Z-Lys-NCA and results in less control of the growing polymer chain end reactivity during the course of the

polymerization. These diblock copolymers were characterized by GPC (Figure 2-12) and ^{1}H NMR and results are summarized in Table 2-2 (expt. 3 and expt. 4).

2-3.5 Self-Assembly behavior of PNIPAm-*b*-PZLys diblock copolymer in aqueous solution

Most prior studies on self-assembly of polypeptides in dilute solution have concentrated on the determination of the influences of various parameters such as molecular weight, solvent, temperature, salt, pH, amino acid composition, etc.[37] However, little attention has been paid to the self-assembly properties based on Cbz-protective side chain polypeptide amphiphilic block copolymers in aqueous medium.[38] It is well-known that polypeptide forms α-helical conformation, a tight spiral stabilized by hydrogen bonds. This ensures that the PNIPAm-*b*-PZLys copolymer has rod-like hydrophobic and flexible hydrophilic segment. In order to investigate the rod-coil self-assembly in aqueous solution, we selected two samples of diblock copolymers, $PNIPAm_{197}$-*b*-$PZLys_{44}$ and $PNIPAm_{90}$-*b*-$PZLys_{71}$, to observe aggregation morphology by transmission electron microscopy (TEM). These two samples were first dissolved in helicogenic common solvent (DMF or THF) and then precipitant (water) was added to the solution. After stirring 2 days for equilibrium, organic solvent was removed from the colloidal solution by dialyzing against DI water and observed by TEM. Depending on the nature of organic solvent employed, the morphology of aggregates formed in DMF/water system may differ to that in THF/water. In addition, the copolymer composition is another effective approach to affect the aggregate morphology. In the system of $PNIPAm_{197}$-*b*-$PZLys_{44}$, the micelle morphologies changed from a spherical micelle in DMF/water system to a mixed spherical and wormlike micelle in THF/water system as shown in Figure 2-13a and 13b. Nakajima *et al.* reported that the Cbz side chain dimension varies in accordance with the kind of solvent dipole moment.[39] The solvent with high dipole moment possesses greater dimension for the side chain originating from the difference in the side chain-solvent interaction. Consequently, when the common solvent is changed from DMF to

THF, a less dipole moment solvent of THF, it tends to induce rod segment side chain to shrink. The rod-like peptide helices can pack side-by-side along their long axes to form more compact micelle core in THF/water than that in DMF/water system. However, there was no enough space to accommodate the relatively longer solvent-compatible PNIPAm block in the corona domain. Consequently, in order to reduce the repulsion contribution of corona-forming PNIPAm block, the morphology shifts to mixed spherical and wormlike micelles for decreasing the corona free energy.[40] Furthermore, all of the spherical micelles observed in THF/water system are smaller than those in DMF/water system, suggesting that the core-forming PZLys chains are packed more densely. The effect of copolymer composition on morphological change was investigated by examining other sample of $PNIPAm_{91}$-*b*-$PZLys_{71}$. When the PZLys composition f_{PZLys} is increased from 0.18 to 0.44, the morphology changes from spherical micelles to giant vesicles in DMF/water system (Figure 2-13c), and from mixed spherical and wormlike micelles to vesicles in THF/water system (Figure 2-13d). Decreasing f_{PNIPAm} reduces the corona crowding and thus permits a larger aggregation number. However, expansion of the sphere is inhibited by the large entropy penalty from increasing f_{PZLys}[41]. Consequently, the micelle morphology changes to giant vesicles to satisfy the less interfacial curvature requirement for the relatively shorter PNIPAm and the stiff interface from packed helices. The common solvent THF also leads to vesicle aggregates but in smaller dimension about 430 nm. According to above discussion in THF/water system, compact vesicles can be attributed to the less stiff interface of the more densely packed helices and its corresponding segments length. In this section, the micelle morphologies of PNIPAm-*b*-PZLys in both DMF/water and THF/water system are characterized. These amphiphilic hybrid rod-coil block copolymers are able to form well-defined universal morphologies upon varying copolymer compositions and the helicogenic common solvents.

2-3.6 Hierarchical Self-Assembly structure of PNIPAm-*b*-PZLys rod-coil block copolymer in solid state

Almost thirty years ago, Gallot *et al.*[42] investigated the solid state behavior of polyvinyl-*b*-polypeptide rod-coil diblock copolymers by small-angle X-ray scattering (SAXS). They found a large-scale hexagonal-in-lamellar morphology of the alternating polyvinyl and polypeptide sheets with the α-helical polypeptide chains arranged in a hexagonal array. In order to investigate this new polypeptide-based rod-coil copolymer, synchrotron SAXS, wide-angle X-ray scattering (WAXS), and TEM techniques were used to examine solid state nano-domain morphology and the polypeptide secondary structure. SAXS and WAXS spectra for the $PNIPAm_{90}$-*b*-$PZLys_{71}$ are shown in Figure 2-14. For SAXS pattern in Figure 2-14a, orders of sharp reflection with relative positions 1:2:3 indicate a very high quality of lamellar microphase separation structure with nano-domain distance of 27.3nm. The WAXS pattern can be used to identify the secondary polypeptide structure. The WAXS curve in Figure 2-14b exhibits PZLys peaks with relative positions $1:\sqrt{3}:\sqrt{4}$ corresponding to hexagonally packed of α-helices secondary structures. The set of diffraction peaks at the largest reflection (~0.43 $Å^{-1}$) corresponds to a *d* spacing of ~14.7 Å which can be attributed to the inter-columnar distance of PZLys chains into a columnar hexagonal lattice. The reflection at 11.5 $Å^{-1}$ corresponds to the pitch of the helix of 5.4 Å. The broad "amorphous halo" centered around 14.1 $Å^{-1}$ (with a corresponding average distance of 4.5 Å) carries a large fraction of the diffracted intensity originating form the long amorphous side chains. In order to gain more information about the structural details, the morphology was also analyzed by TEM to gain the conformation of a single block copolymer chain. In Figure 2-15a, the lamellar morphology was observed and the maximum length of the α-helices (1.5 Å × 71 = 106.5 Å) is comparable to the thickness of poly(Z-L-lysine) layer in TEM graph. This would indicate that the helices are not stacked but are rather interdigitated or rarely folded.[43] This could be attributed to the polypeptide

α-helices produce a strong electric dipole moment along the molecule axis, both interdigitation and helix folding are ways to minimize the energy of the superstructure of helices. The schematic representation of the expected structure is shown in Figure 2-15b. On the basis of these results, the self-assembly structure is a lamellar-in-hexagonal (LH) morphology, referring to the local hexagonal packing of the α-helical polypeptide chains and the phase segregation into a lamellar structure.

2-3.7 Stimuli-responsive behavior of PNIPAm-*b*-PLys diblock copolymer in aqueous solution

^{1}H NMR spectroscopy was used to investigate the dual stimuli-responsive behavior of $PNIPAm_{197}$-*b*-$PLys_{44}$. Upon dissolution of the diblock copolymer in basic or thermal D_2O solution, conformation changed spontaneously as demonstrated by ^{1}H NMR. Spectra of the diblock copolymer were obtained in basic (pH ≈ 13, NaOD/D_2O) or thermal condition at 45 °C and compared with that in neutral D_2O at 25 °C (Figure 2-16a). Under basic condition, the protonated ($-NH_3^+$) poly(L-lysine) block is transformed into neutral and insoluble $-CH_2-NH_2$ groups supported by observation of several chemical shifts. The signal at 2.92 ppm ($-C\underline{H}_2-NH_3^+$) appeared in neutral D_2O becomes a weak intensity at 2.54 ppm, and the α-methine protons of PLys (COC*H*NH) at 4.2 ppm almost completely disappears, indicating that its secondary conformation changes from a charged coil to a neutral and compact α–helical structure, while the PNIPAm segment remains fully solvated. These phenomena are in line with the results previously reported for coil-helix transition of poly(L-lysine).[44] Similarly, when the temperature is elevated up to 45 °C, the signal at 3.81 ppm and 1.06 ppm, corresponding to the PNIPAm methine and methyl protons peak intensity, become attenuated relative to the PLys methylene peak. Although the mechanism for the LCST behavior is complex, it is generally accepted that the LCST behavior or phase transition of NIPAM-based

polymers is associated with the dehydration of the chains, which leads to a more compact structure.[45] Figure 2-16b depicts the proposed model of the dual stimuli-responsive structure.

2-4 Conclusion

We have demonstrated that an amide-linkage hetero-functional initiator was successfully synthesized which allows polymerization to be conducted consecutively by atom transfer radical polymerization then the amine hydrochloride mediated ring opening polymerization of α-amino acid *N*-carboxyanhydrides. Well-defined poly(*N*-isopropylacrylamide)-*b*-poly(Z-L-lysine) was obtained and the protective Cbz-group was successfully removed without cleavage of the block copolymer. We found that the amphiphilic hybrid rod-coil block copolymers were able to form various well-defined universal morphologies including micelles-spherical micelles, wormlike micelles, and vesicles by varying either the copolymer compositions on the helicogenic common solvents. On the basis of synchrotron SAXS, WAXS, and TEM results, we have confirmed the formation of the hierarchical lamellar-in-hexagonal self-assembly structure in $PNIPAm_{90}$-*b*-$PZLys_{71}$ at solid state. By removing the protective Cbz-group, the dual stimuli-responsive behaviors of the PNIPAm-*b*-PLys were investigated by nuclear magnetic resonance spectroscopy in aqueous solution. Coil-to-helix and coil-globule transitions occur by changing the environmental conditions, by elevating the temperature or changing the pH value.

This work has demonstrated the feasibility of using hetero-functional amide linkage initiator to synthesize hybrid block copolymers which both segments are able to response to environmental changes. In the effort to expand potential applications, these results presented here provide a versatile method toward designing polymers to impart stimuli-responsive functionalities.

References

1. Hamley, I. W. *Angew. Chem., Int. Ed.* **2003**, *42*, 1692-1712.
2. Ambade, A. V.; Savariar, E. N.; Thayumanavan, S. *Mol. Pharm.* **2005**, *2*, 264-272.
3. Elbert, D. L.; Herbert, C. B.; Hubbell, J. A. *Langmuir* **1999**, *15*, 5355-5362.
4. Cai, Q.; Zeng, K.; Ruan, C.; Decai, T. A.; Grimes, C. A. *Anal. Chem.* **2004**, 76, 4038-4043.
5. Schild, H. G. *Prog. Polym. Sci.* **1992**, *17*, 163-249.
6. Poe, G. D.; Jarrett, W. L.; Scales, C. W.; McCormick, C. L. *Macromolecules* **2004**, *37*, 2603.
7. Virtanen, J.; Arotcarena, M.; Heise, B.; Ishaya, S.; Laschewsky, A.; Tenhu, H. *Langmuir* **2002**, *18*, 5360-5363.
8. (a) Bellomo, E.; Wyrsta, M. D.; Pakstis, L.; Pochan, D. J.; Deming, T. J. *Nat. Mater.* **2004**, *3*, 244-248. (b) Holowka, E. P., Pochan, D. J., Deming, T. J. *J. Am. Chem. Soc.* **2005**, *127*, 12423-12428. (c) Rodríguez-Hernández, J.; Lecommandoux, S. *J. Am. Chem. Soc.* **2005**, *127*, 2026-2027. (d) Nowak, A. P.; Breedveld, V.; Pakstis, L.; Ozbas, Bl.; Pine, D. J.; Pochan, D.; Deming, T. J. *Nature* **2002**, *417*, 424-428.
9. Mart, R. J.; Osborne, R. D.; Stevens, M. M.; Ulijn, S. V. *Soft Matter* **2006**, *2*, 822-835.
10. Schlaad, H.; Antonietti, M. *Eur. Phys. J. E* **2003**, *10*, 17-23.
11. (a) Babin, J.; Rodríguez- Hernández, J.; Lecommandoux, S.; Klok, H.-A.; Achard, M.-F. *Faraday Discuss.* **2005**, *128*, 179-192. (b) Chécot, F.; Lecommandoux, S.; Gnanou, Y.; Klok, H.-A. *Angew. Chem. Int. Ed.* **2002**, *41,* 5752-5784. (c) Börner, H. G.; Schlaad, H. *Soft Matter* **2007**, *3*, 394-408. (d) Gebhardt, K. E., Ahn, S.; Venkatachalam, G.; Savin, D. A. *Langmuir* **2007**, *23*, 2851-2856.
12. Kricheldorf, H. R. *Angew. Chem. Int. Ed.* **2006**, *45*, 5752-5784.
13. Deming, T. J. *J. Polym. Sci. Part A: Polym. Chem.* **2000**, *38*, 3011-3018.

14. (a) Deming, T. J. *Nature* **1997**, 390, 386-389. (b) Deming, T. J. *Adv. drug deliv. rev.* **2002**, *54*, 1145-1155.

15. Brzezinska, K. R.; Deming, T. J. *Macromolecules*, **2001**, *34*, 4348–4354.

16. Aliferis, T.; Iatrou, H.; Hadjichristidis, N. *Biomacromolecules* **2004**, *5*, 1653-1656.

17. Dimitrov, I.; Schlaad, H. *Chem. Commun.*, **2003**, *23*, 2944-2945.

18. (a) Dimitrov, I.; Kukula, H.; Cölfen, H.; Schlaad, H. *Macromol. Symp*. **2004**, *215*, 383-393. (b) Lutz, J.-F.; Schutt, D.; Kubowicz, S. *Macromol. Rapid Commun.* **2005**, *26*, 23-28. (c) Meyer, M.; Schlaad, H. *Macromolecules*, **2006**, *39*, 3967-3970. (d) Dimitrov, I.; Berlinova, I. V.; Vladimirov, N. G. *Macromolecules*, **2006**, *39*, 2423-2426.

19. (a) Matyjaszewski, K. *Prog. Polym. Sci.* **2005**, *30*, 858-875. (b) Braunecker, W. A.; Matyjaszewski, K. *Prog. Polym. Sci.* **2007**, *32*, 93-146. (c) Matyjaszewski, K.; Xia, J. *Chem. Rev.* **2001**, *101*, 2921- 2990. (c) Kamigaito, M.; Ando, T.; Sawamoto, M. *Chem. Rev.* **2001**, *101*, 3689-3746.

20. Bernaerts, K. V.; Du Prez, F. E. *Prog. Polym. Sci.* **2005**, *30*, 858-875.

21. Rao, J.; Luo, Z.; Ge, Z.; Liu, H.; Liu, S. *Biomacromolecules* **2007**, *8*, 3871-3878.

22. Schild, H. G. *Prog. Polym. Sci.* **1992**, *17*, 163-249.

23. Xia, Y.; Yin, X.; Burke, N. A. D.; Stover, H. D. H. *Macromolecules* **2005**, *38*, 5937-5943.

24. Hawker, C. J.; Bosman, A. W.; Harth, E. *Chem. Rev.* **2001**, *101*, 3661-3688.

25. (a) Ray, B.; Isobe, Y.; Matsumoto, K.; Habaue, S.; Okamoto, Y.; Kamigaito, M.; Sawamoto, M. *Macromolecules* **2004**, *37*, 1702-1710. (b) Convertine, A. J.; Ayres, N.; Scales, C. W.; Lowe, A. B.; McCormick, C. L. *Biomacromolecules* **2004**, *5*, 1177-1180.

26. Poché, D.; Moore, M.; Bowles, J. *Synth. Commun.* **1999**, *29*, 843–854.

27. Ciampolini, M.; Nardi, N. *Inorg. Chem.* **1966**, *5*, 41–44.

28. Baek, K.-Y.; Kamigaito, M.; Sawamoto, M. *J. Polym. Sci., Part A: Polym. Chem.* **2002**, *40*, 1937-1944.

29. (a) Xu, F. J.; Zhong, S. P.; Yung, L. Y. L.; Kang, E. T.; Neoh, K. G. *Biomacromolecules* **2004**, *5*, 2392-2403. (b) Limer, A.; Haddleton, D. M, *Macromolecules* **2006**, *39*, 1353-1358. (c) Venkataraman, S.; Wooley, K. L. *Macromolecules* **2006**, *39*, 9661-9664.

30. (a) Neugebauer, D.; Mtyjaszewski, K. *Macromolecules* **2003**, *36*, 2598-2603. (b) Masci, G.; Giacomelli, L.; Crescenzi, V. *Macromol. Rapid Commun.* **2004**, *25*, 559-564. (c) Teodorescu, M.; Mtyjaszewski, K. *Macromol. Rapid Commun.* **2000**, *21*, 190-194.

31. Matyjaszewski, K.; Shipp, D. A.; Wang, J.-L.; Grimaud, T.; Patten, T. E. *Macromolecules* **1998**, *31*, 6836-6840.

32. Fischer, H. *Chem Rev.* **2001**, *101*, 3581-3610.

33. (a) Tang, W.; Matyjaszewski, *Macromolecules* **2006**, *39*, 4953-4959. (b) Tang, W.; Matyjaszewski, *Macromolecules* **2007**, *40*, 1858-1863.

34. Matyjaszewski, K.; Nakagawa, Y.; Gaynor, S. G. *Macromol. Rapid Commun.* **1997**, *18*, 1057.

35. Harrisson, S.; Wooley, K. L. *Polym. Prep.* **2004**, *45*, 545-546.

36. Postma**,** A**.;** Davis, T. P.; Moad, G.; O'Shea, M. S. *React. Funct. Polym.* **2006**, *66*, 137-147.

37. Schlaad, H. *Adv. Polym. Sci.* **2006**, *202*, 53-73.

38. (a) Naka, K.; Yamashita, R.; Nakamura, T.; Ohki, A.; Maeda, S. *Macromol. Chem. Phys.* **1997**, *198*, 89-100. (b) Cheon, J. B.; Jeong, Y. I.; Cho, C. S. *Polymer* **1999**, *40*, 2041-2050. (c) Toyotama, A.; Kugimiya, S. I.; Yamanaka, J.; Yonese, M. *Chem.*

Pharm. Bull. **2001**, *49*, 169-172. (d) Tang, D.; Lin, J.; Lin, S.; Zhang, S.; Chen, T.; Tian, X. *Macromol. Rapid Commun.* **2004**, *25*, 1241-1246. (e) Dong, C. M.; Sun, X. L.; Fauche, K. M.; Apkarian, R. P.; Chaikof, E. L. *Biomacromolecules* **2004**, *5*, 224-231.

39. Ishimuro, Y.; Hamada, F.; Nakajima, A. *Macromolecules* **1978**, *11*, 382-387.
40. (a) He, Y.; Li, Z.; Simone, P.; Lodge, T. P. *J. Am. Chem. Soc.* **2006**, *128*, 2745-2750. (b) Bhargava, P.; Zheng, J. X.; Li, P.; Quirk, R. P.; Harris, F. W.; Cheng, S. Z. D. *Macromolecules* **2006**, *39*, 4880-4888.
41. Zhang, L.; Eisenberg, A. *Polym. Adv. Technol.* **1998**, *9*, 677-699.
42. (a) Billot, J. P.; Douy, A.; Gallot, B. *Makromol. Chem.* **1976**, *177*, 1889-1893. (b) Billot, J. P.; Douy, A.; Gallot, B. *Makromol. Chem.* **1977**, *178*, 1641-1650.
43. Douy, A.; Gallot, B. *Polymer* **1982**, *23*, 1039-1044.
44. Bradbury, E. M.; Crane-Robinson, C.; Goldman, H.; Rattle, H. W. E. *Biopolymers* **1968**, *6*, 851-862.
45. Ono, Y.; Shikata, T. *J. Am. Chem. Soc.* **2006**, *128*, 10030-10031.

Scheme 2-1: Synthesis of phthalimidoethyl 2-bromo-2-methylpropionamide hetero-functional initiator (2)

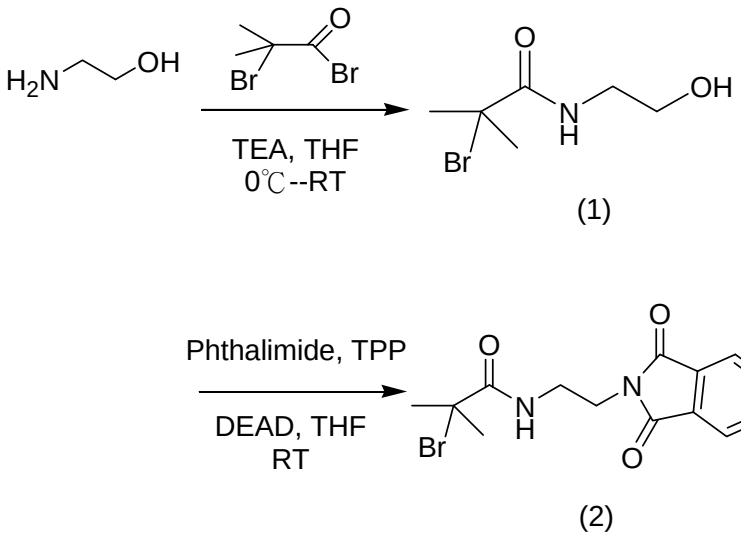

Scheme 2-2: Synthesis of poly(*N*-isopropylacrylamide)-*b*-polypeptides

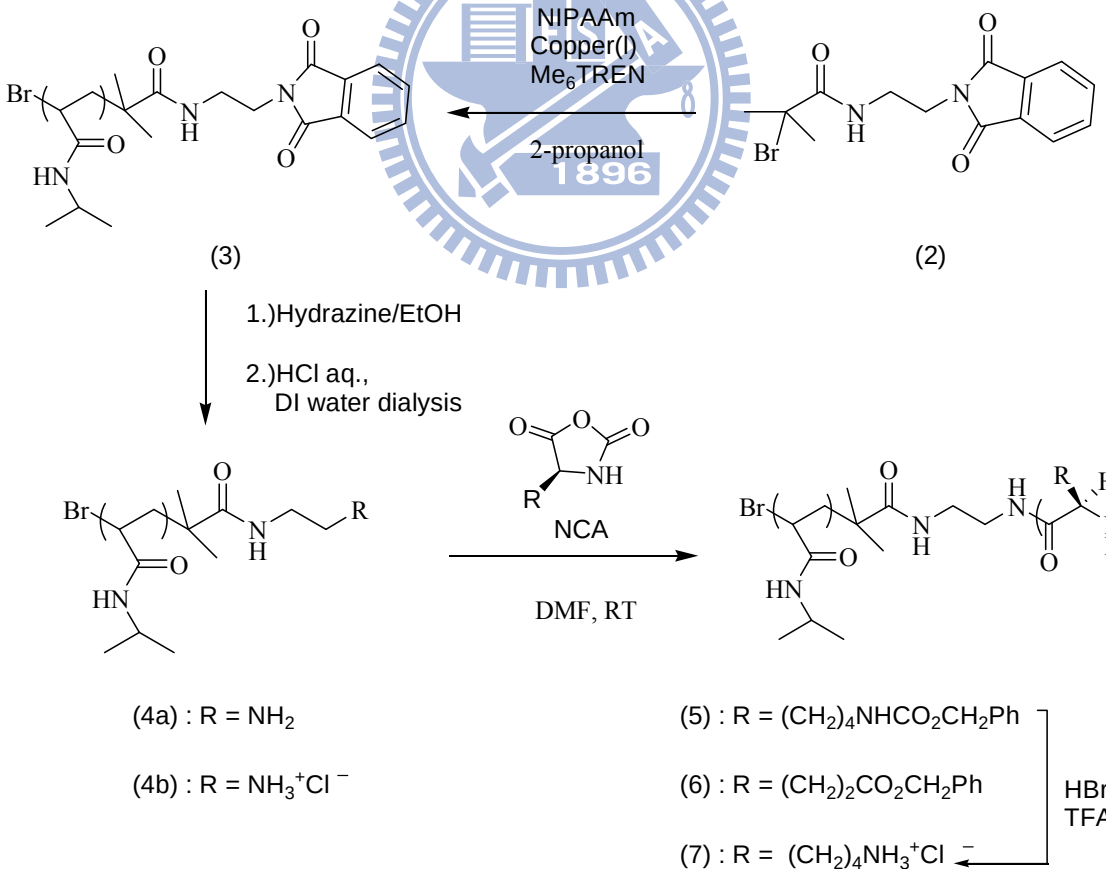

Table 2-1: Experimental Conditions and Properties of PNIPAm Prepared by ATRP: Effect of Catalyst and Temperature.

Entry	Monomer/ Initiator	Catalyst	Temp. °C	Time min	Conv.[b] %	*M*n NMR[c]	*M*n GPC	M_w/M_n
1[a]	250/1	CuBr	20 °C	70	56.19	15874	17747	1.31
2[a]	250/1	CuCl	20 °C	250	70.25	19846	19379	1.32
3[a]	250/1	CuBr	0 °C	720	63.88	18046	18444	1.12

[a] Ratio of reactants: $[NIPAm]_0/[PIBrPA]_0/[Cu(I)]_0/[Me_6TREN]_0$=250/1/1/1; $[NIPAm]_0$ = 3.473M, in 2-propanol (2.0 weight equiv vs. monomer). [b] Monomer conversion was determined from the ^{1}H NMR integration ratio of the monomer double bond at 5.5 ppm to polymer peak at 3.8 ppm in DMSO-d_6. [c] $M_{n,NMR}$ = $([NIPAm]_0/[PIBrPA]_0)$ × conversion $\times M_{monomer}$.

Table 2-2: Results of Synthesis Diblock Copolymers PNIPA-*b*-PZLys and PNIPAm-*b*-PBLG

PNIPAm-*b*-PZLys[a]								
Macroinitiator [MI]			[Z-L-Lys NCA]$_0$/				unit ratio	
expt	DP[b]	M_w/M_n	[MI]$_0$	time(hr)	yield(%)	M_n	m:n	M_w/M_n
1	90	1.12	45	80	80	18515	90:38	1.19
2	90	1.12	90	35	75	28118	90:71	1.26
PNIPAm-*b*-PBLG[a]								
Macroinitiator [MI]			[BLG NCA]$_0$/				unit ratio	
expt	DP[b]	M_w/M_n	[MI]$_0$	time(hr)	yield(%)	M_n	m:n	M_w/M_n
3	90	1.12	45	20	78	9327	90:37	1.39
4	90	1.12	90	45	58	13025	90:55	1.43

[a] Polymerization at 20 °C in DMF (~9 wt%). [b] Calculated from the ratio of the integral of the amide methylene and methine protons peak by ^{1}H NMR.

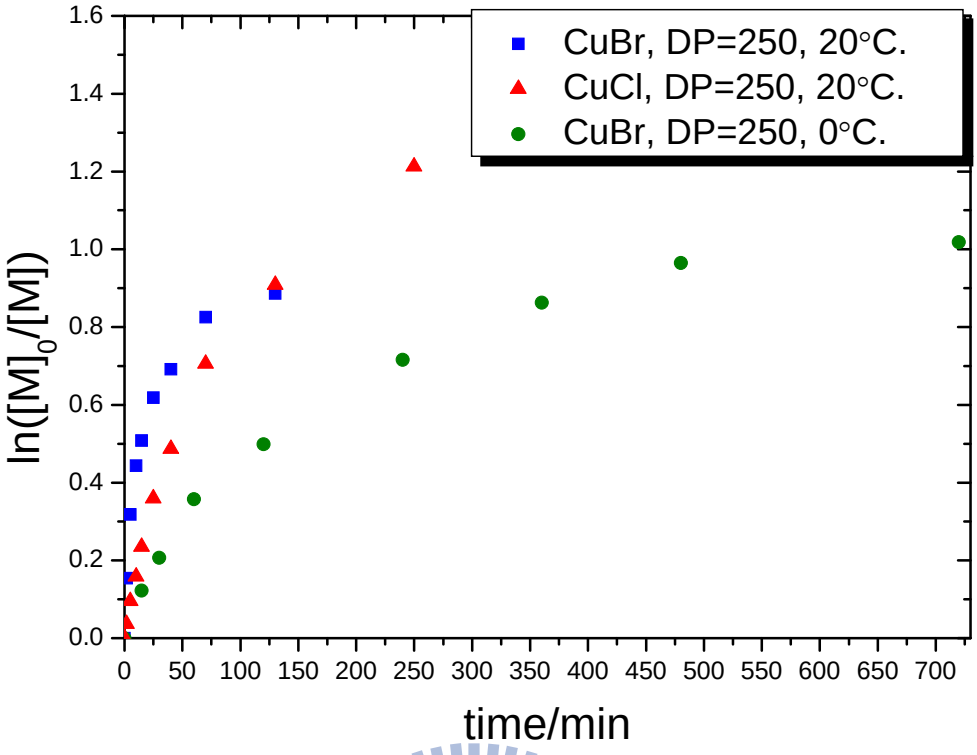

Figure 2-1: Kinetic plots for the polymerization of NIPAm at different temperature and catalyzed by different copper catalyst.

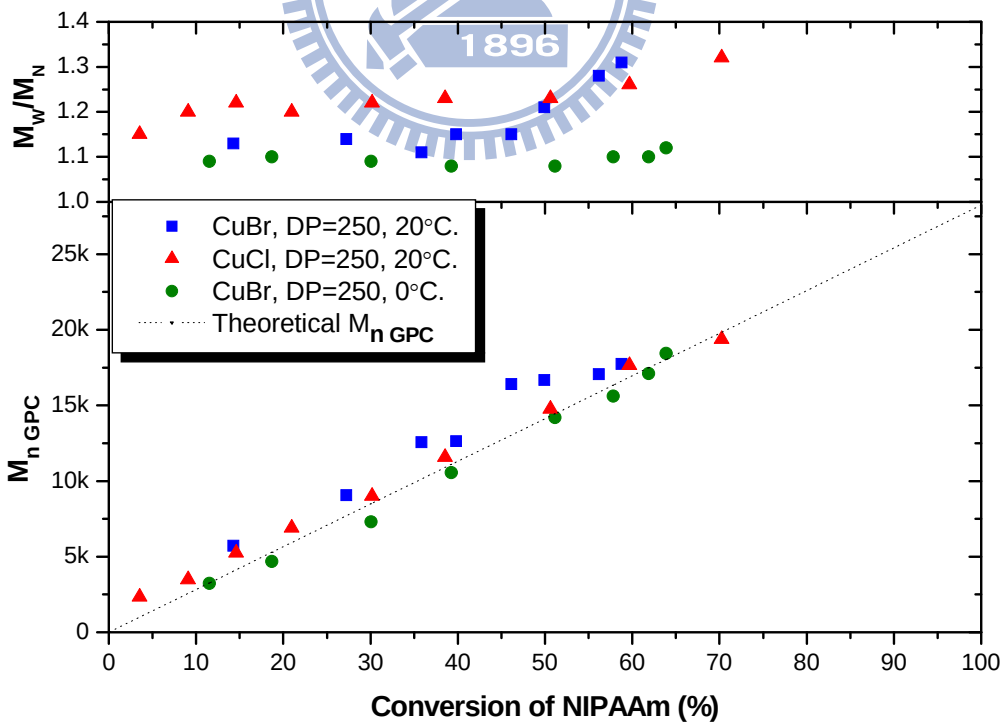

Figure 2-2: Molecular weights and polydispersities of PNIPAm as degree of conversion. Experimental conditions are given in Table 1.

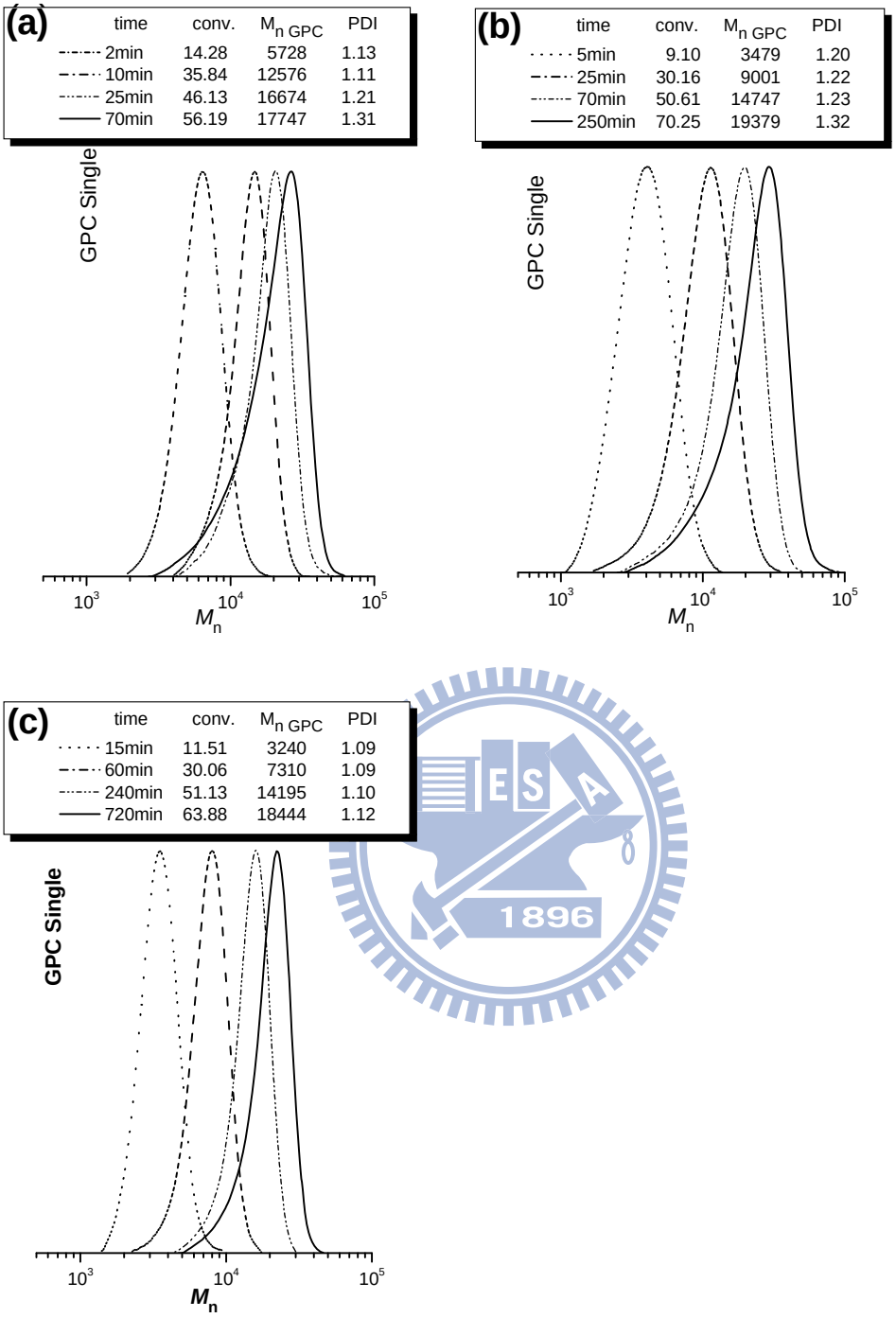

Figure 2-3: Evolution of the molecular weight GPC traces in different polymerization conditions (a) CuBr/20 °C, (b) CuCl/ 20 °C, and (c) CuBr/0 °C.

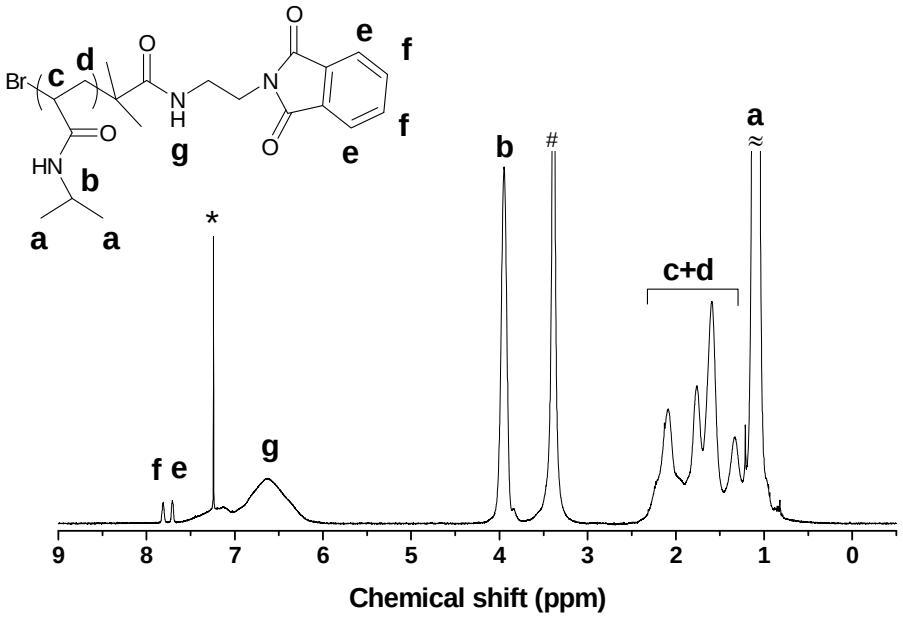

Figure 2-4: ^{1}H NMR spectrum of phthalimide end-capped poly(*N*-isopropylacrylamide) in $CDCl_3$ (*, $CDCl_3$; #, water).

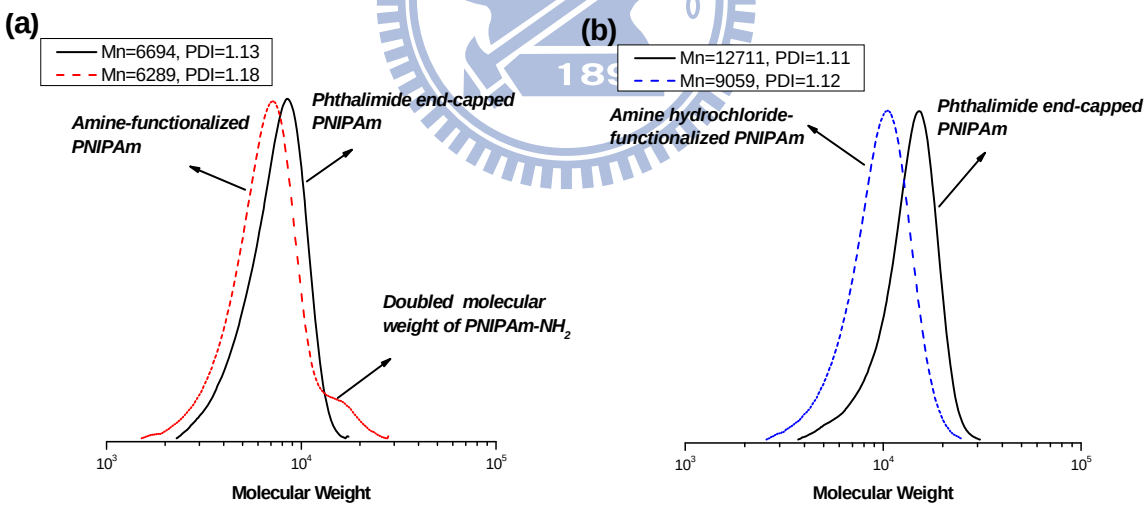

Figure 2-5: GPC profiles comparison of two macroinitiators: (a) PNIPAm-NH_2 dialyzed at ambient temperature 20 °C and (b) PNIPAm-$NH_3^+Cl^-$ dialyzed in cold water at 5 °C.

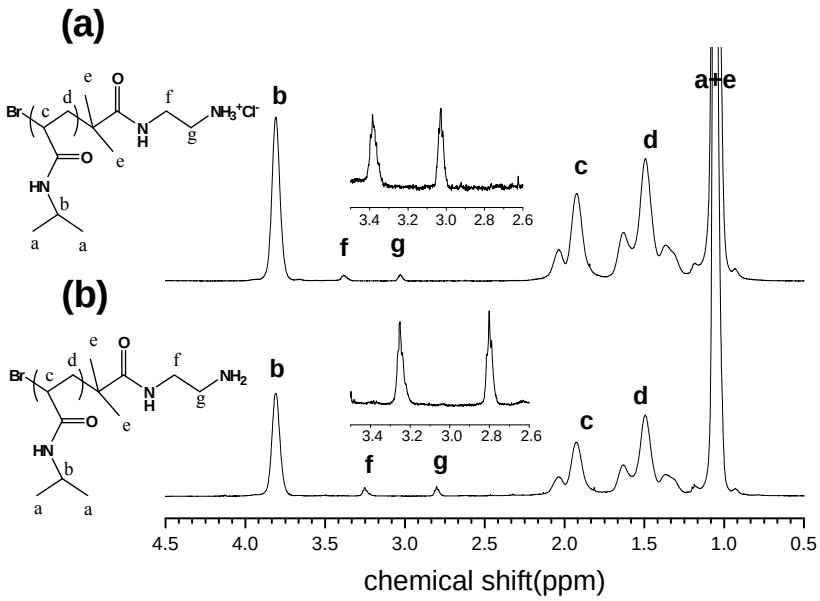

Figure 2-6: ^{1}H NMR spectra of (a) amine hydrochloride-functionalized PNIPAm macroinitiator and (b) amine-functionalized PNIPAm in D_2O at 25 °C; inset shows the amide methylene protons (f) and amine or amine hydrochloride methylene protons (g).

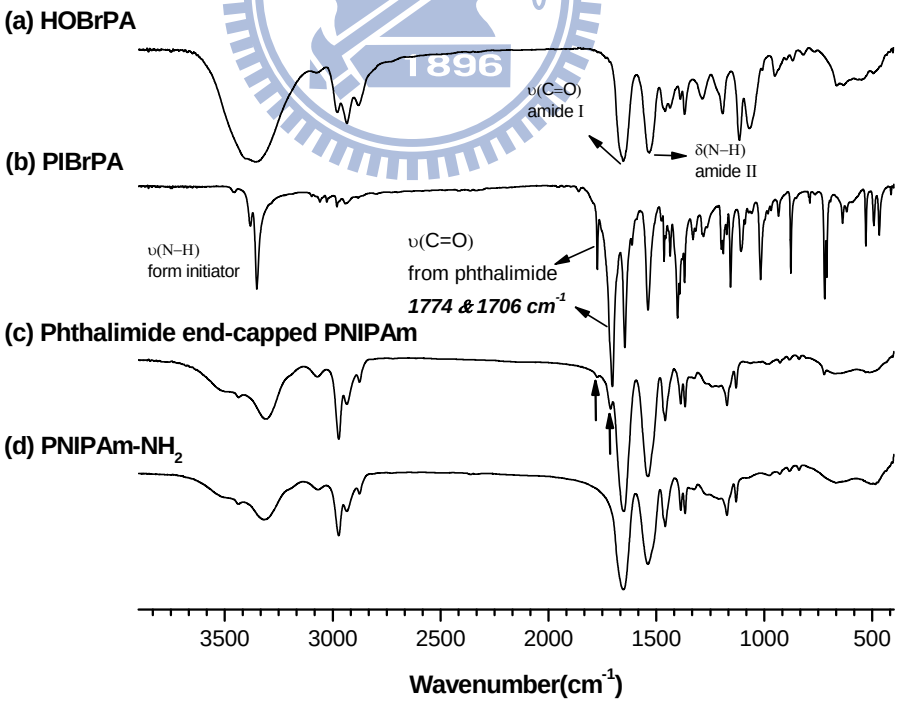

Figure 2-7: FT-IR spectra of (a) HOBrPA, (b) PIBrPA, (c) Phthalimide end-capped PNIPAm, and (d) PNIPAm-NH_2.

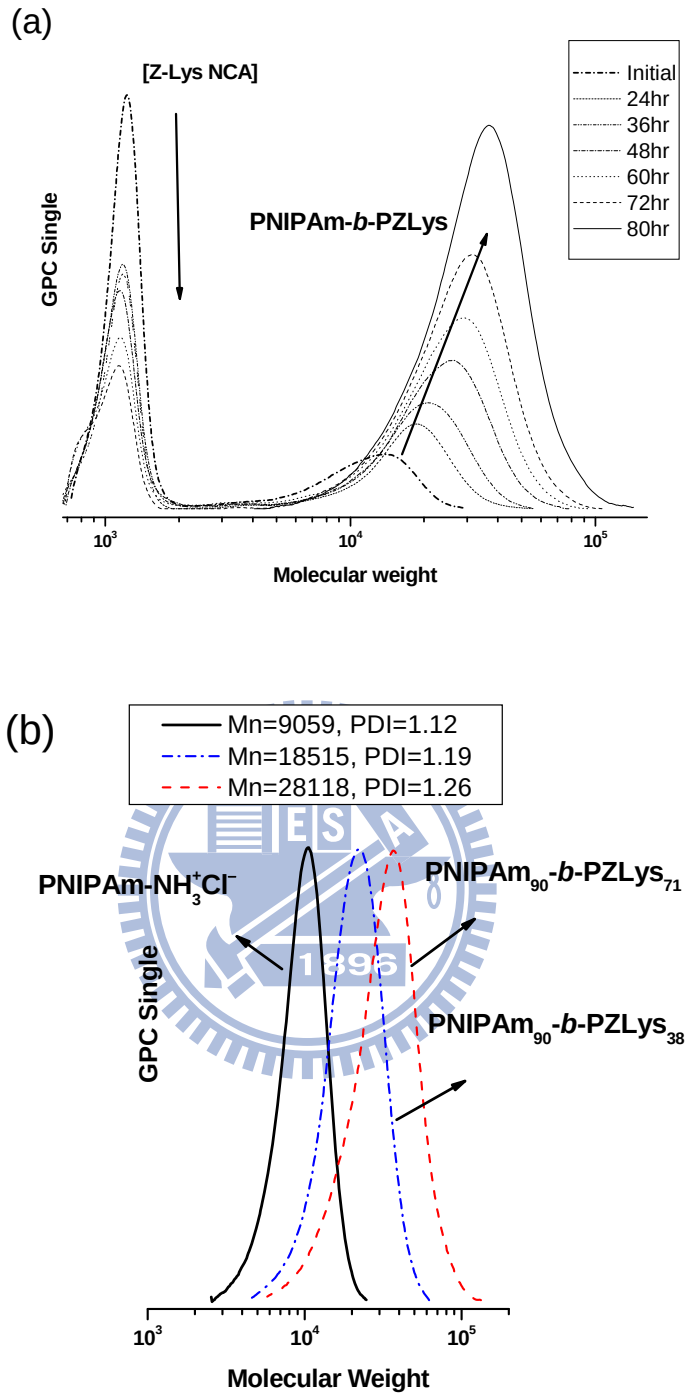

Figure 2-8: (a) GPC traces of monomer Z-Lys-NCA and PNIPAm$_{90}$-*b*-PZLys$_{90}$ (expt.2), (b) GPC signals of PNIPAm$_{90}$-*b*-PZLys$_{38}$, PNIPAm$_{90}$-*b*-PZLys$_{71}$, and PNIPAm-$NH_3^+Cl^-$ macroinitiator.

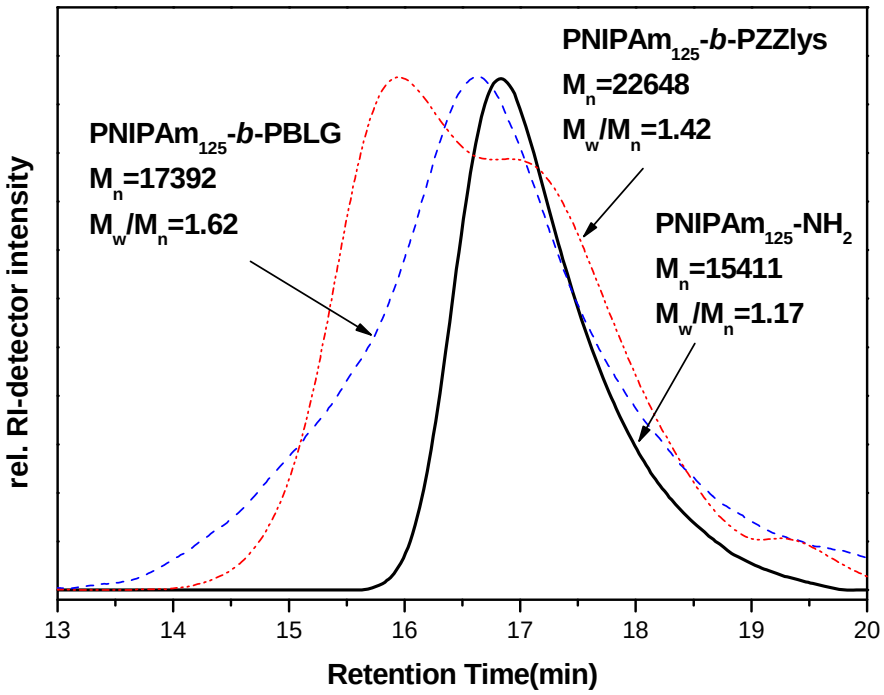

Figure 2-9: GPC signals of PNIPAm-*b*-polypeptides and amine-functionalized PNIPAm macroinitiator. Ratio of reactants: $[NIPAm]_0/[NCA]_0 = 1/100$.

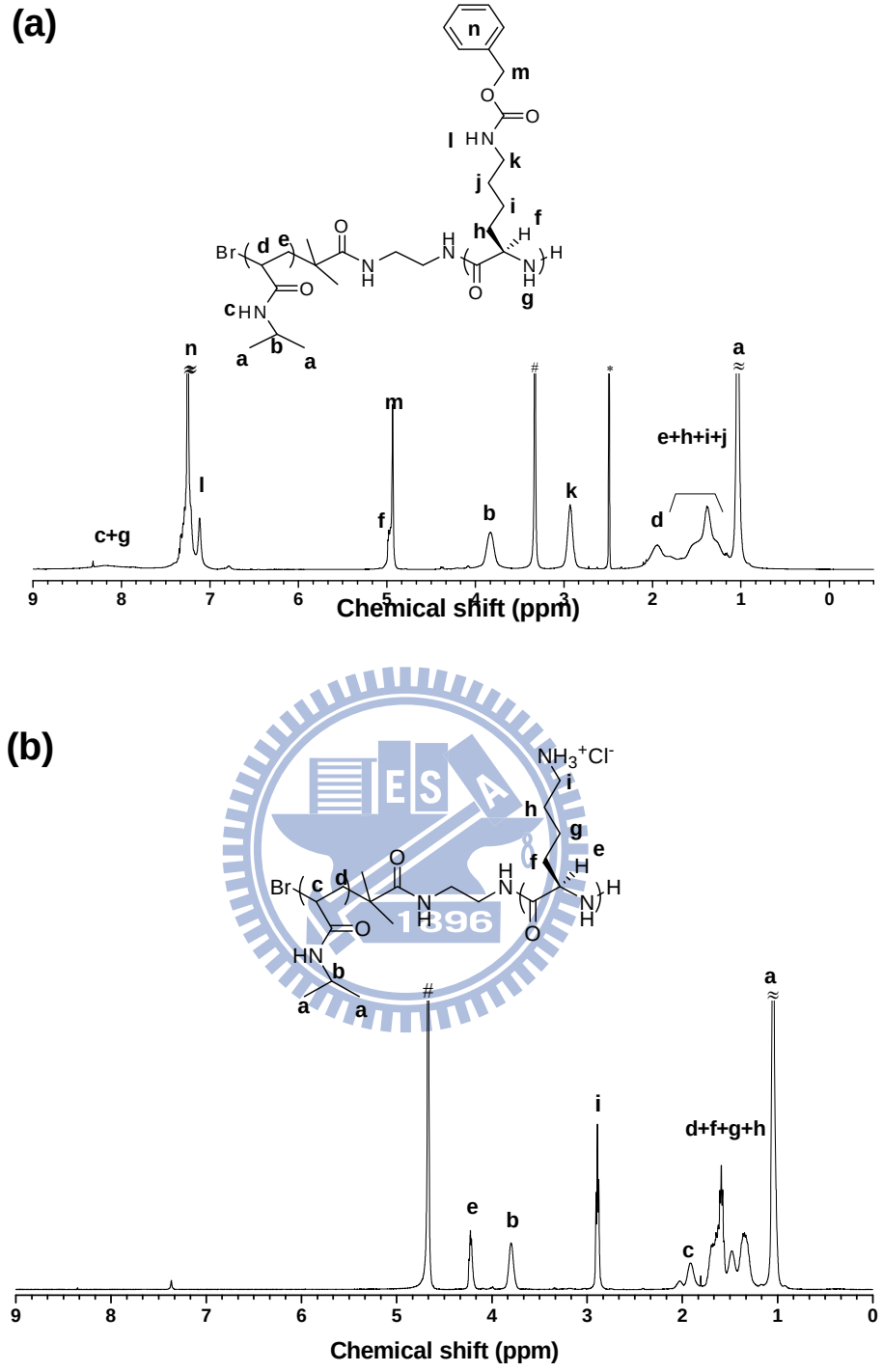

Figure 2-10: ^{1}H NMR spectra of (a) PNIPAm$_{90}$-*b*-PZLys$_{71}$ in dimethyl-d$_6$ sulfoxide at 25 °C and (b) PNIPAm$_{90}$-*b*-PLys$_{72}$ in D_2O at 25 °C (*, dimethyl sulfoxide; #, water).

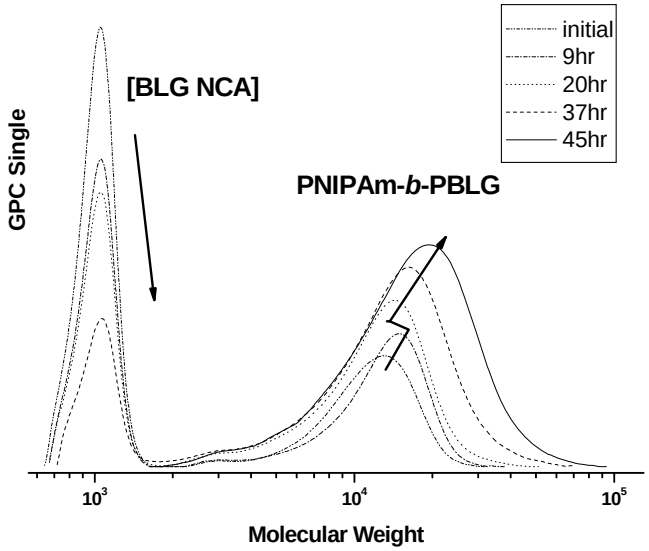

Figure 2-11: CPC traces of monomer BLG-NCA and PNIPAm$_{90}$-*b*-PBLG$_{90}$ (expt.4).

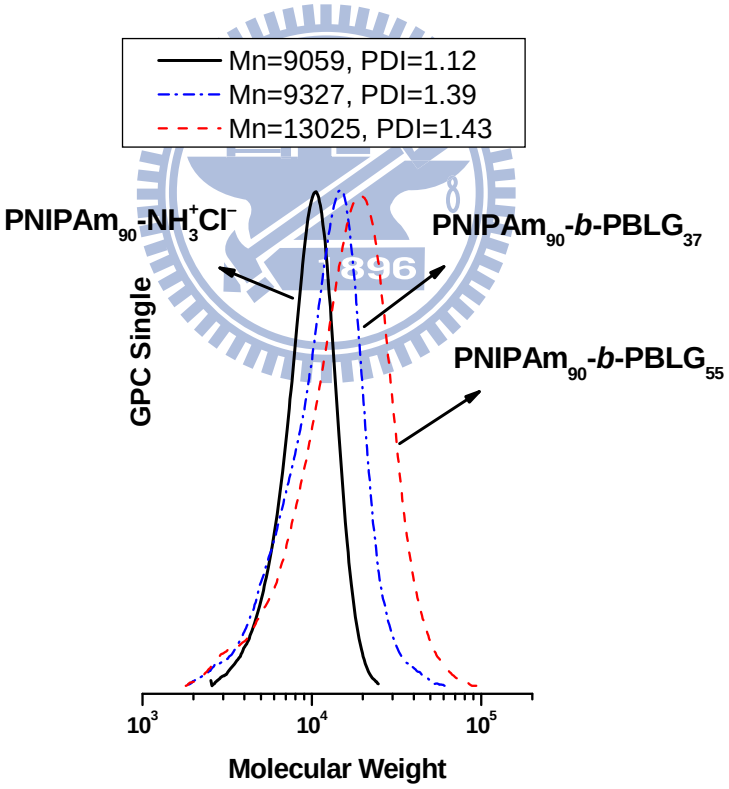

Figure 2-12: GPC signals of PNIPAm$_{90}$-*b*-PBLG$_{37}$, PNIPAm$_{90}$-*b*-PBLG$_{55}$ and PNIPAm-$NH_3^+Cl^-$ macroinitiator.

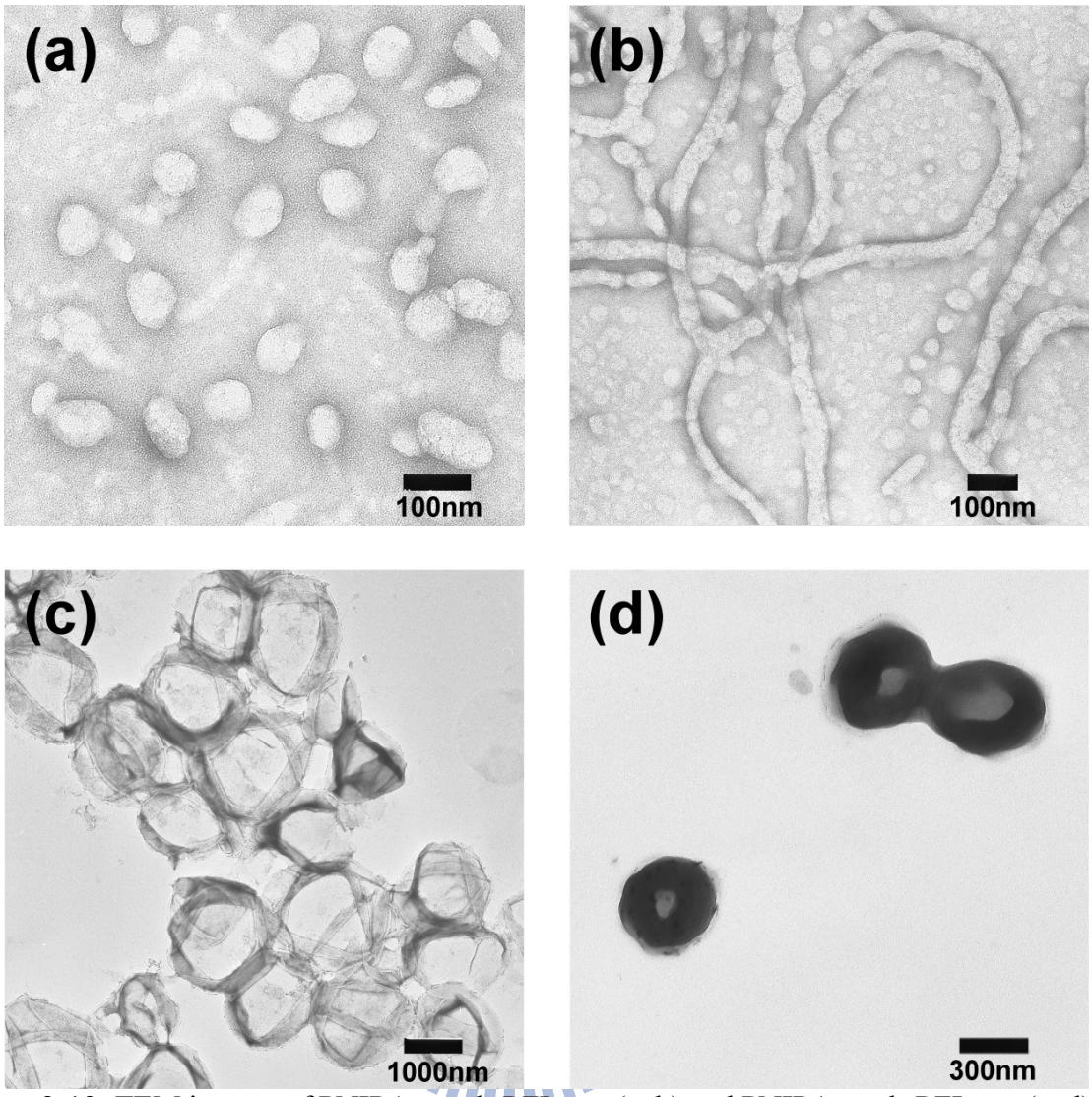

Figure 2-13: TEM images of $PNIPAm_{197}$-b-$PZLys_{44}$ (a, b) and $PNIPAm_{90}$-b-$PZLys_{71}$ (c, d). (a) a spherical micelles morphology, (b) a mixed spherical and wormlike micelles morphology, (c) a giant vesicles morphology, and (d) a compact vesicles morphology.

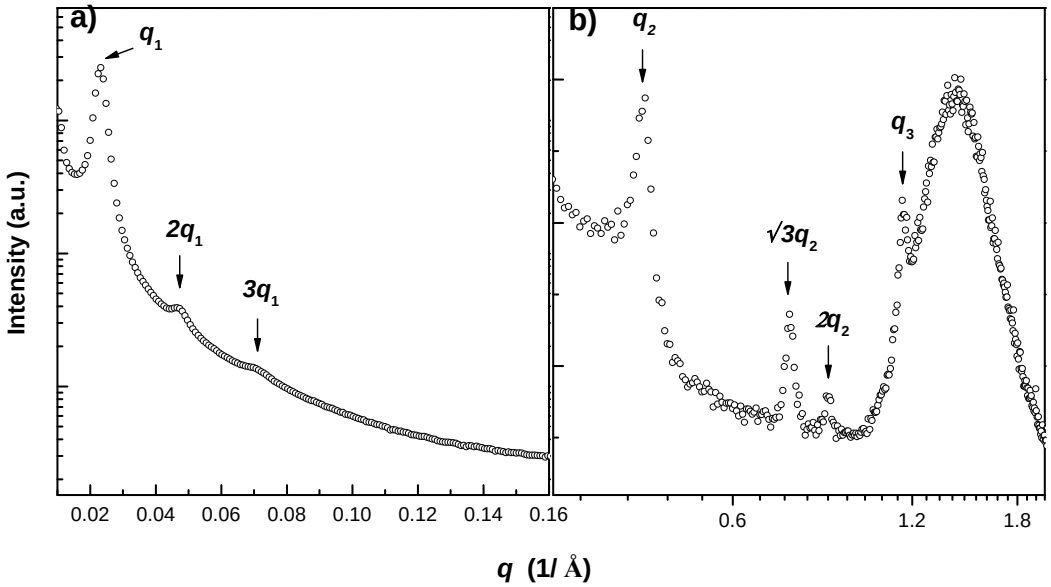

Figure 2-14: (a) SAXS and (b) WAXS patterns of the PNIPAm$_{90}$-*b*-PZLys$_{71}$ recorded at room temperature.

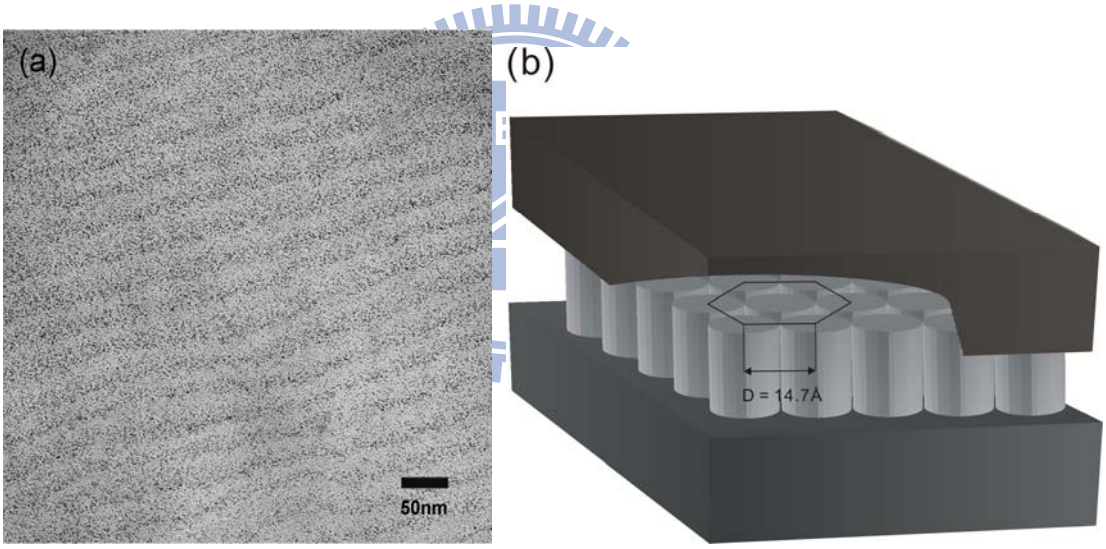

Figure 2-15: (a) TEM image of the PNIPAm$_{90}$-*b*-PZLys$_{71}$ lamellar phase separation morphology. Note that polypeptide regions appear black due to staining with RuO_4. (b) Proposed schematic representation of the hexagonal-in-lamellar solid-state morphology of PNIPAm-*b*-PZLys block copolymer.

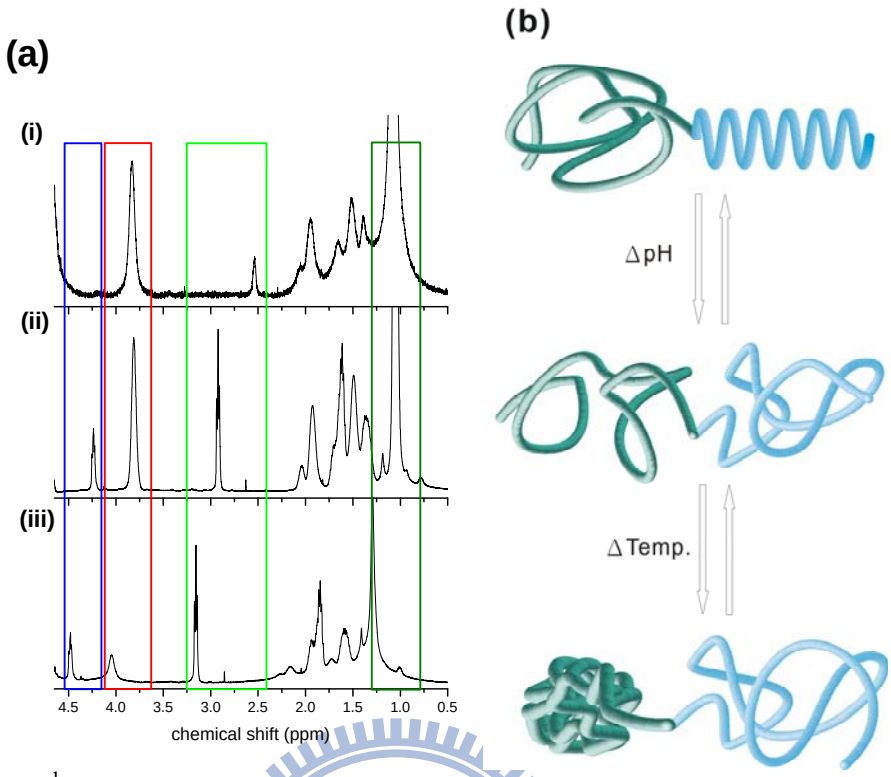

Figure 2-16: (a) ^{1}H NMR spectra recorded in D_2O: (i) $PNIPAm_{197}$-*b*-$PLys_{44}$ at pH＝13, (ii) $PNIPAm_{197}$-*b*-$PLys_{44}$ at pH＝7, and (iii) $PNIPAm_{197}$-*b*-$PLys_{44}$ at 45 °C. (b) Proposed schematic representation of the $PNIPAm_{197}$-*b*-$PLys_{44}$ stimuli-responsive behavior of the pH-induced coil-to-helix and thermo-induced coil-to-globule transition in aqueous solution.

Chapter 3

Using Click Chemistry to Fabricate Ultrathin Thermoresponsive Microcapsules through Direct Covalent Layer-by-Layer Assembly

Abstract

We report the syntheses of azido- and acetylene-functionalized poly(*N*-isopropylacrylamide) (PNIPAm) copolymers and their use in the fabrication of ultrathin thermoresponsive microcapsules through direct covalent layer-by-layer (LbL) assembly using click chemistry. The clickable copolymers poly[*N*-isopropylacrylamide-*co*-(trimethylsilyl)propargyl acrylamide] and poly(*N*-isoropylacrylamide-*co*-3-azideopropylacrylamide) were prepared through atom transfer radical polymerization (ATRP) at 0 °C using a synthesized dansyl-labeled initiator and the CuBr/Me_6TREN (hexamethylated tris[2-(dimethylamino)ethyl]amine) catalyst complex in 2-propanol. After removing the protective trimethylsilyl groups, these clickable PNIPAm copolymers assemble alternately onto azido-modified silica particles in aqueous media through click reactions catalyzed by copper sulfate and sodium ascorbate. After removing the template, the microcapsules remained stable because of the presence of the covalently bonded triazole units; the microcapsules exhibited thermoresponsive and thermo-reversible swelling/de-swelling behaviors upon changing the temperature of the medium. Adjusting the number of clickable functionalities resulted in changes to the degree of cross-linking, thereby allowing control over the surface morphology and thickness of the covalently stabilized PNIPAm multilayer thin films. The microcapsules fabricated close to the lower critical solution temperature of

PNIPAm exhibited extremely low surface roughnesses and thick multilayer films as a result of their compact chain conformation in aqueous solution, leading to tighter packing of the PNIPAm structure. We further post-functionalized the surface of the multilayer thin film through click reactions with an azido-modified lissamine rhodamin dye to demonstrate the feasibility of further modification with potentially useful functionalities. Finally, preliminary study on the permeability of microcapsules was presented by using different molecular weigh tetramethylrhodamine isothiocyanate (TRITC)-labelled dextran and rhodamine 6G as probe molecules and the results revealed that the microcapsules with tighter packing wall are selectively permeable to molecules and show potential applications for the encapsulation of variety of materials.

3-1 Introduction

In recent years, functional hollow spheres — referred to as capsules or vesicles — with well-defined structures and tailorable properties have attracted intense research interest because of the variety of their potential applications, such as in delivery vesicles for drugs,[1] protection shield for proteins, enzymes, and DNA,[2] and catalysis.[3] For many potential applications, microcapsules that are environmentally sensitive to light,[4] temperature,[5] or pH[6] are required to control the transport and delivery of guest materials into their hollow spheres.

For over a decade, the layer-by-layer (LbL) assembly has been a versatile method for the fabrication of hollow capsules.[7] Since its first introduction in the early 1990s,[8] the LbL method has been widely used to deposit multilayers of various materials (e.g. peptides, oligonucleotides, and inorganic nanoparticles) onto colloidal supports.[9] Typically, LbL films are assembled through the alternate deposition of oppositely charged polyelectrolytes (PEs), with the buildup primarily facilitated through electrostatic forces. After the formation of PEs multilayers, the templates are removed to yield hollow capsules. So far, the field of LbL assembly has expanded to include films prepared using other non-electrostatic interactions — such as hydrogen bonding,[10] host-guest interactions,[11] and hybridization of DNA base pairs[12] — to fabricate hollow capsules.

The use of covalent bonds to assemble LbL films has several significant advantages over traditional assembly methods because the stability of the resulting cross-linked polymer networks makes them good candidates for special applications. Covalent assembly multilayers of planar substrates has been performed using a variety of reactions between different kinds of functional molecules.[13] These studies have confirmed the benefits of covalent bonding LbL assembly, providing systems that are stable under a range of conditions. For colloidal curved surfaces, post-modifications are often applied — through

oxidization,[14] UV-irradiation,[15] carbodiimide formation,[16] and glutaraldehyde modification[17] —to enhance the capsules' binding strength in multilayers. There are relatively few reports describing the use of the LbL method to directly deposit covalently bonded multilayer thin films onto the colloidal templates.[18]

Recently, direct covalent assembly on colloidal particles has been performed through the reactions of complementary functional polymers — for example, poly(allylamine hydrochloride) (PAH) and poly(glycidyl methylacrylate), which react through their amino and epoxide functionalities, respectively.[18a] Single component polyelectrolyte microcapsules have also been reported from the glutaraldehyde-mediated direct covalent assembly of PAH onto $MnCO_3$ particles.[18b] In addition, a novel method has been introduced to create pH-sensitive degradable capsules based on poly(methacrylic acid) cross-linked via disulfide linkages.[19] These strategies have opened the door to the fabrication of directly covalently bonded multilayer films.

Recently, a general click chemistry approach[20] for the direct covalent LbL assembly of polymer films onto particles has been developed to create a new class of ultrathin, single-component poly(acrylic acid) (PAA) pH-responsive microcapsules. The development of click chemistry[21] employing the highly efficient copper(I)-catalyzed Huisgen 1,3-dipolar cycloaddition[22] between azides and acetylenes affords superior regioselectivity and almost quantitative transformation under mild conditions with virtually no side reactions or byproducts. Moreover, the resultant aromatic 1,2,3-triazoles linkages are extremely stable making the reaction of particular interest for the formation of covalently linked multilayer thin films. This strategy suggests the potential of using click chemistry techniques for the direct covalent LbL assembly of polymer multilayers on colloidal templates and subsequent formation of single-component capsules.

Poly(*N*-isopropylacrylamide) (PNIPAm) is perhaps the most widely studied thermoresponsive polymer. In aqueous media, PNIPAm exhibits a lower critical solution temperature (LCST) of ca. 32 °C.[23] Below the LCST, the polymer is fully soluble in water because of the formation of hydrogen bonds between water molecules and the polymer's amide side chains. As the temperature is increased, the polymer undergoes a "coil-to-globule" phase transition[24] as a result of the disruption of these hydrogen bonds, as well as the release of hydrophobically structured water around the isopropyl groups. One of the earliest processes for making hollow thermo-sensitive spheres was developed by Zha et al. who used the colloid-templated polymerization of cross-linked PNIPAm shells on silica particles presenting polymerizable units on their surfaces; the subsequent hollow spheres were obtained after dissolving the silica particles in hydrofluoric acid (HF) solution.[25] Since then, many other techniques have been developed to fabricate thermoresponsive hollow spheres based on PNIPAm, including precipitation polymerization,[26] LbL assembly[27] and interfacial polymerization.[28] Because PNIPAm is uncharged, the use of secondary, non-electrostatic interactions is vital for its LbL assembly into functional films with nano-scale precision.

In recent years, an extensive range of new polymeric materials for macromolecular engineering and biological applications have been developed using a combination of click chemistry and controlled radical polymerization (CRP).[29] There are many CRP methods for incorporating clickable functionalities into a polymer side-chain, including ring opening metathesis polymerization (ROMP),[30] nitroxide- mediated polymerization (NMP),[31] living cationic ring opening polymerization,[32] atom transfer radical polymerization (ATRP)[33] and ring opening polymerization (ROP).[34] Among these techniques, ATRP has several advantages when combined with click chemistry, such as good tolerance toward most functional groups and excellent manipulation of the polymer architecture.

In this paper, we report a method for the fabrication of thermoresponsive microcapsules

through direct covalent LbL assembly via click chemistry using clickable azido- and acetylene-functionalized PNIPAm copolymers. Recently, Matyjaszewski et al.[33a] reported that azide moieties are compatible with ATRP and Hawker et al.[31] demonstrated that pendant acetylene-functionalized copolymer can be prepared through NMP. Based on these results, we investigated the copolymerization of poly[*N*-isopropylacrylamide-*co*-(trimethylsilyl)propargyl acrylamide] [PNIPAm-*co*-(TMS)Ace] and poly(*N*-isoropylacrylamide-*co*-3-azideopropylacrylamide) (PNIPAm-*co*-Az) using ATRP techniques with a synthesized dansyl-labeled ATRP initiator. After removing the protective trimethylsilyl group, the clickable PNIPAm copolymers were able to assemble alternately onto azido-modified silica particles in aqueous media using click reactions catalyzed by copper sulfate and sodium ascorbate. Using copolymers containing 10 and 20 mol% contents of clickable functionalities (azide and acetylene units), we examined the effect of the degree of cross-linking on the preparation of microcapsules containing multilayer thin films. In addition to this effect, we found that the LbL assembly temperature also significantly influences the morphology and thickness of the multilayer thin films, depending on the conformation of the PNIPAm chains in aqueous solution. The growth of the PNIPAm-Ace/PNIPAm-Az clicked multilayer thin films on silica particles was monitored by measuring their fluorescence intensities using confocal laser scanning microscopy (CLSM). Furthermore, we also characterized the microcapsules using transmission electron microscopy (TEM) and atomic force microscopy (AFM) in the tapping mode. Taking advantage of the LCST characteristics of PNIPAm, we also used AFM and TEM to examine the thermoresponsive behavior of the swelling and de-swelling of the microcapsules upon elevating the temperature of the medium. Finally, we demonstrate the feasibility of post-functionalization of the microcapsules through the reaction of an azido-modified lissamine rhodamine dye with the remaining excess of free acetylene functional groups of the

surface of the multilayer thin films.

3-2 Experimental Section

3-2.1 Materials

The following reagents and solvents were purchased from commercial suppliers and used as received unless otherwise noted: L-ascorbic acid sodium salt (TCI, ＞98%), bromoisobutyryl bromide (ACROS, 98%), acryloyl chloride (Alfa Aesar, 96%), 3-bromopropyltrichlorosilane (Aldrich, 96%), cupric sulfate pentahydrate (SHOWA, 99.5%), chlorotrimethylsilane (Lancaster, 98+%), 3-chloropropylamine hydrochloride (ACROS, 98%), dansyl chloride (ACROS, 98%), *N*,*N*-diisopropylethylamine (DIPEA) (ACROS, 98%), 1, 8-diazabicyclo[5.4.0]undec-7-ene (DBU; ACROS, 98%), propargyl amine (ACROS, 99%), rhodamine 6G (Aldrich, ~ 95%), tetrabutylammonium fluoride (1 M solution in THF; ACROS), tetramethylrhodamine isothiocyanate (TRITC)-labeled dextran (M_w ~ 4,400, 65,000 ~ 76,000 g mol^{-1}) (Aldrich), silver chloride (ACROS, 99+%), sodium azide (SHOWA, 98%), and 2-propanol (Tedia, 99.5%). The monomer *N*-isopropylacrylamide (NIPAm, 99%, TCI) was recrystallized from hexane/toluene and dried under vacuum prior to use. *N*,*N*-Dimethylformamide (DMF) (Tedia, 99.8%) and toluene (Tedia, 99.5%) were dried over CaH_2 (ACROS, 93%) and distilled under reduced pressure. Tetrahydrofuran (Tedia, 99.8%) was distilled over Na/benzophenone. The deionized (DI) water used in all reactions, solution preparations, and polymer isolations was purified to a resistance of 18 MΩ (Milli-Q Reagent Water System, Millipore Corporation). Silica particles (diameter: 3 μm) were obtained from Polysciences, Inc. (USA). Hexamethylated tris[2-(dimethylamino)ethyl]amine (Me_6TREN) was synthesized according to the method described by Ciampolini.[35] Copper(I) bromide (Acros, 98%) was washed with glacial acetic acid to remove any soluble oxidized species and then it was filtered, washed with ethanol, and dried. (Trimethylsilyl)propargyl acrylamide,[31] 1-azido-3-aminopropane,[36] azido-modified lissamine rhodamine (LRAz)[37] and $Cu(PPh_3)_3Br$[38]

were synthesized using previously described procedures.

3-2.2 Synthesis of Propargyl 2-Bromo-2-methylpropionamide (1)

A solution of propargyl amine (6.00 g, 5.45 mmol) and triethylamine (11.4 mL, 8.18 mmol) dissolved in THF (300 mL) was fed into a 500-mL two-necked round-bottom flask equipped with an Ar inlet and a rubber septum and then cooled in an ice bath. After adding α-bromoisobutyryl bromide (12.5 g, 5.45 mmol) dropwise to the solution, a white precipitate of triethylammonium bromide was formed. The mixture was stirred at room temperature overnight, the precipitate was filtered off, the solvent was evaporated, and the crude product was purified through column chromatography (*n*-hexane/EtOAc, 4:1) to give **1** as a pale yellow solid (7.84 g, 70.5%). ^{1}H NMR (500 MHz, $CDCl_3$), δ_H: 6.88 (br s, 1H, N**H**), 4.05 (dd, J = 5.25, 2.57 Hz, 2H, CC**H**$_2$NH), 2.27 (t, J = 2.56 Hz, 1H, C**H**≡C), 3.37 [s, 6H, C(C**H**$_3$)$_2$Br]. ^{13}C NMR (125 MHz, $CDCl_3$), δ_C: 171.7 (**C**O), 78.8 (CH≡**C**), 72.0 (**C**H≡C), 62.2 [**C**C(CH$_3$)$_2$Br], 32.4 [(**C**H$_3$)$_2$Br], 30.3 (**C**CH$_2$NH).

3-2.3 Synthesis of 5-Dimethylaminonaphthalene-1-sulfonic Acid (3-Azidopropyl)amide (Dansyl-N$_3$, 2)

1-Azido-3-aminopropane (2.23 g, 2.67 mmol) was added to a solution of dansyl chloride (4.00 g, 14.8 mmol) in dry THF (100 mL). Triethylamine (3 mL) was added and then the mixture was stirred at room temperature for 16 h. The solvent was evaporated under vacuum and the crude product was purified through column chromatography (EtOAc) to give **2** as a yellow oil (3.78 g, 76.5%). ^{1}H NMR (500 MHz, $CDCl_3$) δ_H: 8.56 (d, J = 8.49 Hz, 1H, Ar**H**), 8.28–8.24 (m, 2H, Ar**H**), 7.58 (t, J = 8.10 Hz, 1H, Ar**H**), 7.54 (t, J = 7.50 Hz, 1H, Ar**H**), 7.20 (d, J = 7.53 Hz, 1H, Ar**H**), 4.90 (br s, 1H, N**H**), 3.26 (t, J = 6.40, 2H, CH$_2$C**H**$_2$N$_3$), 2.98 (q, J = 6.44 Hz, 2H, NHC**H**$_2$CH$_2$), 2.90 [s, 6H, N(C**H**$_3$)$_2$], 1.67–1.60 (m, 2H, CH$_2$C**H**$_2$CH$_2$). ^{13}C NMR (125 MHz, $CDCl_3$), δ_C: 152.1, 134.3, 130.6, 129.9, 129.8, 129.5, 128.5, 123.2, 118.5,

115.3 (naphthalene carbons), 48.8 (**C**CH_2N_3), 45.4 [N(**C**$H_3)_2$], 40.8 (NH**C**H_2), 28.8 (CH_2**C**H_2CH_2).

3-2.4 Synthesis of Dansyl-Labeled ATRP Initiator (3)

N,*N*-Diisopropylethylamine (0.075 g, 5.2 mmol) and $Cu(PPh_3)_3Br$ (223 mg, 2.40 μmol) were added to a solution of propargyl 2-bromo-2-methylpropionamide (**1**; 2.45 g, 1.20 mmol) and dansyl-N_3 (**2**; 4.00 g, 1.20 mmol) in THF (30 mL) and then the mixture was stirred at room temperature for 12 h. The solvent was evaporated and the crude product was purified through column chromatography (*n*-hexane/EtOAc, 2:1) to give **3** as a yellow solid (5.76 g, 89.5%). ^{1}H NMR (500 MHz, $CDCl_3$), δ_H: 8.56 (d, J = 8.41 Hz, 1H, Ar**H**), 8.28 (d, J = 8.59 Hz, 1H, Ar**H**), 8.18 (d, J = 9.29 Hz, 1H, Ar**H**), 7.51 (m, 2H, Ar**H**), 7.47 (s, 1H, triazole *H*), 7.20 (d, J = 7.55 Hz, 1H, Ar**H**), 5.78 (br s, 1H, N**H**), 4.47 (d, J = 5.04 Hz, CC**H**$_2$NH, 2H), 4.33 (t, J = 6.11 Hz, 2H, CH_2C**H**$_2$N), 2.89 [s, 6H, N(C**H**$_3)_2$], 2.87 (m, 2H, NHC**H**$_2$$CH_2$), 2.92–2.81 (m, 2H, CH_2C**H**$_2$$CH_2$), 1.90 [s, 6H, C(C**H**$_3)_2$Br]. ^{13}C NMR (125 MHz, $CDCl_3$), δ_C: 172.2 (**C**ONH), 151.4 (**C**N$(CH_3)_2$), 144.1 (**C**CH_2NH), 134.5, 130.5, 129.7, 129.6, 129.5, 128.5, 123.4, 122.9 119.0 (naphthalene carbons), 115.5 (N**C**HC), 62.2 [**C**C$(CH_3)_2$Br], 47.1 (**C**H_2N), 45.5 [N(**C**$H_3)_2$], 39.9 (NH**C**$H_2$$CH_2$), 35.8 (C**C**$H_2$NH), 32.2 [(**C**$H_3)_2$Br], 30.1 ($CH_2$**C**$H_2$$CH_2$).

3-2.5 Synthesis 3-Azidopropylacrylamide (4)

1-Azido-3-aminopropane (5.00 g, 5.00 mmol) and triethylamine (10.45 mL, 7.50 mmol) were dissolved in dry CH_2Cl_2 (200 mL) and cooled to 0 °C. Acryloyl chloride (4.53 g, 5.00 mmol) was added slowly over 30 min and then stirring was continued for an additional 16 h at room temperature. The reaction mixture was washed with brine and water, dried ($MgSO_4$), and concentrated under reduced pressure. The crude product was further purified through column chromatography (*n*-hexane/EtOAc, 1:1) to give **4** as a colorless oil (5.33 g, 69.2%). ^{1}H NMR (500 MHz, $CDCl_3$), δ_H: 6.24 (dd, J = 1, 17 Hz, 1H, trans C**H**$_2$=CH), 6.19 (br s, 1H, N**H**),

6.09 (dd, *J* = 10.5, 17 Hz, 1H, CH_2=C**H**), 5.61 (dd, J = 1, 10.5 Hz, 1H, cis C**H**$_2$=CH), 3.40–3.38 (br m, 4H, C**H**$_2$$CH_2$C**H**$_2$−$N_3$), 1.82–1.77 (m, 1H, C**H**$_2$$CH_2$−$N_3$). ^{13}C NMR (125 MHz, $CDCl_3$), δ_C: 165.8 (**C**=O), 130.7 (CH_2=**C**H), 126.5 (**C**H_2=CH), 49.3 (CH_2**C**H_2−N_3), 37.1 (NH-**C**H_2), 28.7 (CH_2**C**$H_2$$CH_2$).

3-2.6 Trimethylsilyl-Protected Acetylenic Acrylamide Copolymers {Poly[NIPAm-*co*-(trimethylsilyl)propargyl Acrylamide], 5}

NIPAm (2.32 g, 2.05 mmol), (trimethylsilyl)propargyl acrylamide (0.93 g, 0.51 mmol), and the dansyl-labeled initiator (0.069 g, 1.28 μmol) were mixed at a 180:20:1 molar ratio in 2-propanol (2.5 mL). The solution was deoxygenated by performing freeze/pump/thaw cycles. Upon equilibration at 20 °C after the third cycle, the flask was immersed in an ice bath. An oxygen-free solution of 2-propanol (1.00 mL) containing CuBr (0.0184 g, 1.28 μmol) and Me_6TREN (29.65 mg, 35.00 μL) was prepared separately. This solution was added to the monomer/initiator mixture through an argon-purged syringe to initiate the polymerization; stirring was performed for an additional 12 h. The reaction mixture was exposed to air to terminate the polymerization; the sample was then evaporated to dryness and the residue dissolved in THF (50 mL). The copper catalyst was removed by passing the solution through a neutral alumina column. The eluate was concentrated and added to *n*-hexane to precipitate **5**, which was collected as a pale yellow powder. ^{1}H NMR (500 MHz, $CDCl_3$), δ_H: 0.13 [br s, Si(C**H**$_3$)$_3$], 1.12 [br s, CH(C**H**$_3$)$_2$], 1.38–2.14 (br m, polymer backbone), 3.98 [br s, C**H**$(CH_3)_2$].

3-2.7 Acetylenic Acrylamide Copolymers {Poly(NIPAm-*co*-propargyl Acrylamide, 6}

Excess tetrabutylammonium fluoride was added to a solution of poly[NIPAm-*co*-(trimethylsilyl)propargyl acrylamide] in dry THF to 0 °C. The mixture was then stirred for 2 h at 0 °C. The solution was dialyzed extensively against DI water and the

product was isolated via lyophilization to give **6** as a pale yellow powder. ^{1}H NMR (500 MHz, D_2O), δ_H:1.08 [br s, CH(C**H**$_3$)$_2$], 1.25–1.77 (br m, C**H**$_2$CH, copolymer backbone), 1.78–2.22 (br m, CH$_2$C**H** polymer backbone and C≡C**H**) 3.71–3.97 [br m, C**H**(CH$_3$)$_2$ and NHC**H**$_2$C].

3-2.8 Azido-Functionalized PNIPAm Copolymers {Poly(NIPAm-*co*-3-azidopropyl Acrylamide, 7}

NIPAm (1.95 g, 1.73 mmol), 3-azidopropylacrylamide (0.67 g, 0.43 mmol), and the dansyl sulfonyl azide amide ATRP initiator (0.058 g, 1.08 μmol) were dissolved at an approximate 180:20:1 molar ratio in 2-propanol (1.5 mL) and then the solution was deoxygenated by performing freeze/pump/thaw cycles. Upon equilibration at 20 °C after the third cycle, the flask was immersed in an ice bath. An oxygen-free solution of 2-propanol (0.5 mL) containing CuBr (0.0155 g, 1.08 μmol) and Me$_6$TREN (24.99 mg, 29.68 μL) was prepared separately. This solution was added to the monomer/initiator mixture through an argon-purged syringe to initiate the polymerization; the mixture was then stirred for 12 h. The reaction mixture was exposed to air to stop the polymerization; after evaporation to dryness, the residue was dissolved in THF (30 mL) and the copper catalyst was removed by passing the solution through a neutral alumina column. The eluate was concentrated and added to *n*-hexane to precipitate **7**, which was collected as a pale yellow powder (1.95 g, 42.3%). ^{1}H NMR (500 MHz, D_2O), δ_H: 1.08 [br s, CH(C**H**$_3$)$_2$], 1.26–1.78 (m, C**H**$_2$CH polymer backbone and NHCH$_2$C**H**$_2$), 1.79–2.16 (br m, CH$_2$C**H** polymer backbone), 2.82 (br s, N(C**H**$_3$)$_2$ from initiator), 3.08–3.26 (br m, NHC**H**$_2$), 3.27–3.36 (br m,C**H**$_2$N$_3$), 3.83 [br s, C**H**(CH$_3$)$_2$].

3-2.9 Synthesis of 3-μm Azido-Modified Silica Particles[39]

Anhydrous toluene (7 mL) was added under an Ar atmosphere to a Schlenk flask containing 3-μm silica microparticles (500 mg) and then the flask was placed into an oil bath at 80 °C.

After stirring for 30 min, a solution of 3-bromopropyltrichlorosilane (0.5 mL) in anhydrous toluene (3 mL) was added dropwise, and then the mixture was maintained at 80 °C for an additional 18 h. After centrifuging and removal of the supernatant solution, the particles were washed three times with toluene and ethanol to remove excess bromopropyltrichlorosilane and then the product bromo-modified silica particles were dried under reduced pressure. A sample of the bromo-modified silica particles (300 mg) was combined with sodium azide (1.0 g) in DMF (5 mL) and then the suspension was stirred at 80 °C for 18 h. After centrifugation and removal of the supernatant, the product was washed three times with distilled water, acetone, and ethanol and then dried under reduced pressure.

3-2.10 General Procedure for Direct Covalent LbL Assembly of PNIPAm Multilayer Thin Films on Azido-Modified Silica Particles

An aqueous solution (4 mL) containing the azide-modified silica particles (10 mg) and the acetylene-functionalized PNIPAm copolymers (5 mg) was combined with copper(II) sulfate (2 mg). The suspension was sonicated for 5 min, sodium ascorbate solution (5 mg/mL, 1 mL) was added, and then the mixture was incubated for 8 h at 25 °C. After the click reaction was complete, the dispersion of particles was centrifuged and the supernatant was removed and replaced with DI water. This rinsing process, aided by ultrasonication, was repeated three times to ensure removal of the excess copolymer; at this point, the next copolymer solution was added to the dispersion. Upon the addition of the sodium ascorbate solution, the reaction mixture turned brownish for the azide-functionalized PNIPAm copolymer solution and yellowish for the acetylene-functionalized PNIPAm copolymer solution; this color persisted for several hours. To ensure that the clickable groups on the thin film's surface were completely consumed and covered by the deposited copolymers, the mixtures were stirred for at least 8 h until the solution had turned pale blue, signifying the reaction's completion. After the desired number of bilayers had been formed, the microcapsules were obtained by

immersing the coated silica particles in 2 M HF for 5 min at ambient temperature to etch out the silica cores completely. The resulting microcapsules were purified through extensive dialysis against DI water.

3-2.11 Post-Functionalization of Multilayer Thin Films

The three-layer (PNIPAm-Ace$_{22}$/PNIPAm-Az$_{10}$)PNIPAm-Ace$_{22}$-coated silica particles (1.25 mg/mL, 4 mL) were combined with copper(II) sulfate pentahydrate (2 mg) and LRAz dye (5 mg). Sodium ascorbate (5 mg) in DI water (1.0 mL) was then added to the mixture, which was then incubated for 6 h. The particles were dialyzed extensively with DI water until no fluorescence was detectable in the supernatant.

3-2.12 Characterizations

Analytical TLC was performed on commercial Merck Plates coated with silica gel GF254 (0.24 mm thick). Silica Gel for flash chromatography was Merck Kieselgel 60 (230 – 400 mesh, ASTM). ^{1}H NMR (500 MHz) and ^{13}C NMR (125 MHz) were recorded using a Varian Unity Inova spectrometer using $CDCl_3$ or D_2O as the solvent. Fourier transform infrared (FT-IR) spectra of solid samples were recorded at room temperature using a Nicolet AVATAR 320 FT-IR Spectrometer. Gel permeation chromatography (GPC) was performed a HITACHI L-7100 pump and a RI 2000 refractive index detector (Schambeck SFD GmbH); the elution rate was 1.0 mL/min and the temperature was 80 °C; a Polymer Laboratories PLgel guard column (5 μm particles; 50 × 7.5 mm) and a PLgel 5 μm Mixed-D column (300 × 7.5 mm; particle size: 5 μm,) were connected in series. The molecular weight calibration curve was obtained using poly(ethylene oxide) standards of defined molecular weights (1,010－163,000 g/mol) (Polymer Laboratories Inc., MA). TEM images were obtained using a JEOL TEM-1200EX II instrument operated at 120 KV. Height measurements of the

microcapsules were determined using tapping-mode AFM (Digital Instrument NS4/D3100CL/MultiMode AFM; Veeco-Digital Instruments, Santa Barbara, CA) with silicon cantilevers (Pointprobe® Silicon AFM Probe) at room temperature, in air. The swelling samples of PNIPAm microcapsules were prepared by drying a droplet of capsule suspension on the surface of a clean silicon wafer or copper grid and allowing it to dry freely in air. In order to maintain its shrunk morphology, the de-swelling samples were prepared by heating the capsules suspension solution up to 50°C for 20 min and allowing a droplet of heated capsule suspension to be dried quickly in this oven at 50 ℃ on silicon wafer or copper grid. CLSM and DIC (differential interference contrast) images were recorded using a Leica TCS SP5 confocal microscope imaging system equipped with a diode laser (excitation wavelength: 403 and 561 nm) to quantify the fluorescence of the coated particles. Thermal analyses of the homo- and copolymer solutions were performed using a Q-20 calorimeter (TA instruments, Delaware, USA). Heating scans were recorded in the range of 0–50 ℃ at a scan rate of 2 °C min^{-1}.

3-3 Results and Discussion

3-3.1 ATRP Synthesis and Characterization of Clickable Thermoresponsive PNIPAm Copolymers

To incorporate clickable functionalities and take advantage of click chemistry for the direct covalent LbL assembly of multilayer thin films on colloidal particles, our general strategy began with the preparation of thermoresponsive copolymers presenting reactive side chain substituents from PNIPAm backbones. Bergbreiter and Chance reported water-soluble PNIPAm copolymers featuring pendent azide and acetylene groups for covalent LbL grafting on polyethylene via click reactions; they used conventional free radical copolymerization of NIPAm and acrylate-based co-monomers, followed by post-functionalization, to afford these clickable functionalities.[40] We recently demonstrated the ATRP polymerization of well-defined PNIPAm polymers using an amide-linked initiator.[41] Following similar experimental conditions in this study, we employed two acrylamide-based monomers—3-azidopropylacrylamide[42] (AzPAM) and (trimethylsilyl)propargyl acrylamide[31]—for ATRP copolymerization with NIPAm, catalyzed by CuBr/Me_6TREN, using a synthesized fluorescent amide-linked initiator in isopropyl alcohol at 0 °C (Scheme 1). To incorporate the clickable functionalities into PNIPAm while retaining its thermoresponsive behavior, these copolymer materials were designed to contain only 10 and 20 mol% of either the azide or the acetylene functional monomers. Table 1 provides a detailed summary of the results and the polymer characterization. The acetylene unit in the monomer was protected with a trimethylsilyl (TMS) group to circumvent its complexation with the copper catalyst during ATRP copolymerization.[43] After removing this protective group with tetrabutylammonium fluoride (TBAF) in THF, we obtained the desired acetylene-functionalized PNIPAm copolymer. We used ^{1}H NMR spectroscopy (Figure 3-1) to determine the number of repeating units (from the relative integration of the peaks of the

dimethylamino protons of the initiator) and the composition of copolymers (by comparing the integration of the signals of the methylene protons neighboring to the azido groups and with methyl protons of TMS). We found that the compositions of the azide and acetylene moieties were very close to their monomer contents of 10 and 20 mol%; we denote these samples as PNIPAm-Ace$_a$ and PNIPAm-Az$_a$, where "a" represents the molar percentage of clickable functionalities in the copolymers. Figure 3-2 displays the FT-IR spectra of the copolymers, revealing the characteristic absorptions of the TMS-protected acetylene, the fingerprint weak acetylene, and the strong azide peaks at ca. 2181, 2122 and 2098 cm^{-1}, respectively. The GPC traces in Figure 3-3 display a clear monomodal and symmetric peaks, without any discernible tailing or shoulders at the lower or higher molecular weight side. These data reveal that we had successfully prepared the click-functionalized PNIPAm copolymers through ATRP.

The LCST of PNIPAm copolymers is strongly influenced by the nature and molar concentration of the co-monomer and by the overall hydrophilicity of the copolymer.[44] In general, hydrophobic compounds lower the LCST, whereas hydrophilic compounds raise it.[45] Figure 3-4 presents DSC thermograms of our four azido- and acetylene-functionalized samples in relation to that of the homo-PNIPAm. We consider the temperature at the maximum of the DSC endotherm to be the LCST of the copolymer. The transition temperatures of the acetylene-functionalized copolymers were slightly lower than that of the homo PNIPAm. When the co-monomer AzPAM content was 8.7 mol%, however, the transition temperature became broader and the LCST decreased to 30.0 °C, i.e., lower than that of PNIPAm-Ace$_{0.17}$. Furthermore, we observed a much lower and broader LCST region for PNIPAm-Az$_{0.22}$; its LCST was ca. 24.9 °C. This result indicates that by the hydrophobic azide groups and alkyl chains dominate the hydrophilicity over the hydrophilic amide groups in the AzPAM, leading to a decrease in the LCST.[46] In contrast, the shorter propargyl group results in a less-hydrophobic copolymer, which, thus, provided less of a change in the LCST.

Because aqueous PNIPAm solutions undergo coil-to-globule phase transitions when the temperature is increased, we expected the LbL assembly behavior to depend strongly on the reaction temperature and, hence, the conformation of the copolymer chain.

3-3.2 Click Reactions for the Direct Covalent LbL Assembly of Multilayer Thin Films on Silica Particles

We chose silica particles as our sacrificial template material because of its ready availability over a broad range of sizes with monodispersity and because their surface can be readily modified with silylating agents. We treated the hydroxyl groups on the surface of the particles with an excess of 3-bromopropyltrichlorosilane and then exchanged the bromine atoms into azide groups through nucleophilic substitution with NaN_3 in DMF. Next, we began the LbL assembly at 25 °C, mediated through 1,3-dipolar cycloaddition between the azide units on the surfaces of silica particles and the acetylene-functionalized PNIPAm copolymer, to form the first thin film layer (Scheme 2). Because of the coil-to-globule phase transition, these copolymers adopted coil structures in aqueous solution at temperatures below their LCSTs. We expected that these conformations led to steric restriction, with only a portion of these clickable functionalities of the copolymers being consumed.[20] Consequently, we exploited the remaining free acetylene groups on the surface of the first thin film layer in the next assembly step. Repeating this process provided the desired number of layers on the surface of the silica particles, leaving behind single-component covalently stabilized PNIPAm microcapsules after core-removal through HF etching.

We used CLSM to confirm the growth of multilayer thin films on the silica particles by measuring the fluorescence intensities after depositing each bilayer. Figure 3-5a reveals a steady increase in the fluorescence intensity upon increasing the number of deposited PNIPAm-$Ace_{9.8}$/PNIPAm-Az_{10} layers. The CLSM image in Figure 3-5b reveals the uniform

coverage and regular spherical shape of the dansyl-labeled copolymers on the silica particle templates, confirming the buildup of multilayer thin films on the particles. The AFM images in Figure 3-5c display the continuous morphology and intact shell structure of the microcapsules after removal of the template. We observe creases and folds, which are characteristic of ultrathin walls resulting from collapse of the microcapsules after drying. The TEM images in Figure 3-5d confirm that these shells retained their integrity after dissolution of the core. We calculated the thickness of the multilayer thin films by examining the AFM height profiles of the microcapsules from regions in which they had folded only once. The thickness of the five-bilayer PNIPAm-$Ace_{9.8}$/PNIPAm-Az_{10} thin film was ca. 5.5 nm. Cross-linking of PNIPAm provides temperature-sensitive polymer networks that swell in water at temperatures below their LCST and de-swell at temperatures above it.[47] As expected, the sizes of our microcapsules changed dramatically upon increasing the aqueous solution temperature from 25 to 50 °C (Figure 3-5e). We conducted the LbL assembly in aqueous solutions to observe its thermoresponsive behavior and the result indicates the success of our click reaction-mediated fabrication of covalently stabilized microcapsules. This novel clickable functionalized PNIPAm derivatives provided the microcapsules with covalent linkages and also retained its thermoresponsive characteristics, thereby allowing them to exhibit swelling and de-swelling behavior.

3-3.3 Effect of Cross-Linking Degree on Multilayer Thin Films Thickness and Morphology

To further investigate the properties of the PNIPAm-$Ace_{9.8}$/PNIPAm-Az_{10} multilayer thin films, we fabricated them from copolymers containing various contents of their click-functionalities. The AFM images in Figure 3-6 reveal an increase in the thickness of the films upon increasing the number of bilayers. Because of the instability of the microcapsules containing less than one bilayer, it was difficult to measure the thickness of these systems.

The average thickness of the microcapsules assembled from PNIPAm-Ace_{22}/PNIPAm-Az_{10} (Figure 3-6, circles) was greater than that of its counterparts prepared from PNIPAm-$Ace_{9.8}$/PNIPAm-Az_{10}. For example, two-bilayer microcapsules assembled from PNIPAm-Ace_{22}/PNIPAm-Az_{10} had a thickness of ca. 8 nm, whereas the five-bilayer PNIPAm-$Ace_{9.8}$/PNIPAm-Az_{10} microcapsule was 5.5 nm thick (Figure 3-5c). This result clearly indicates that the increase in film thickness was influenced by the degree of cross-linking. We found, however, that the increase in thickness was nonlinear—the thickness of the bilayers decreased progressively as the number of deposited bilayers increased. This behavior can be explained by considering that as the multilayer thin films assembled in the second layer, the number of clickable functionalities of the PNIPAm-Az_{10} polymer decreased, leaving an insufficient number of free clickable azide groups on the surface. As a result, the subsequent LbL assembly was restricted, leading to sequentially thinner bilayers in the multilayer thin films. As mentioned above, increasing the content of azide functionalities to 22 mol% dramatically lowered the LCST, the copolymer became insoluble in aqueous solution at 25 °C. To avoid serious aggregation, we conducted the buildup of (PNIPAm-Ace_{22}/PNIPAm-Az_{22}) multilayers at 20 °C to examine the effect of higher degrees of cross-linking. We observed a regular increase in the multilayer thickness, providing films that were thicker than those of the (PNIPAm-$Ace_{9.8}$/PNIPAm-Az_{10})$_n$ systems (Figure 3-6, squares). Thus, the direct covalent LbL multilayer growth also depends on the degree of cross-linking. In addition, we found that the thickness of the microcapsule shells obtained from height measurements increased gradually with respect to the number of bilayers. This behavior confirms unambiguously the success of our direct covalently bonded LbL assembly procedure for the fabrication of microcapsules possessing ultrathin walls. Indeed, the thickness of the microcapsules can be adjusted through control of the degree of cross-linking.

3-3.4 Tailoring Multilayer Thin Film Morphologies by Adjusting the Reaction Temperature

In addition to the degree of cross-linking, the temperature at which LbL assembly of PNIPAm films is performed is another important factor affecting the morphologies of the resulting thin films. Quinn et al. demonstrated that the adsorption temperature of PNIPAm on planar templates was affected significantly by both the mass proportion of PNIPAm in the film and the morphology of the film's surface;[48] when the adsorption was conducted at temperatures close to the LCST, the amount of PNIPAm in the film increased significantly and the total film mass increased. Using the same concept, in this study we examined the effect of the temperature on the covalent assembly on the colloidal template. Figure 3-7 displays AFM images of the surface roughnesses of three microcapsule samples assembled with different compositions and at different temperatures. The microcapsule with two PNIPAm-Ace$_{22}$/PNIPAm-Az$_{10}$ bilayers assembled at 25 °C (Figure 3-7a) features numerous polymer grains on the surface, i.e., it possessed a coarse morphology. Increasing the degree of cross-linking resulted in a microcapsule having a smoother surface morphology, as demonstrated by the AFM image of a two-bilayer thin film prepared from PNIPAm-Ace$_{22}$/PNIPAm-Az$_{22}$ (Figure 3-7b). The formation of polymer grains on the surface can be attributed to the lack of a sufficient number of the remaining free azide functionalities from PNIPAm-Az$_{10}$ as mentioned above. Surprisingly, when we increased the reaction temperature to 30 °C—close to the LCST of the PNIPAm-Ace$_{22}$/PNIPAm-Az$_{10}$ copolymers—the resulting microcapsule featured only one bilayer, but it displayed a continuous and intact shell structure (Figure 3-7c; thickness: ca. 10 nm). This surface was also smoother than that prepared at lower temperature (cf. Figures 3-7a and c). These results reveal that when we performed the assembly at temperatures close to the LCST, the resulting microcapsules exhibited extremely smooth surfaces and thicker multilayer thin films because

of the tighter packing of the PNIPAm derivative as a result of a more compact chain conformation in aqueous solution.

To further investigate the thermoresponsive de-swelling behavior of microcapsules fabricated with more tightly packed multilayers, we recorded AFM and TEM images (Figure 3-8) of the microcapsules possessing two bilayers of PNIPAm-Ace_{22}/PNIPAm-Az_{10} that had been assembled at 30 °C. When comparing the AFM images and the height measurements of the microcapsules in their air-dried and thermally dried states (Figures 3-8a and c), we observe a clear increase in the thickness of the thin film—with a size variation confirming that the microcapsule de-swelled and shrank—when the microcapsules were dried at 50 °C in the oven. In addition, the TEM images in Figures 8b and d provide additional evidence suggesting that the dimensions of the microcapsule decreased considerably upon increasing the temperature above its LCST. To examine the important thermo-reversible characteristics, we conducted the heating/cooling processes of the microcapsules suspension solution between 50 °C and 25 °C repeatedly. As shown in Figure 3-9, the dimension variation of these microcapsules remained distinguishable between the swelling and de-swelling states even after five heating/cooling cycles. This result reveals that the microcapsules show good thermo-reversible characteristics in the swelling/de-swelling behavior of the ultrathin PNIPAm microcapsules.

3-3.5 Post-Functionalization of PNIPAm Clicked Thin Films Through Click Reactions With a Fluorogenic Small Molecule and Preliminary Permeability Study

Because our direct covalent LbL assembly process is based on alternating reactions between remaining free clickable groups on the surface and their complementary copolymers, the presence of unreacted free acetylene or azide moieties can be used for further conjugation with functional materials. To examine the potential for post-functionalization, we reacted the

three-layer (PNIPAm-Ace_{22}/PNIPAm-Az_{22})PNIPAm-Ace_{22}-coated silica particles with a small fluorogenic molecule, namely an azido-modified lissamine rhodamine dye. We then used CLSM to analyze the post-functionalized silica particles by simultaneously exciting the fluorescent dansyl-labeled PNIPAm thin films and the rhodamine molecules on the surface at excitation wavelengths of 403 and 561 nm, respectively. Figure 3-10a and b reveal that both green and red fluorescence emissions were visible from the thin films on the periphery of the silica particles. In order to demonstrate that the unreacted free clickable group is affected at the outer surface, the four-layer coated silica particles (with azide functional group on the surface) were also reacted with the azide-modified rhodamine dye (Figure 3-10c and d). CLSM analyses show that weak rhodamine fluorescence emission was visible when compared to the three-layer surface-modified silica particles. This result indicates that the clickable group is exclusively affected at the outer surface of the click multilayer and only few reactive groups remain inside the multilayer thin film. These experiments further demonstrate that the clickable functionalities on the multilayer thin films surface are accessible after each click assembly. Consequently, the microcapsules fabricated through direct covalent LbL assembly allow the surface for post-functionalization to conjugate a variety of small molecules or larger biomacromolecules.[49] Finally, preliminary study on the permeability of two-bilayer (PNIPAm-Ace_{22}/PNIPAm-Az_{10})$_2$ microcapsule assembled at 30 °C was presented and shown in Figure 3-11. For microcapsules incubated with probe molecules, rhodamine 6G or 4.4–kDa TRITC–labelled dextran, it was found that theses microcapsules had the same fluorescence intensity inside as the bulk solution (Figures 3-11a–f), implying that these low-molecular-weight probe molecules can penetrate into these microcapsules. When the microcapsules incubated with high-molecular-weigh TRITC–labelled dextran (65kDa), however, the dark appearance of capsules interior contrasted with the bright fluorescent outside (Figures 3-11g–i). These results reveal that the

microcapsules with tighter packing wall are selectively permeable to molecules and show potential applications for the encapsulation of variety of materials.

3-4 Conclusion

Using click chemistry, we have developed a novel approach to fabricate thermoresponsive PNIPAm microcapsules based on direct covalent bonding LbL assembly. This method not only provides a unique approach toward microcapsule construction with direct covalent bonding under mild reaction conditions but also opens a platform to better understand the effects of the degree of cross-linking on the thin film thickness and morphology. The fabrication of these microcapsules can be tailored by adjusting the aqueous reaction temperature close to the LCST (30 °C), resulting in multilayer film materials exhibiting extremely low surface roughness and high thickness as a result of tighter packing of PNIPAm, a special characteristic of the LbL assembly of PNIPAm on the colloidal template. These microcapsules also undergo a thermo-reversible swelling/de-swelling transition upon changing the temperature of the medium. The surfaces of these multilayer thin films are easily modified using, for example, an azido-modified lissamine rhodamine dye, thereby allowing post-functionalization with a variety of small molecules or larger biomacromolecules. Finally, permeability study reveals that the microcapsules with tighter packing wall are selectively permeable to molecules depending on molecular weight and show potential applications for the encapsulation of variety of materials.

References

1. (a) Wang, Y.; Bansal, V.; Zelikin, A. N.; Caruso, F. *Nano Letters* **2008**, *8*, 1741–1745. (b) Tamber, H.; Johansen, P.; Merkle, H. P.; Gander, B. *Adv. Drug Delivery Rev.* **2005**, *57*, 357–376. (c) Trehan, A.; Sinha, V. R. *J. Controlled Release* **2003**, *90*, 261–280.
2. (a) Zelikin, A. N.; Becker, A. L.; Johnston, A. P. R.; Wark, K. L.; Turatti, F.; Caruso, F. *ACS Nano* **2007**, *1*, 63–69. (b) Zelikin, A. N.; Li, Q.; Caruso, F. *Angew. Chem. Int. Ed.* **2006**, *45*, 7743–7745.
3. (a) Molvinger, K.; Quignard, F.; Brunel, D.; B Angelatos, A. S.; Radt, B.; Caruso, F. *J. Phys. Chem. B* **2005**, *109*, 3071–3076.
4. (a) Nayak, S.; Gan, D.; Serpe, M. J.; Lyon, L. A. *Small* **2005**, *1*, 416–421. (b) Sun, Q.; Deng, Y. *J. Am. Chem. Soc.* **2005**, *127*, 8274–8275. (c) Qian, J.; Wu, F. *Chem. Mater.* **2007**, *19*, 5839–5841. (d) Zha, L.; Zhang, Y.; Yang, W.; Fu, S. *Adv. Mater.* **2002**, *14*, 1090–1092. (e) Zhang, Y.; Jiang, M.; Zhao, J.; Ren, X.; Chen, D.; Zhang, G. *Adv. Funct. Mater.* **2005**, 15, 695–699. (f) Glinel, K.; Sukhorukov, G. B.; Möhwald, H.; Khrenov, V.; Tauer, K. *Macromol. Chem. Phys.* **2003**, *204*, 1784–1790.
5. (a) Sukhishvili, S. A.; Granick, S. *J. Am. Chem. Soc.* **2000**, *122*, 9550–9551. (b) Kozlovskaya, V.; Kharlampieva, E.; Mansfield, M. L.; Sukhishvili, S. A. *Chem. Mater.* **2006**, *18*, 328–336. (c) Such, G. K.; Tjipto, E.; Postma, A.; Johnston, A. P. R.; Caruso, F. *Nano Lett.* **2007**, *7*, 1706–1710. (d) Feng, Z.; Wang, Z.; Gao C.; Shen, J. *Chem. Mater.* **2007**, *19*, 4648–4657.
6. Molvinger, K.; Quignard, F.; Brunel, D.; Boissiere, M.; Devoissèlle, J.-M. *Chem. Mater.* **2004**, *16*, 3367–3372. (b) Zhang, J.; Xu, S.; Kumacheva, E. *J. Am. Chem. Soc.* **2004**, *126*, 7908–7914.
7. (a) Peyratout, C. S.; Dahne, L. *Angew. Chem. Int. Ed.* **2004**, *43*, 3762–3783. (b) Johnston, A. P. R.; Cortez, C.; Angelatos, A. S.; Caruso, F. *Curr. Opin. Colloid Interface Sci.* **2006**,

11, 203–209. (c) Quinn, J. F.; Johnston, A. P. R.; Such, G. K.; Zelikin, A. N.; Caruso, F. *Chem. Soc. Rev.* **2007**, *36*, 707–718. (d) Sukhorukov, G.; Fery, A.; Möhwald, H. *Prog. Polym. Sci.* **2005**, *30*, 885–897.

8. (a) Caruso, F.; Caruso, R. A.; Möhwald H. *Science*, **1998**, *282*, 1111–1114. (b) Donath, E.; Sukhorukov, G. B.; Caruso, F.; Davis, S. A.; Möhwald H. *Angew. Chem. Int. Ed.* **1998**, *37*, 2202–2205.
9. Decher, G.; Schlenoff, J. *Multilayer Thin Films*; Wiley-VCH: Weinheim, Germany, 2003.
10. (a) Zhang, Y. J.; Guan, Y.; Yang, S. G.; Xu, J.; Han, C. C. *Adv. Mater.* **2003**, *15*, 832–835. (b) Kozlovskaya, V.; Ok, S.; Sousa, A.; Libera, M.; Sukhishvili, S. A. *Macromolecules* **2003**, *36*, 8590–8592. (c) Yang, S. Y.; Lee, D.; Cohen, R. E.; Rubner, M. F. *Langmuir* **2004**, *20*, 5978–5981.
11. Wang, Z.; Feng, Z.; Gao, C. *Chem. Mater.* **2008**, *20*, 4194–4199.
12. (a) Johnston, A. P. R.; Read, E. S.; Caruso, F. *Nano Lett.* **2005**, *5*, 953–956. (b) Johnston, A. P. R.; Mitomo, H.; Read, E. S.; Caruso, F. *Langmuir*, **2006**, *22*, 3251–3258.
13. (a) Liu, Y. L.; Bruening, M. L.; Bergbreiter, D. E.; Crooks, R. M. *Angew. Chem. Int. Ed.* **1997**, *36*, 2114–2116. (b) Major, J. S.; Blanchard, G. J. *Langmuir* **2001**, *17*, 1163–1168. (c) Serizawa, T.; Matsukuma, D.; Nanemeki, K.; Uemura, M.; Kurusu, F.; Akashi, M. *Macromolecules* **2004**, *37*, 6531–6536. (d) Liang, Z.; Wang, Q. *Langmuir* **2004**, *20*, 9600–9606. (e) Tian, Y.; He, Q.; Tao, C.; Li, J. *Langmuir* **2006**, *22*, 360–362. (f) Buck, M. E.; Zhang, J.; Lynn, D. M. *Adv. Mater.* **2007**, *19*, 3951–3955.
14. Moya, S.; Dähne, L.; Voigt, A.; Leporatti, S.; Donath, E.; Möhwald, H. *Colloids Surf. A* **2001**, *183–185*, 27–40.
15. (a) Nardin, C.; Hirt, T.; Leukel, J.; Meier, W. *Langmuir* **2000**, *16*, 1035–1041. (b) Pastoriza-Santos, I.; Schöler, B.; Caruso, F. *Adv. Func. Mater.* **2001**, *11*, 122–128. (c) Zhu, H. G.; McShane, M. J. *Langmuir* **2005**, *21*, 424–430.

16. (a) Tong, W. J.; Gao, C. Y.; Möhwald, H. *Chem. Mater.* **2005**, *17*, 4610–4616. (b) Zhang, Y. J.; Guan, Y.; Zhou, S. *Biomacromolecules* **2005**, *6*, 2365–2369.

17. (a) Schuetz, P.; Caruso, F. *Adv. Funct, Mater.* **2003**, *13*, 929–937. (b) Kozlovskaya, V.; Ok, S.; Sousa, A.; Libera, M.; Sukhishvili, S. A. *Macromolecules* **2003**, *36*, 8590–8592. (c) Lee, D.; Rubner, M. F.; Cohen, R. E. *Chem. Mater.* **2005**, *17*, 1099–1105. (d) Yang, S. Y.; Lee, D.; Cohen, R. E. *Langmuir* **2004**, *20*, 5978–6981.

18. (a) Feng, Z.; Wang, Z.; Gao, C.; Shen, J. *Adv. Mater.* **2007**, *19*, 3687–3691. (b) Tong, W.; Gao, C.; Möhwald, H. *Macromol. Rapid Commun.* **2006**, *27*, 2078–2083. (c) Duan, L.; He, Q.; Yan, X. H.; Cui, Y.; Wang, K. W.; Li, J. B. *Biochem. Biophys. Res. Commun.* **2007**, *354*, 357–362.

19. (a) Zelikin, A. N.; Quinn, J. F.; Caruso, F. *Biomacromolecules* **2006**, *7*, 27–30. (b) Zelikin, A. N.; Li, Q.; Caruso, F. *Angew. Chem. Int. Ed.* **2006**, *45*, 7743–7745. (c) Zelikin, A. N.; Li, Q.; Caruso, F. *Chem. Mater.* **2008**, *20*, 2655–2661.

20. (a) Such, G. K.; Quinn, J. F., Quinn, A.; Tjipto, E.; Caruso, F. *J. Am. Chem. Soc.* **2006**, *128*, 9318–9319. (b) Such, G. K.; Tjipto, E.; Postma, A.; Johnston, A. P. R.; Caruso, F. *Nano Lett.* **2007**, *7*, 1706–1710. (c) Ochs, C. J.; Such, G. K.; Städler, B.; Caruso, F. *Biomacromolecules* **2008**, 9, 3389–3396.

21. (a) Kolb, H. C.; Finn, M. G.; Sharpless, K. B. *Angew. Chem. Int. Ed.* **2001**, *40*, 2004–2021. (b) Kolb, H. C.; Sharpless, K. B. *Drug Discov. Today* **2003**, *8*, 1128–1137. (c) Lewis, W. G.; Green, L. G.; Grynszpan, F.; Radic, Z.; Carlier, P. R.; Taylor, P.; Finn, M. G.; Sharpless, K. B. *Angew. Chem., Int. Ed.* **2002**, *41*, 1053–1057. (d) Hawker, C. J.; Wooley, K. L. *Science* **2005**, *309*, 1200–1205.

22. (a) Huisgen, R. *Angew. Chem., Int. Ed.* **1968**, *7*, 321–328. (b) Bock, V. D.; Hiemstra, H.; van Maarseveen, J. H. *Eur. J. Org. Chem.* **2006**, 51–68.

23. Schild, H. G. *Prog. Polym. Sci.* **1992**, *17*, 163–249.

24. (a) Pelton, R. H.; Chibante, P. *Colloids Surf.* **1986**, *20*, 247–256. (b) Zhang, J.; Pelton, R.; Deng, Y. *Langmuir* **1995**, *11*, 2301–2302.

25. Zha, L. S.; Zhang, Y.; Yang, W. L.; Fu, S. K. *Adv. Mater.* **2002**, *14*, 1090–1092.

26. (a) Nayak, S.; Gan, D. J.; Serpe, M. J.; Lyon, L. A. *Small* **2005**, *1*, 416–421. (b) Zhang, Y. W.; Jiang, M.; Zhao, J. X.; Ren, X. W.; Cheng, D. Y.; Zhang, G. Z. *Adv. Funct. Mater.* **2005**, *15*, 695–699. (c) Qian, J.; Wu, F. *Chem. Mater.* **2007**, *19*, 5839–5841.

27. Glinel, K.; Sukhorukov, G. B.; Möhwald, H.; Khrenov, V.; Tauer, K. *Macromol. Chem. Phys.* **2003**, *204*, 1784–1790.

28. (a) Sun, Q. H.; Deng, Y. L. *J. Am. Chem. Soc.* **2005**, *127*, 8274–8275. (b) Cheng, C.-J.; Chu, L.-Y.; Ren, P.-W.; Zhang, J.; Hu, L. *J. Colloid Interface Sci.* **2007**, *313*, 383–388. (c) Lawrence, D. B.; Cai, T.; Hu, Z.; Marquez, M.; Dinsmore, A. D. *Langmuir* **2007**, *23*, 395–398.

29. (a) Lutz, J. F. *Angew. Chem. Int. Ed.* **2007**, *46*, 1018–1025. (b) Binder, W. H.; Sachsenhofer, R. *Macromol. Rapid Commun.* **2007**, *28*, 15–54. (c) Fournier, D.; Hoogenboom, R.; Schubert, U. S. *Chem. Soc. Rev.* **2007**, *36*, 1369–1380. (d) Golas, P. L.; Matyjaszewski, K. *QSAR Comb. Sci.* **2007**, *11–12*, 1116–1134.

30. (a) Binder, W. H.; Kluger, C. *Macromolecules* **2004**, *37*, 9321–9330. (b) Binder, W. H.; Kluger, C.; Josipovic, M.; Straif, C. J.; Friedbacher, G. *Macromolecules* **2006**, *39*, 8092–8101.

31. Malkoch, M.; Thibault, R. J.; Drockenmuller, E.; Messerschmidt, M.; Voit, B.; Russell, T. P.; Hawker, C. J. *J. Am. Chem. Soc.* **2005**, *127*, 14942–14949.

32. Luxenhofer, R.; Jordan, R. *Macromolecules* **2006**, *39*, 3509–3516.

33. (a) Sumerlin, B. S.; Tsarevsky, N. V.; Louche, G.; Lee, R. Y.; Matyjaszewski, K. *Macromolecules* **2005**, *38*, 7540–7545. (b) Ladmiral, V.; Mantovani, G.; Clarkson, G. J.; Cauet, S.; Irwin, J. L.; Haddleton, D. M. *J. Am. Chem. Soc.* **2006**, *128*, 4823–4830. (c)

Zhang, J.; Zhou, Y.; Zhu, Z.; Ge, Z.; Liu, S. *Macromolecules* **2008**, *41*, 1444–1454.

34. (a) Riva, P.; Schmeits, S.; Stoffelbach, F.; Jérôme, C.; Jérôme, R.; Lecomte, P. *Chem. Commun.* **2005**, 5334–5336. (b) Lecomte, P.; Riva, P.; Schmeits, S.; Rieger, J.; Butsele, K. V.; Jérôme, C.; Jérôme, R. *Macromol. Symp.* **2006**, *240*, 157–165.
35. Ciampolini, M.; Nardi, N. *Inorg. Chem.* **1966**, *5*, 41–44.
36. Carboni, B.; Benanlil, A.; Vaultier, M. *J. Org. Chem.* **1993**, *58*, 3736–3741.
37. Rozkiewicz, D.; Janczewski, D.; Verboom, W.; Ravoo, B. J.; Reinhoudt, D. N. *Angew. Chem. Int. Ed.* **2006**, *45*, 5292–5296.
38. Gujadhur, R.; Venkataraman, D.; Kintigh, J. T. *Tetrahedron Lett.* **2001**, *42*, 4791–4793.
39. Ranjan, R.; Brittain, W. J. *Macromolecules* **2007**, *40*, 6217–6223.
40. Bergbreiter, D. E.; Chance, B. S. *Macromolecules* **2007**, *40*, 5337–5343.
41. Huang, C.-J.; Chang, F.-C. *Macromolecules* **2008**, *41*, 7041–7052.
42. Jiang, X.; Zhang, J.; Zhou, Y.; Xu, J.; Liu, S. *J. Polym. Sci., Part A: Polym. Chem.* **2008**, *46*, 860–871.
43. Opsteen, J. A.; van Hest, J. C. M. *Chem. Commun.* **2005**, 57–59.
44. Feil, H.; Bae, Y. H.; Feijen, J.; Kim, S. W. *Macromolecules* **1993**, *26*, 2496–2500.
45. (a) Chen, G.; Hoffman, A. S. *Macromol. Chem. Phys.* **1995**, *196*, 1251–1259. (b) Kuckling, D.; Adler, H.-J.; Arndt, K.-F.; Ling, L.; Habicher, W. D. *Macromol. Symp.* **1999**, *145*, 65–74. (c) Kunugi, S.; Yamazaki, Y.; Takano, K.; Tanaka, N. *Langmuir* **1999**, *15*, 4056–4061. (d) Deng, Y.; Pelton, R. *Macromolecules* **1995**, *28*, 4617–4621.
46. Kuckling, D.; Adler, H.-J. P.; Arndt, K.-F.; Ling, L.; Habicher, W. D. *Macromol. Chem. Phys.* **2000**, *201*, 273–280.
47. (a) Hoare, T.; Pelton, R. *Macromolecules* **2004**, *37*, 2544–2550. (b) Jones, C. D.; Lyon, L. A. *Macromolecules* **2003**, *36*, 1988–1993.
48. (a) Quinn, J. F.; Caruso, F. *Langmuir* **2004**, *20*, 20–22. (b) Kharlampieva, E.; Kozlovskaya,

V.; Ankner, J. F.; Sukhishvili, S. A. *Langmuir* **2008**, *24*, 11346-11349.

49. Nystrom, A. M.; Wooley, K. L. *Tetrahedron* **2008**, *64*, 8543–8552.

Scheme 3-1: Synthesis of the Fluorescent Amide-Linked Dansyl-Labeled ATRP Initiator **3** Using a Click Reaction; Preparation of Acetylene- and Azido-Functionalized PNIPAm Random Copolymers Using ATRP.

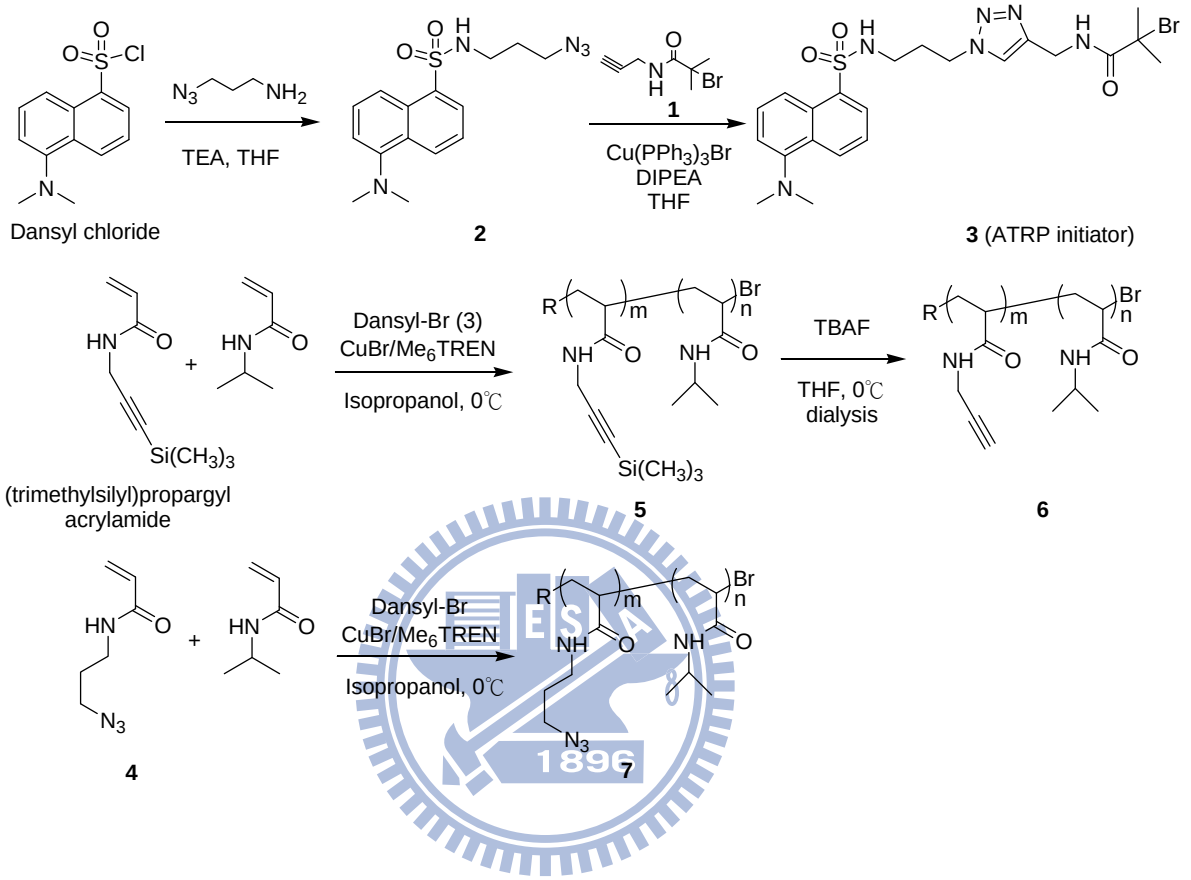

Scheme 3-2: Schematic Representation of the Preparation of Covalently Stabilized Thermoresponsive Microcapsules Through Layer-by-Layer Assembly Using Click Chemistry.

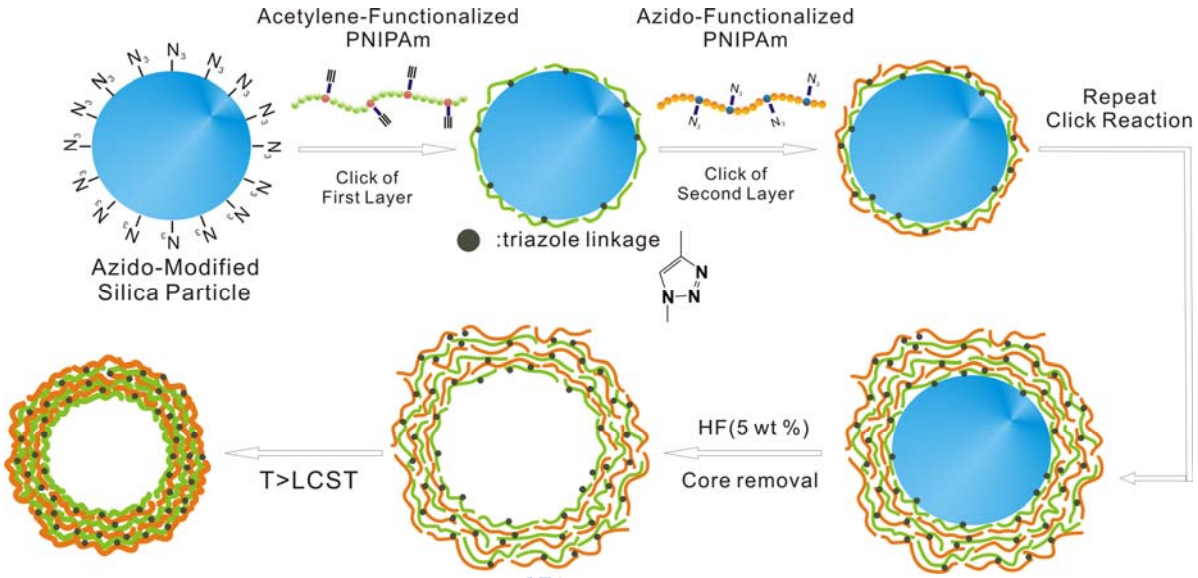

Table 3-1: Characterization Data for the Acetylene- and Azido-Functionalized Copolymers.

entry	click-functionalized copolymer sample	$M_{n,\,GPC}$ (kg/mol)	$M_{n,\,NMR}$ (kg/mol)	M_w/M_n	F_{azide} [a]	$F_{acetylene}$ [b]	maximum of endothermic peak (℃)
1	PNIPAm$_{138}$-*co*-Ace$_{15}$	13,900	17,200	1.23	—	9.8	31.5
2	PNIPAm$_{113}$-*co*-Az $_{13}$	13,300	14,800	1.21	10	—	30.0
3	PNIPAm$_{137}$-*co*-Ace$_{39}$	19,600	19,700	1.25	—	22	30.9
4	PNIPAm$_{73}$-*co*-Az$_{20}$	9,500	11,300	1.16	22	—	24.9

[a] F_{azide}: mole percentage of azide functionality; [b] $F_{acetylene}$: mole fraction of acetylene functionality in D_2O at 20 °C, measured using ^1H NMR spectroscopy.

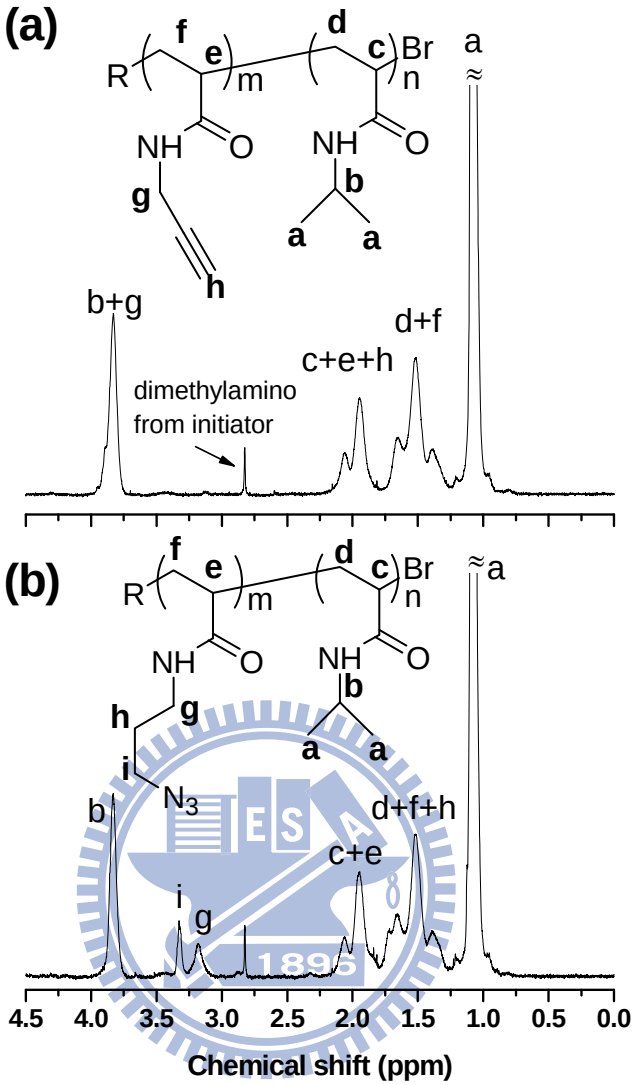

Figure 3-1: ^{1}H NMR spectra of (a) PNIPAm-Ace$_{9.8}$ and (b) PNIPAm-Az$_{10}$ in D_2O at 20 °C.

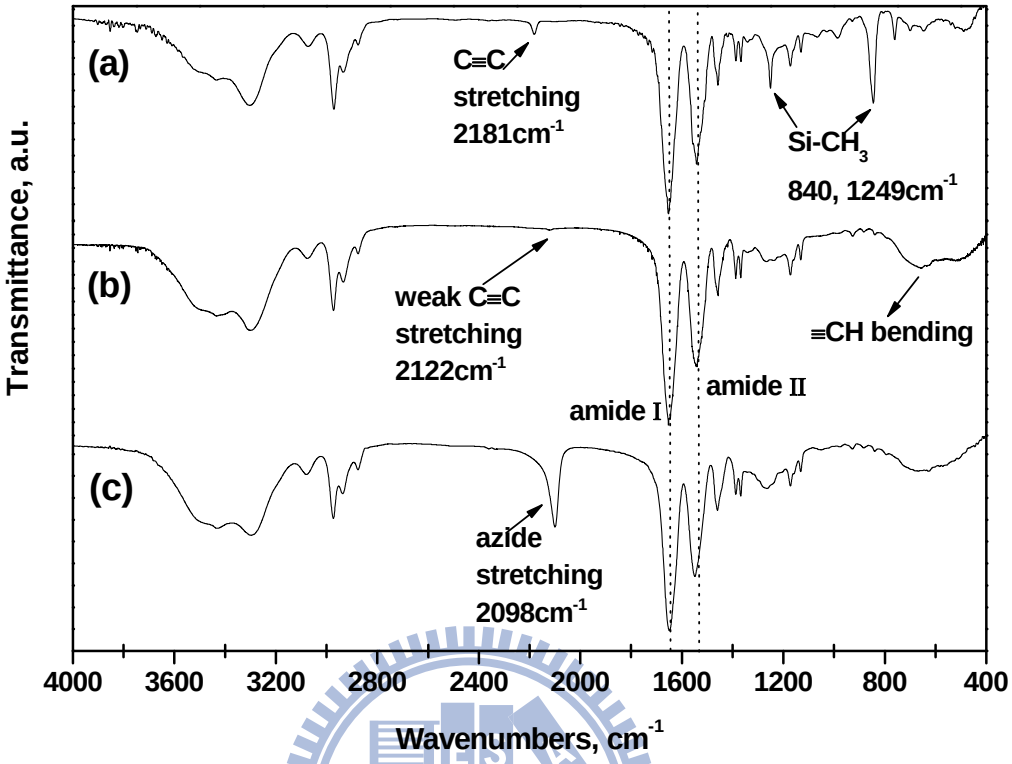

Figure 3-2: IR spectra of (a) PNIPAm-(TMS)Ace, (b) PNIPAm-Ace and (c) PNIPAm-Az.

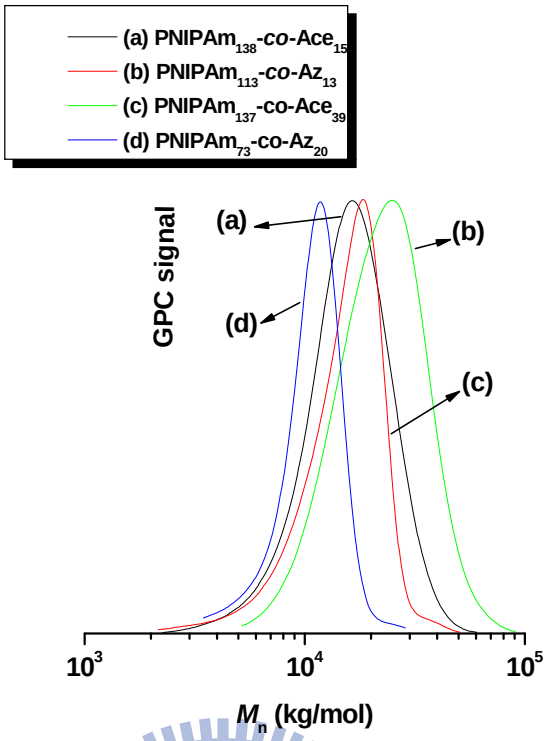

Figure 3-3: GPC traces of click-functionalized PNIPAm copolymer samples.

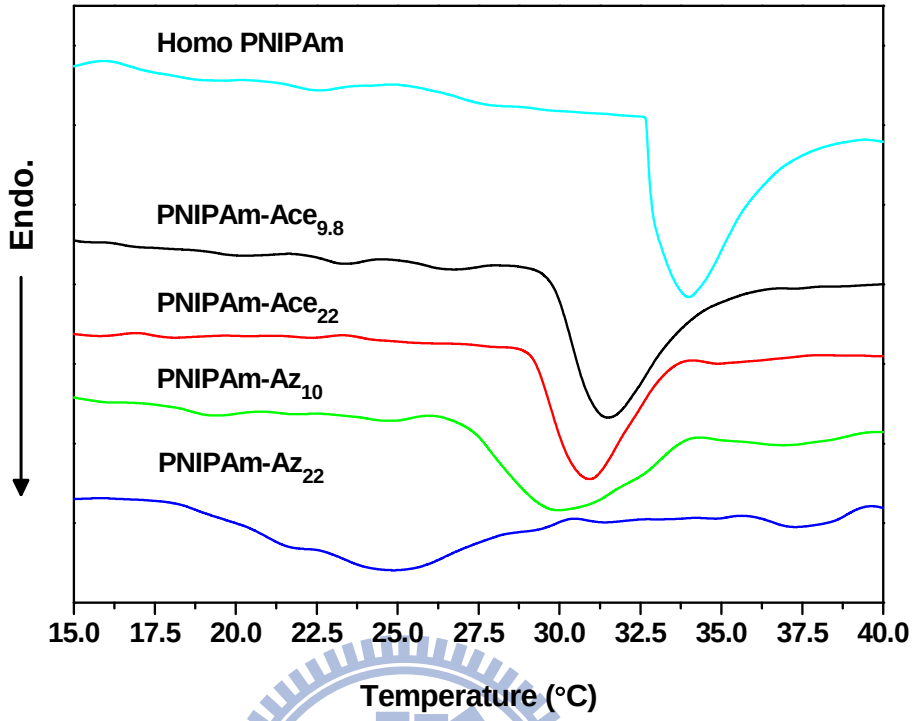

Figure 3-4: DSC thermorgrams of click-functionalized PNIPAm copolymers and a PNIPAm homopolymer in aqueous solution (1 wt %; heating rate: 2 °C/min).

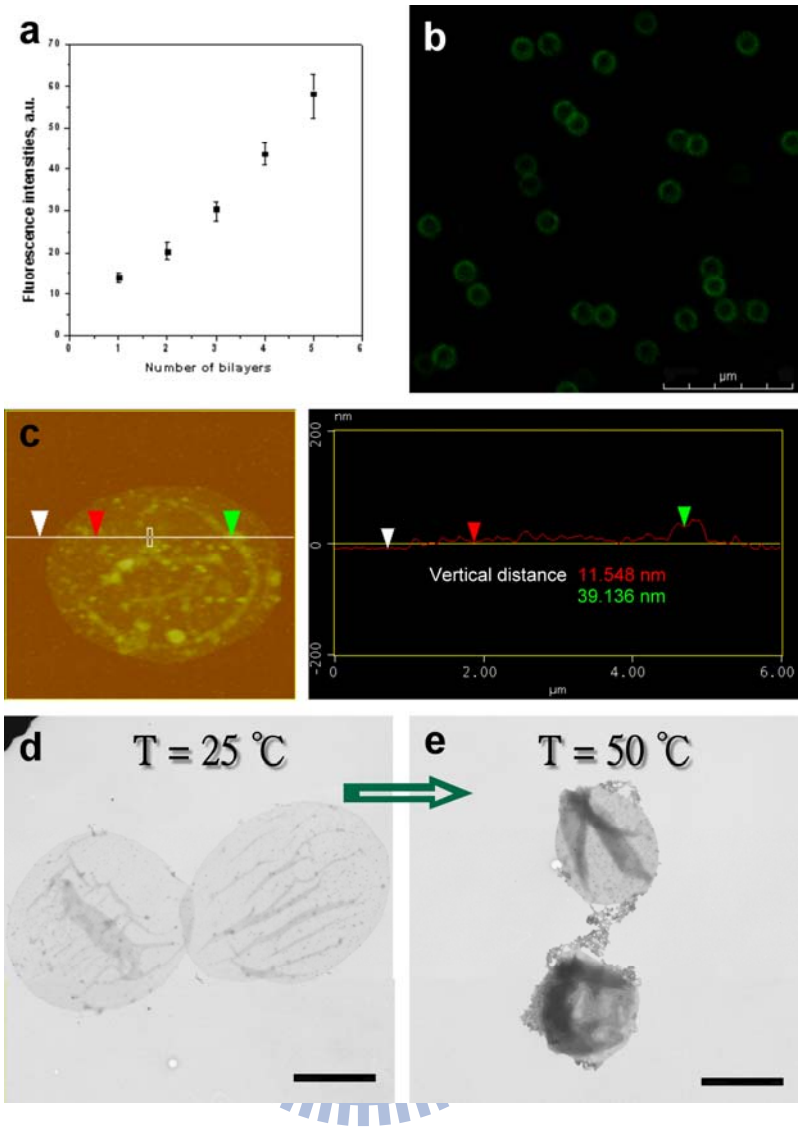

Figure 3-5: (a) Fluorescence intensity of 3-μm SiO_2 particles plotted as a function of the number of deposited PNIPAm-$Ace_{9.8}$/PNIPAm-Az_{10} bilayers. (b) CLSM image of 3-μm SiO_2 particles featuring five bilayers of PNIPAm-$Ace_{9.8}$/PNIPAm-Az_{10} bilayers in aqueous solution; the scale bar: 20 μm. (c) Tapping-mode AFM image of a collapsed PNIPAm microcapsule (dried state) featuring five PNIPAm-$Ace_{9.8}$/PNIPAm-Az_{10} bilayers; the AFM-derived thickness of the multilayer was measured in terms of the difference in heights at the points marked by the arrows. (d, e) TEM images of (PNIPAm-$Ace_{9.8}$/PNIPAm-Az_{10})$_5$ microcapsules prepared in the (d) dried state and (e) thermally dried state (50 °C); the scale bar: 2 μm.

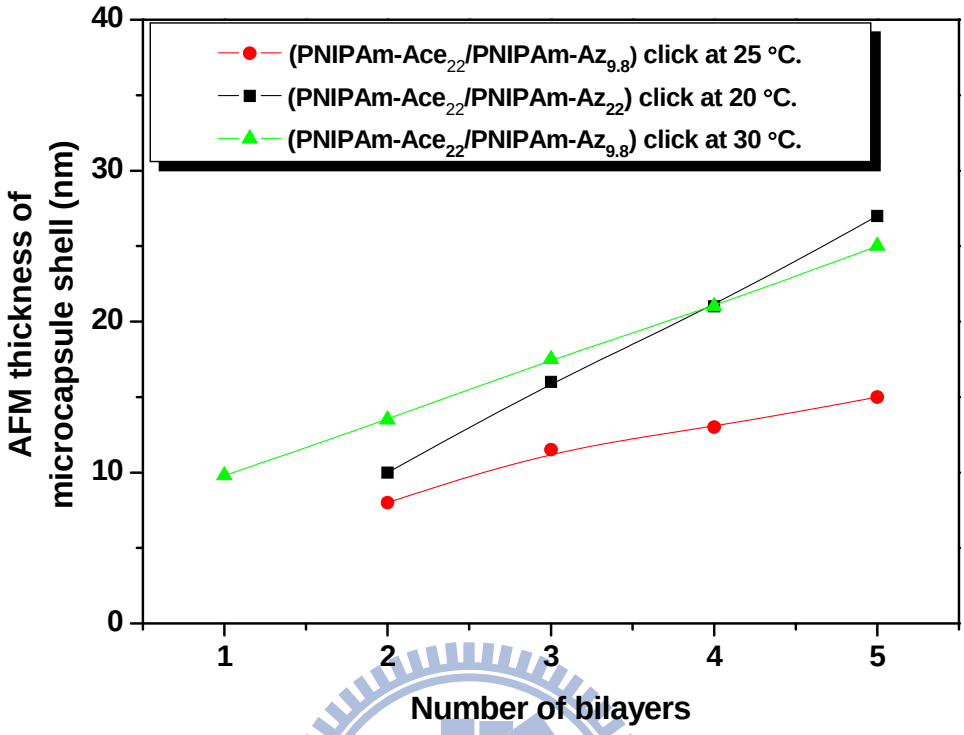

Figure 3-6: PNIPAm microcapsules multilayer thicknesses—measured using tapping-mode AFM—plotted with respect to the number of bilayers, the cross-linking degree, and the reaction temperature.

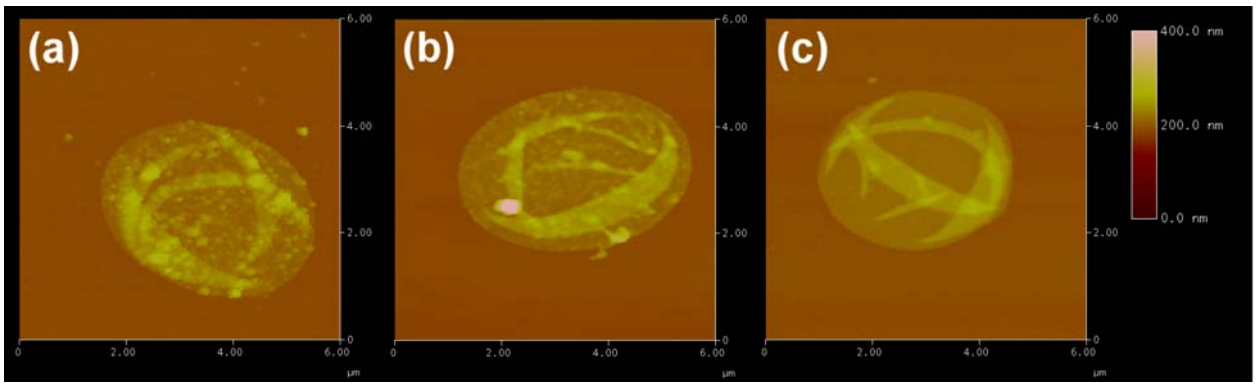

Figure 3-7: AFM images of PNIPAm microcapsules fabricated at various temperatures and with different compositions: (a) $(PNIPAm\text{-}Ace_{22}/PNIPAm\text{-}Az_{10})_2$ at 25 °C. (b) $(PNIPAm\text{-}Ace_{22}/PNIPAm\text{-}Az_{22})_2$ at 20 °C. (c) $(PNIPAm\text{-}Ace_{22}/PNIPAm\text{-}Az_{10})_1$ at 30 °C.

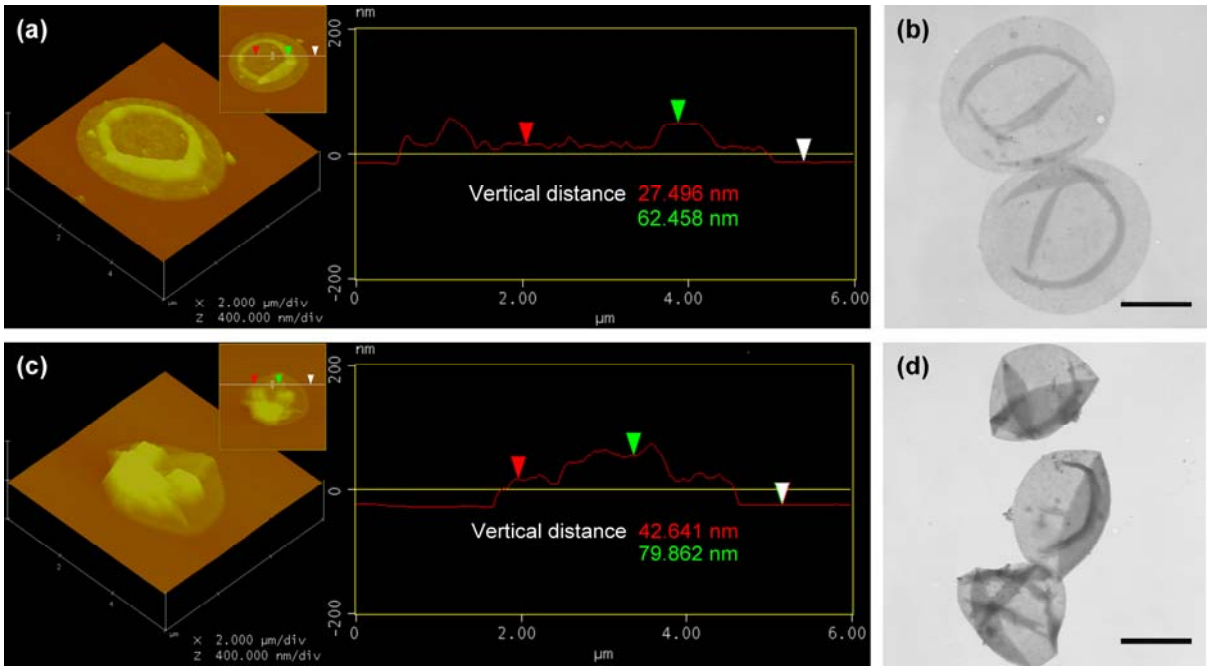

Figure 3-8: (a, c) AFM and (b, d) TEM images of the (PNIPAm-Ace$_{22}$/PNIPAm-Az$_{10}$)$_2$ microcapsules assembled closely to LCST at 30 °C. Samples prepared at 25 °C (a, b) and at 50 °C (c, d); the scale bar: 2 μm.

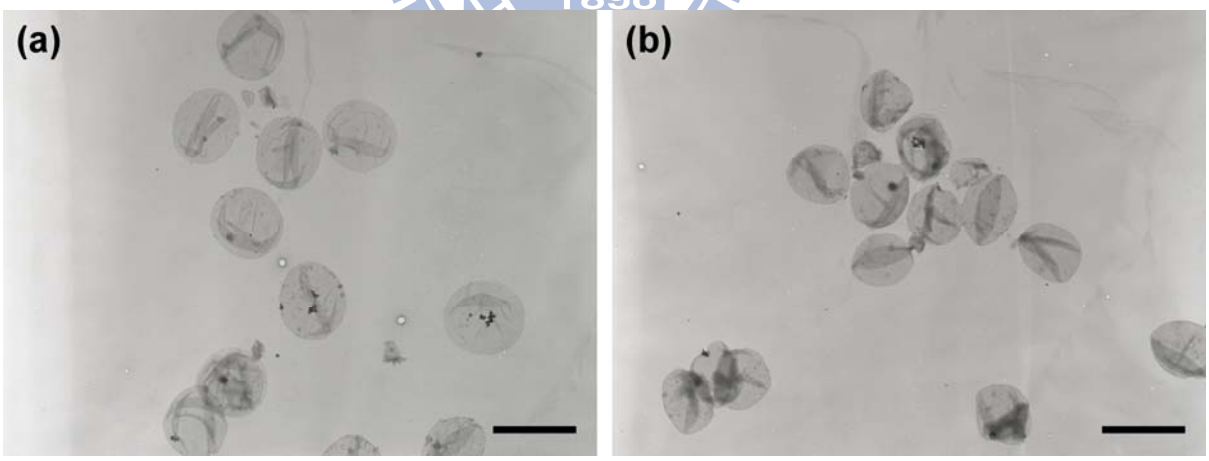

Figure 3-9: TEM images of the two-bilayer (PNIPAm-Ace$_{22}$/PNIPAm-Az$_{10}$)$_2$ microcapsules assembled at 30 °C after five heating/cooling cycles process. (a) swelling capsules prepared at 25 °C and (b) de-swelling capsules prepared at 50 °C; the scale bar: 5 μm.

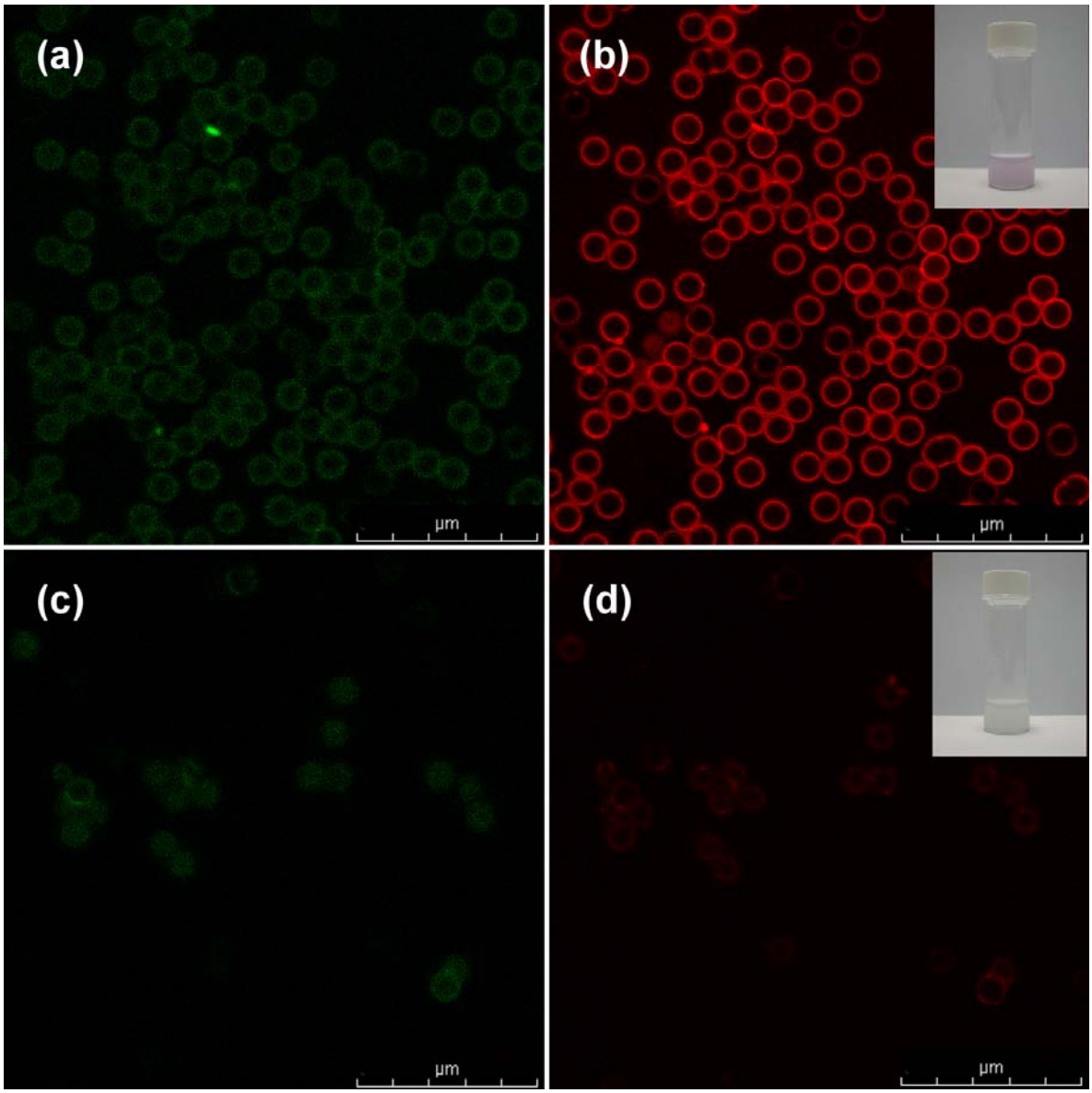

Figure 3-10: CLSM images of (a, b) three-layer (PNIPAm-Ace$_{22}$/PNIPAm-Az$_{22}$)PNIPAm-Ace$_{22}$ and (c, d) four-layer (PNIPAm-Ace$_{22}$/PNIPAm-Az$_{22}$)$_2$-coated silica particles functionalized with azido-modified lissamine rhodamine dye. The insets of panels (b and d) show photographs of vials containing lissamine rhodamine surface modified PNIPAm-coated silica particles suspension. Excitation wavelength (a, c) 403 and (b, d) 561 nm; the scale bar: 20 µm.

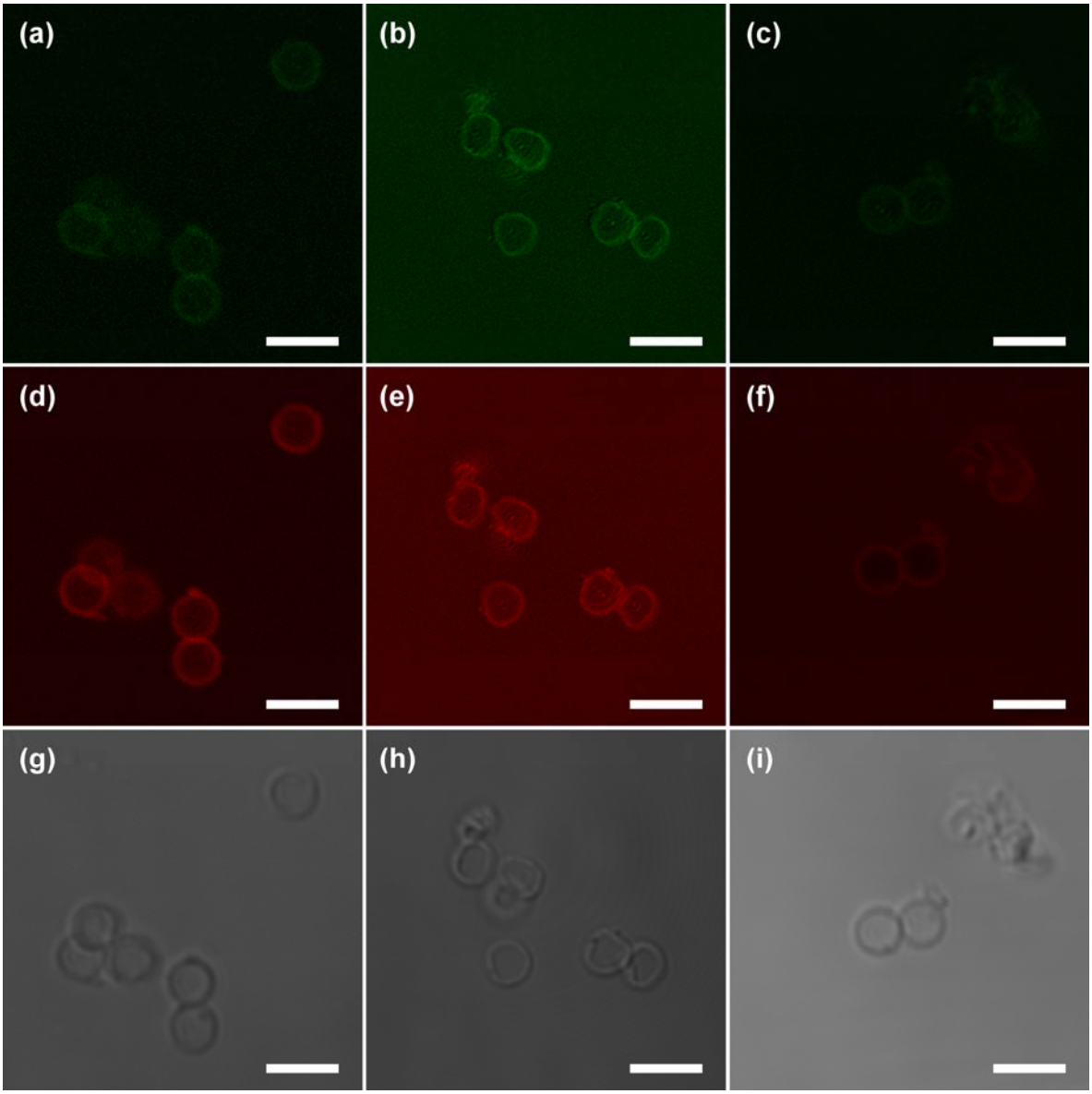

Figure 3-11: CLSM and DIC images of the two-bilayer (PNIPAm-Ace_{22}/PNIPAm-Az_{10})$_2$ PNIPAm microcapsules assembled at 30 °C after mixing with probe molecule solutions of (a, d, g) rhodamine 6G and TRITC-dextran (b, e, h) M_w ~ 4.4 kDa, (c, f, i) M_w ~ 6.5 – 7.6 kDa. Excitation wavelength (a, b, c) 403 nm and (d, e, f) 561 nm; the scale bar: 5 μm.

Chapter 4

Fabrication of Vesicle-like Dual-responsive Click Capsules by Direct Covalent Layer-by-Layer Assembly

Abstract

We report a click chemistry approach for the consecutive layer-by-layer assembly of thermo and pH-sensitive clickable copolymers on silica particles and the subsequent formation of a vesicle-like dual-responsive click capsules. This click capsules exhibit both thermo and pH-responsive behaviors by elevating the solution temperature and incubating in acidic or basic solutions respectively. These stimuli-responsive behaviors were examined by using confocal laser scanning microscopy (CLSM), transmission electron microscopy (TEM), and atomic force microscopy (AFM). This approach provides potential applications in preparing well-defined vesicle-like capsules with covalent stabilization and flexibility in introducing a range of new materials including different functional polymers.

4-1 Introduction

In the early 1990s, Decher and co-workers developed a technique for constructing ultrathin organic films, creating multilayer assemblies by consecutive, layer-by-layer (LbL) adsorption of anionic and cationic polyelectrolytes.[1]. So far, the field of LbL assembly has expanded to include films prepared using other non-electrostatic interactions—such as hydrogen bonding,[2] host-guest interactions,[3] and hybridization of DNA base pairs.[4] For over a decade, the LbL assembly has also been a versatile method for the fabrication of hollow capsules with well-defined structures, composition and tailorable physicochemical properties.[5] To prepare stable polymer capsules under various conditions (e.g., temperature, ionic strength), the use of covalent bonds to enhance the capsules' binding strength has been proved to be an efficient method.[6] These strategies include post-modifications through oxidization,[7] UV-irradiation,[8] carbodiimide formation,[9] and glutaraldehyde modification.[10] Furthermore, the direct covalent LbL assemble performed through chemical reaction between two kinds of functional groups on polymer materials allows new properties to be engineered into the capsules.[11]

These strategies have opened the door to the fabrication of directly covalently bonded multilayer films. Recently, Caruso and co-workers demonstrated a promising approach to introduce covalent bonds in capsules via click chemistry,[12] the philosophy of being selective and high yielding under mild conditions,[13] based on the promising Huisgen 1,3-dipolar cycloaddition of azides and alkynes and thiol-ene click reactions. This general applicable and modular approach opened the door to the fabrication of directly covalently bonded multilayer films.

We recently reported the feasibility of directly covalent LbL assembly using click chemistry to fabricate ultrathin thermoresponsive capsules.[14] It was demonstrated that the single component Poly(*N*-isopropylacrylamide) (PNIPAm) capsules stabilized by aromatic

1,2,3-triazoles linkages exhibited unique thermo-sensitive assembly behavior and thermo-reversible swelling/deswelling transition upon changing the temperature of the medium. We sought to exploit this LbL approach to fabricate a dual-component polymer capsules that have the same basic architecture as polymer vesicles. In most cases, the polymer vesicles,[15] also known as "polymersomes",[16] are generally built through self-assembly from amphiphilic block copolymers, which phase separate in selective solvents as a result of the solubility difference between the blocks. Although polymer vesicles self-assembled through phase separation in dilute solution can be tailored for response to external stimuli including pH,[17] light,[18] and temperature,[19] some of these vesicles can be susceptible to disassembly upon a variation of such conditions, which may limit their use in biomedical applications. There are limited literature reports have been employed to cross-linking the walls of polymersomes and stabilize the construction, such as radical polymerization,[20] photoinduced [2+2] cycloaddition,[21] base-catalyzed self-condensation of siloxanes,[22] and ring opening of epoxides.[23] Our studies are motivated in part by the potential for controllably cross-linked the bilayers as drug-delivery vehicles.

To broaden the realm of multilayer architectures, herein we report the use the LbL technique via click chemistry to alternately assemble thermo and pH responsive clickable copolymers on silica template, leading to a vesicle-like ultrathin multilayer with dual stimuli-responsive behaviors, as illustrated in Scheme 1. Such LbL assembled polymer capsules not only possess the robust covalent-stabilized nanostructure but also exhibit reversible swelling/deswelling behaviors upon changing the condition of the medium.

4-2 Experimental Section

4-2.1 Materials

All reagents and solvents were purchased from commercial suppliers and used as received unless otherwise noted, including L-ascorbic acid sodium salt (TCI, ＞98%), acryloly chloride (Alfa Aesar, 96%), Cupric sulfate pentahydrate (SHOWA, 99.5%), sodium azide (SHOWA, 98%), and 2-propanol (Tedia, 99.5%). The monomer *N*-isopropylacrylamide (NIPAm, 99%, TCI) was recrystallized in hexane/toluene and dried under vacuum before use. *N*,*N*-dimethylformamide (DMF) (Tedia, 99.8%) and toluene (Tedia, 99.5%) were dried over CaH_2 (ACROS, 93%) and distilled under reduced pressure. Tetrahydrofuran (Tedia, 99.8%) was distilled over Na/benzophenone. Deioned (DI) water used in all reactions, solution preparations, and polymer isolations was purified to a resistance of 18 MΩ (Milli-Q Reagent Water System, Millipore Corporation). Copper(I) bromide (Acros, 98%) was washed with glacial acetic acid for the removal of any soluble oxidized species, filtered, washed with 2-propanol, and dried. *N*-Acryloylalanine (AAL), dansyl-labeled ATRP initiator, 2-(1-Carboxy-1-methylethylsulfanylthiocarboylsulfanyl)-2-methylpropionic acid (CMP), hexamethylated tris(2-(dimethylamino)ethyl)amine (Me_6TREN), (trimethylsilyl)propargyl acrylamide, and 5-μm azido-modified Silica Particles were synthesized according to previous described procedures.

4-2.2 Synthesis of 2-(2-(2-azidoethoxy)ethoxy)ethanol (Scheme 4-1, (2))

2-(2-(2-chloroethoxy)ethoxy)ethanol (25.0 g, 148.3 mmol) and sodium azide (14.46 g, 222.3 mmol) were added in 400 mL DMF. The mixture was stirred at 100 °C for 15 h and then cooled to RT. After the precipitate was filtered off, the solvent was evaporated under vacuum to afford the product **2**, (24.2 g, 93 %) as a colorless oil.

4-2.3 Synthesis of 2-(2-(2-azidoethoxy)ethoxy)ethyl methanesulfonate (Scheme 4-1, (3))

A solution of 20.0 g (114 mmol) of compound **2** and 25 mL of Et_3N in 500 mL of dry CH_2Cl_2 was cooled to 0 °C under a nitrogen atmosphere. A solution of methanesulfonyl chloride (13.7 g, 120 mmol) in CH_2Cl_2 (25 mL) was added dropwise to this mixture over a 30-min period, and the solution was warmed to room temperature and stirred for 1.5 h. After the precipitate was filtered off, the solvent was evaporated and the crude product was purified by column chromatography eluting with a 2:1 mixture of *n*-hexane and ethyl acetate to give **3** as a pale yellow oil (21.8 g, 75.5 %). ^{1}H NMR (500MHz, $CDCl_3$): δ 4.33 (m, C**H**$_2$OSO$_2$CH$_3$, 2H), 3.74 (m, C**H**$_2$CH$_2$OSO$_2$CH$_3$, 2H), 3.66-3.61 (br, C**H**$_2$OC**H**$_2$C**H**$_2$O, 6H), 3.35 (m, C**H**$_2$N$_3$, 2H). 3.03 (s, OSO$_2$C**H**$_3$, 3H). ^{13}C NMR: δ 70.55 (**C**H$_2$CH$_2$OCH$_2$CH$_2$N$_3$, 1C), 70.50 (**C**H$_2$OCH$_2$CH$_2$N$_3$, 1C), 69.94 (O**C**H$_2$CH$_2$N$_3$, 1C), 69.13 (**C**H$_2$CH$_2$OSO$_2$CH$_3$, 1C), 68.97 **C**H$_2$OSO$_2$CH$_3$, 1C), 50.56 (**C**H$_2$N$_3$, 1C), 37.52 (OSO$_2$**C**H$_3$, 1C).

4-2.4 Synthesis of 2-(2-(2-(2-azidoethoxy)ethoxy)ethyl)isoindoline-1,3-dione (Scheme 4-1, (4))

A solution of 20.0 g (79 mmol) of compound **3** and 22.0 g (118.5 mol) of potassium phthalimide in 400 mL of dry DME was heat at reflux for 18 h under a nitrogen atmosphere. After cooling to room temperature and concentration in vacuo, the resulting residue was diluted with ethyl acetate and the solids were filtered. Concentration of the filtrate in vacuo

followed by purification of the crude product by column chromatography eluting with a 4:1 mixture of *n*-hexane and ethyl acetate to give **4** as a colorless oil (15.3 g, 63.5 %). ^{1}H NMR (500MHz, $CDCl_3$): δ 7.78 (m, phthalyl aromatic, 2H), 7.66 7.78 (m, phthalyl aromatic, 2H), 3.85 (m, C**H**$_2$N, 2H), 3.70 (m, C**H**$_2$CH$_2$N, 2H), 3.60 (m, C**H**$_2$CH$_2$N$_3$, 2H), 3.55 (br, OC**H**$_2$C**H**$_2$O, 4H), 3.25 (m, C**H**$_2$N$_3$, 2H). ^{13}C NMR: δ 168.12 (**C**O, 2C), 133.81 (aryl-***C***, 2C), 131.98 (aryl-***C***, 2C), 123.08 (aryl-***C***, 2C), 70.48 (**C**H$_2$OCH$_2$CH$_2$N, 1C), 70.04 (**C**H$_2$OCH$_2$CH$_2$N$_3$, 1C), 69.87 (**C**H$_2$CH$_2$N$_3$, 1C), 67.87 (**C**H$_2$CH$_2$N, 1C), 50.48 (**C**H$_2$N$_3$, 1C), 37.15 (**C**H$_2$N, 1C).

4-2.5 Synthesis of 2-(2-(2-azidoethoxy)ethoxy)ethanamine, (Scheme 4-1,(5))

A solution of 10.0 g (32.9 mmol) of compound 4 and 4.0 mL of 80% hydrazine hydrate in 100 mL of absolute ethanol was heated at 55 °C for 2 h, during which time a white precipitate formed. The mixture was cooled to room temperature and concentrated in vacuo, after which the crude residue was diluted with xxx mL of dry CH_2Cl_2. After the precipitate was filtered off, the solvent was dried and concentrated in vacuo to afford pale yellow oil, which was used in the next step without further purification (5.04 g, 88 %). ^{1}H NMR (500MHz, $CDCl_3$): δ 3.66-3.60 (br, C**H**$_2$OC**H**$_2$C**H**$_2$O, 6H), 3.50 (m, C**H**$_2$CH$_2$NH$_2$, 2H), 3.37 (m, C**H**$_2$N$_3$, 2H), 2.86 (m, C**H**$_2$NH$_2$, 2H). ^{13}C NMR: δ 73.12 (**C**H$_2$CH$_2$NH$_2$, 1C), 70.62 (**C**H$_2$CH$_2$N$_3$, 1C), 70.26 (**C**H$_2$ CH$_2$OCH$_2$CH$_2$NH$_2$, 1C), 70.02 (**C**H$_2$OCH$_2$CH$_2$NH$_2$, 1C), 50.63 (**C**H$_2$N$_3$, 1C), 41.59 (**C**H$_2$NH$_2$, 1C).

4-2.6 Synthesis of *N*-(2-(2-(2-azidoethoxy)ethoxy)ethyl)acrylamide (Scheme 4-1, (1))

A mixture of triethylamine (5.2 mL, 37.3 mmol) and compound **5** (5.0 g, 28.7 mmol) dissolved in dry CH_2Cl_2 (250 mL) were fed into a 250 mL two-necked round-bottomed flask fitted with a Ar inlet and a rubber septum and were cooled in an ice bath. The acryloyl chloride (3.12 g, 34.4 mmol) was added into the mixture dropwise over 30 mins. White

precipitate was observed and the reaction was allowed to stir at room temperature overnight. After the precipitate was filtered off, the solvent was evaporated and the crude product was purified by column chromatography eluting with a 1:2 mixture of *n*-hexane and ethyl acetate to give **1** as a pale yellow oil (3.84 g, 58.5 %). ^{1}H NMR (500MHz, $CDCl_3$): δ 6.27 (dd, *J* = 16.99, 1.48 Hz, $CH_2C\mathbf{H}NH$, 1H), 6.21 (br s, N**H**, 1H), 6.10 (dd, *J* = 16.99, 10.28 Hz, trans $C\mathbf{H}_2CH$, 1H), 5.62 (dd, *J* = 10.28, 1.48 Hz, cis $C\mathbf{H}_2CH$, 1H), 3.67 (m, $NHCH_2C\mathbf{H}_2O$, 2H), 3.63 (m, $OC\mathbf{H}_2C\mathbf{H}_2O$, 4H), 3.58 (m, $OC\mathbf{H}_2CH_2N_3$, 2H), 3.53 (m, $NHC\mathbf{H}_2$, 2H), 3.38 (m, $C\mathbf{H}_2N_3$, 2H). ^{13}C NMR: δ 165.51 (**C**=O, 1C), 130.76 (CH_2=**C**H, 1C), 126.36 (**C**H_2=CH, 1C), 70.43 ($NHCH_2\mathbf{C}H_2O$, 1C), 70.16 ($NH(CH_2)_2O\mathbf{C}H_2$, 1C), 70.06 ($NH(CH_2)_2OCH_2\mathbf{C}H_2$, 1C), 69.76 ($O\mathbf{C}H_2CH_2N_3$, 1C), 50.56 ($\mathbf{C}H_2N_3$, 1C), 39.02 ($NH\mathbf{C}H_2$, 1C).

4-2.7 Preparation of Alkyne-functionalized Acrylamide Random polymer, Poly[NIPAm-*r*-propargyl acrylamide] (PNIPAm-*r*-PPAm), (Scheme 4-2 (6))

The initial reactants were mixed at a 80: 20: 1 molar ratio of NIPAm (2.32 g, 2.05 mmol), (trimethylsilyl)propargyl acrylamide (0.93 g, 0.51 mmol), dansyl-labeled ATRP initiator (0.064 g, 0.119 mmol), and 2-propanol (2.5 mL). The solution was deoxygenated by performing freeze-pump-thaw cycle. Upon equilibration at 20 ℃ after the third cycle, the flask was immersed into an ice bath. To allow the buildup of the complex between the metal and ligand, an oxygen free solution of 2-propanol (0.5 mL) containing CuBr (0.0184 g, 1.28 μmol) and Me_6TREN (29.65 mg, 35.00 μL) was prepared separately. This solution was then added to the monomers and initiator mixture via an argon-washed syringe to start polymerization (6 hr). The reaction mixture was exposure to air to stop polymerization, then evaporated to dryness and the residue was dissolved in 50mL of THF, and the copper catalyst was removed by passing through a neutral alumina column. Excess tetrabutylammonium fluoride was added to the solution of poly[NIPAm-*r*-(trimethylsilyl)propargyl acrylamide] in

dry THF to 0 °C. The mixture was then stirred for 2 h at 0 °C. The solution was dialyzed extensively against DI water and the product was isolated via lyophilization to give 6 as a pale yellow powder. ^{1}H NMR (500 MHz, D_2O), δ 1.08 (br, CH(C**H**$_3$)$_2$), 1.25–1.77 (br, CH_2CH, copolymer backbone), 1.78–2.22 (br, CH_2CH polymer backbone and C≡C**H**) 3.71–3.97 (br, C**H**(CH_3)$_2$ and NHC**H**$_2$C≡CH).

4-2.8 Preparation of Azido-functionalized Acrylamide Random polymer, Poly[NIPAm-*r*-*N*-(2-(2-(2-azidoethoxy)ethoxy)ethyl) acrylamide] (PNIPAm-*r*-PEOAm), (Scheme 4-2 (7))

The initial reactants were mixed at an approximate 80: 20: 1 molar ratio of NIPAm (2.0 g, 17.7 mmol), *N*-(2-(2-(2-azidoethoxy)ethoxy)ethyl) acrylamide (1.0 g, 4.4 mmol), dansyl-labeled ATRP initiator (0.064 g, 0.119 mmol), and 2-propanol (0.5 mL). The solution was deoxygenated by performing freeze-pump-thaw cycle. Upon equilibration at 20 °C after the third cycle, the flask was immersed into an ice bath. To allow the buildup of the complex between the metal and ligand, an oxygen free solution of 2-propanol (0.5 mL) containing CuBr (0.0184 g, 0.129 mmol) and Me_6TREN (38.8 mg, 46 μL) was prepared separately. This solution was then added to the monomers and initiator mixture via an argon-washed syringe to start polymerization (6 h). The reaction mixture was exposure to air to stop polymerization, then evaporated to dryness and the residue was dissolved in 30 mL of THF, and the copper catalyst was removed by passing through a neutral alumina column. The solution was concentrated and precipitated in *n*-hexane to give **7** as a pale yellow powder. ^{1}H NMR (500MHz, D_2O): δ 1.00 (br, CH(C**H**$_3$)$_2$), 1.15-1.67 (br, C**H**$_2$CH, copolymer backbone), 1.70-2.07 (br, CH_2C**H**, copolymer backbone), 2.76 (br, N(CH_3)$_2$,), 3.25 (br, C**H**$_2$N$_3$), 3.36 (br, NHC**H**$_2$CH$_2$), 3.48 (br, C**H**$_2$CH$_2$N$_3$), 3.57 (br, NHC**H**$_2$C**H**$_2$OC**H**$_2$), 3.75 (br, C**H**(CH_3)$_2$).

4-2.9 Synthesis of Poly(*N*-acryloylalanine)-*r*-Poly(propargyl acrylamide) (PAAL-*r*-PPAm), (Scheme 4-3 (8))

The initial reactants were mixed at an approximate 60: 15: 1: 0.2 molar ratio of *N*-acryloylalanine (1.5 g, 10.5 mmol), propargyl acrylamide (0.286 g, 2.63 mmol), chain transfer agent CMP (49.25 mg, 0.1744 mmol) and V-501 (9.8 mg) were mixed together in deionized water. After the pH was adjusted to 6.5, the mixture was purged with nitrogen at 5 °C for 30 min prior to the reaction. The polymerization was allowed to proceed for 3 h at 45 °C and then was quenched by immersion in liquid nitrogen. The product was purified by dialysis against deionized water and isolated by lyophilization (1.49 g, 83.5 %, $M_{n\ PEO}$ = 8,650 g/mol, PDI = 1.60). ^{1}H NMR (500MHz, D_2O): δ 0.93 (br, SC(C**H**$_3$)$_2$), 1.23 (br, CH(C**H**$_3$)$_2$), 1.32-1.78 (br, C**H**$_2$CH, copolymer backbone), 1.78-2.36 (br, CH$_2$C**H**, copolymer backbone), 2.44-2.71 (br, C≡C**H**), 3.60-4.22 (br, C**H**$_2$C≡CH and C**H**(CH$_3$)$_2$).

4-2.10 Synthesis of poly(*N*-acryloylalanine)-*r*-Poly[*N*-(2-(2-(2-azidoethoxy)ethoxy)ethyl) acrylamide] (PAAL-*r*-PEOAm), (Scheme 4-3 (9))

The initial reactants were mixed at an approximate 60: 15: 1: 0.2 molar ratio of *N*-acryloylalanine (1.5 g, 10.5 mmol), *N*-(2-(2-(2-azidoethoxy)ethoxy)ethyl) acrylamide (0.6 g, 2.63 mmol), chain transfer agent CMP (49.25 mg, 0.1744 mmol) and V-501 (9.8 mg) were mixed together in deionized water. After the pH was adjusted to 6.5, the mixture was purged with nitrogen at 5 °C for 30 min prior to the reaction. The polymerization was allowed to proceed for 3 h at 45 °C and then was quenched by immersion in liquid nitrogen. The product was purified by dialysis against deionized water and isolated by lyophilization (1.79 g, 85.4 %, $M_{n\ PEO}$ = 10,280 g/mol, PDI = 1.83). ^{1}H NMR (500MHz, D_2O): δ 0.93 (br, SC(C**H**$_3$)$_2$), 1.23 (br, CH(C**H**$_3$)$_2$), 1.32-1.78 (br, C**H**$_2$CH, copolymer backbone), 1.78-2.36 (br, CH$_2$C**H**,

copolymer backbone), 3.40 (br, C**H**$_2$N$_3$), 3.52 (br, NHC**H**$_2$), 3.61 (br, C**H**$_2$CH$_2$N$_3$), 3.61 (br, NHCH$_2$C**H**$_2$OC**H**$_2$C**H**$_2$O), 3.98 (br, C**H**(CH$_3$)$_2$).

4-2.11 Procedure for Layer-by-Layer Multilayer Coating of Azide Modified Silica Particles

An aqueous solution (8 mL) containing the azido-modified silica particles (20 mg) and the alkyne-functionalized PNIPAm copolymers (5 mg) was combined with copper(II) sulfate (4 mg). The suspension was sonicated for 5 min, sodium ascorbate solution (5 mg/mL, 2 mL) was added, and then the mixture was incubated for 8 h. After the click reaction was complete, the dispersion of particles was centrifuged and the supernatant was removed and replaced with DI water. This rinsing process, aided by ultrasonication, was repeated three times to ensure removal of the excess copolymer; at this point, the resulting particles were redispersed by combining with an azido-functionalized PNIPAm copolymer solution, and the dispersion was allowed to proceed the second layer assembly by adding copper(II) sulfate and sodium ascorbate solution. The method of assembly inner core pH-responsive PAAL bilayer was assembled at pH 3 to ensure that the carboxylic acid groups were in the protonated state. After the desired number of bilayers had been formed, the capsules were obtained by immersing the coated silica particles in 2 M HF for 5 min at ambient temperature to etch out the silica cores completely. The resulting capsules were purified through extensive dialysis against DI water.

4-3 Results and Discussion

In order to obtain capsules with desired properties leading toward their "smart" responsive, one of the prerequisites is to design their built-up polymer materials. To implement this ideal, we prepared two kinds of alkyne- and azido-functionalized stimuli-responsive random copolymers via controlled radical polymerization, as shown in Figure 4-1.

We first synthesized a water-soluble azide-containing monomer, *N*-(2-(2-(2-azidoethoxy)ethoxy)ethyl)acrylamide (Scheme 4-1), containing ethylene oxide repeat unit to increase the hydrophilicity. These thermo-sensitive Poly(*N*-isopropylacrylamide) (PNIPAm) and pH-sensitive Poly(*N*-acryloylalanine) (PAAL) clickable random copolymers were successfully prepared via atom transfer radical polymerization (ATRP) (Scheme 4-2) and reversible addition-fragmentation chain transfer (RAFT) (Scheme 4-3) polymerization respectively. Controlled radical copolymerization via ATRP and RAFT were chosen because of its monomer compatibility, good control over the molecular weigh distribution, and chain composition.[24] This allowed us to design and synthesize the molar ratio of either the azide or the alkyne while retaining its stimuli-responsive behavior. These copolymer materials were designed to contain 20 mol % of either azide or the alkyne functional monomers. By nuclear magnetic resonance (NMR) (Figure 4-2 and Figure 4-3) spectroscopy, we found that the compositions of azide and alkyne moieties were close to their monomer contents of 20 mol %. Table 4-1 provides a detailed summary of the results and the polymer characterization. These novel clickable functionalized PNIPAm and PAAL random copolymers provided the capsules with covalent linkages and also retained its responsive characteristics, thereby allowing them to exhibit swelling/deswelling behaviors.

In this study, consecutive layer-by-layer was performed with a sequence of PNIPAm/PAAL/PNIPAm to fabricate a vesicle-like click capsules with thermo-sensitive outer

shell bilayers and pH-responsive inner core bilayer (Scheme 4-4). The first layer of alkyne-functionalized PNIPAm was assembled through 1,3-dipolar cycloaddition on the azido-modified silica particles close to the lower critical solution temperature (LCST) of PNIPAm-*r*-PPAm at 32 °C. In our previous study, we have demonstrated a promising method for low surface roughness and thick multilayer films of PNIPAm single component capsules.[14] Therefore, the PNIPAm LbL processes were facilitated by adjusting the solution temperature closely to LCST as a result of coil-to-globule transition characteristic of PNIPAm leading to tighter packing assembled thin film structure. The remaining clickable groups in the multilayers on the surface of the particles are available for covalent attachment of subsequent layers because of the steric hindrance of adsorbed layers. Accordingly, the second layer of PNIPAm-*r*-PEOAm was assembled at 33°C by using the remaining free alkyne groups to establish the first PNIPAm bilayer. The pH-responsive PAAL was introduced at pH 3 to ensure that the carboxylic acid groups were in the protonated state. As a result, the deposition of PAAL on PNIPAm surface was facilitated by the hydrogen bonding between the amide hydrogen of the PNIPAm and the acid carbonyl of the PAAL and the acid hydrogen of the PAAL and amide carbonyl of the PNIPAm.[25] Finally, the outer PNIPAm bilayer was assembled to build up the three bilayers core-shell particles.

After removing the silica template by hydrogen fluoride etching, and incubation at pH 7, the vesicle-capsules were obtained. A uniform coverage with fluorescently labeled polymer, a regular spherical shape, and a uniform size of the capsules were observed as shown in Figure 2. Electrostatic interactions[26] and hydrogen bonding[12b] induced by changes in pH are known to be a driving force for capsule swelling and shrinkage. The pH-sensitive of the click capsules were first examined by immersion of the capsules into low and high pH solutions, where the carboxylic acid side chain of PAAL protonate or deprotonate. As shown in Figure 4-4a, the capsule diameter at pH 3 of approximately 5.5 μm (Figure 4-4a, inset) is larger than

the 5.0 μm particle template.

Because of the thermo reversible characteristic, the PNIPAm bilayers assembled at temperature closely to LCST would undergo phase transition from globule to coil state leading the swelling of the capsules after core removing below LCST. In contrast to the swelling of PNIPAm outer shells, PAAL intramolecular association of the protonated carboxylic acid units and hydrogen bonding complex of PAAL with PNIPAm in acidic condition at pH 3 would lead to shrinkage of the inner core bilayer of the click capsules. Therefore, we can ascribe the slightly swelling rather than shrinkage of the click capsules at pH 3 to the balance between the swelling of PNIPAm outer shells after core removing and the shrinkage of PAAL inner core. In comparison with acidic condition, the carboxylic acid groups are deprotonated in basic condition leading to electrostatic repulsion (negative charge) in the PAAL bilayer. As shown in Figure 4b, the click capsules swelled to 6.5 μm at pH 11 after treating with sodium hydroxide solution. Similar swellability was also observed for the single-component poly(acrylic acid) (PAA) click capsules.[12b] In comparison with highly swelling/deswelling behaviors of the PAA click capsules, we may attribute the reduced swellability in this study to the higher degree of cross-linking density of the PAAL bilayer and the outer surrounding PNIPAm shells. These results demonstrated that the PAAL bilayer was successfully incorporated within the click multilayer and exhibited pH response.

The morphologies of the air-dried capsules in acidic, basic, and thermo conditions were also examined by using TEM and AFM. AFM analysis of the air-dried capsules in Figures 4-5a–c show spherical structures with features of folds and creases that are typical of polymer capsules prepared by LbL assembly on particle templates.[27] TEM analyses shown in Figures 4-5d–f also reveals folds and creases in the click capsules and diameters similar to those obtained by AFM. These dried click capsules also display smooth surfaces as a result of the outer tighter packing PNIPAm shells as we discussed earlier. AFM and TEM measurements

also provided stimuli-responsive behaviors evidences from size and thickness variation of the dried click capsules. The dimension of the dried click capsules was increased considerably upon changing the pH value from 3 to 11. By increasing the temperature to 50 °C, the dimension of click capsules at pH 3 was further decreased because of shrunk of the outer PNIPAm shells. Figure 4 shows the AFM section analyses of stimuli-responsive samples indicating that the increase in wall thickness correspond with the degree of the shrinkage of these click capsules.

In addition to click capsules with both PNIPAm outer shells and PAAL inner core bilayers are fully deswelling (at pH 11 and below LCST), we also investigated the thermo-responsive behavior when the PAAL inner core bilayer was in swelling state at pH 11. After elevating the solution temperature of the swelled PAAL core click capsules to 50 °C, the only slight increase in wall thickness (Figure 4-6d) compared with fully deswelling capsules at pH 3 and 50 °C (Figure 4-6c) is probably due to the hydrophilic deprotonated PAAL inner core bilayer raises the LCST of PNIPAm outer shells. It's well-known that the LCST of PNIPAm copolymer is strongly influenced by the overall hydrophilicity of the copolymer.[28] In general, hydrophobic compounds lower the LCST, whereas hydrophilic compounds raise it.[29] Consequently, we suggest that the LCST of PNIPAm outer shells in this covalently bonded multilayer is substantially affected by the hydrophilicity of the PAAL inner core bilayer.

4-4 Conclusions

In summary, we have developed a new and convenient method based on click chemistry for the direct covalent layer-by-layer assembly of vesicle-like capsules with dual stimuli-responsive characteristics. Consecutive layer-by-layer of these synthesized responsive clickable random copolymers was performed with a sequence of PNIPAm/PAAL/PNIPAm to fabricate the vesicle-like click capsule consisting of thermo-sensitive outer shell bilayers and pH-responsive inner core bilayer. The vesicle-like click capsules exhibited thermo and pH-responsive behaviors by elevating the solution temperature and incubating in acidic or basic solutions respectively. This combination of two widely employed techniques, layer-by-layer and copper-catalyzed 1,3-dipolar cycloaddition, is promising for introducing a broad range of new materials including different functional polymers with covalent stabilization. Furthermore, excess azide/alkyne groups that have not been utilized in the assembly can be used to postfunctionalize the outer multilayer films of the click capsules. The versatility and generality of this approach is expected to enable us to further design advanced and stimuli-responsive capsules.

References

1. Shi, X. Y.; Shen, M. W.; Mohwald, H. *Prog. Polym. Sci.* **2004**, *29*, 987–1019. (b) Decher, G.; Hong, J. D.; Schmitt, J. *Thin Solid Films* **1992**, *210*, 831–835.
2. (a) Zhang, Y. J.; Guan, Y.; Yang, S. G.; Xu, J.; Han, C. C. *Adv. Mater.* **2003**, *15*, 832–835. (b) Kozlovskaya, V.; Ok, S.; Sousa, A.; Libera, M.; Sukhishvili, S. A. *Macromolecules* **2003**, *36*, 8590–8592. (c) Yang, S. Y.; Lee, D.; Cohen, R. E.; Rubner, M. F. *Langmuir* **2004**, *20*, 5978–5981.
3. Wang, Z.; Feng, Z.; Gao, C. *Chem. Mater.* **2008**, *20*, 4194–4199.
4. (a) Johnston, A. P. R.; Read, E. S.; Caruso, F. *Nano Lett.* **2005**, *5*, 953–956. (b) Johnston, A. P. R.; Mitomo, H.; Read, E. S.; Caruso, F. *Langmuir*, **2006**, *22*, 3251–3258.
5. Peyratout, C. S.; Dahne, L. *Angew. Chem., Int. Ed.* **2004**, *43*, 3762–3783. (b) Johnston, A. P. R.; Cortez, C.; Angelatos, A. S.; Caruso, F. *Curr. Opin. Colloid Interface Sci.* **2006**, *11*, 203–209. (c) De Geest, B. G.; De Koker, S.; Sukhorukov, G. B. ; Kreft., O. ; Parak, W. J. ; Skirtach, A. G. ; Demeester, J.; De Smedt, S. C.; Hennink, W. E. *Soft Matter* **2009**, *5*, 282–291.
6. Quinn, J. F.; Johnston, A. P. R.; Such, G. K.; Zelikin, A. N.; Caruso, F. *Chem. Soc. Rev.* **2007**, *36*, 707–718.
7. Moya, S.; Dähne, L.; Voigt, A.; Leporatti, S.; Donath, E.; Möhwald, H. *Colloids Surf. A* **2001**, *183–185*, 27–40.
8. (a) Nardin, C.; Hirt, T.; Leukel, J.; Meier, W. *Langmuir* **2000**, *16*, 1035–1041. (b) Pastoriza-Santos, I.; Schöler, B.; Caruso, F. *Adv. Func. Mater.* **2001**, *11*, 122–128. (c) Zhu, H. G.; McShane, M. J. *Langmuir* **2005**, *21*, 424–430.
9. (a) Tong, W. J.; Gao, C. Y.; Möhwald, H. *Chem. Mater.* **2005**, *17*, 4610–4616. (b) Zhang, Y. J.; Guan, Y.; Zhou, S. *Biomacromolecules* **2005**, *6*, 2365–2369.
10. (a) Feng, Z.; Wang, Z.; Gao, C.; Shen, J. *Adv. Mater.* **2007**, *19*, 3687–3691. (b) Tong, W.;

Gao, C.; Möhwald, H. *Macromol. Rapid Commun.* **2006**, *27*, 2078–2083. (c) Duan, L.; He, Q.; Yan, X. H.; Cui, Y.; Wang, K. W.; Li, J. B. *Biochem. Biophys. Res. Commun.* **2007**, *354*, 357–362.

11. (a) Schuetz, P.; Caruso, F. *Adv. Funct, Mater.* **2003**, *13*, 929–937. (b) Kozlovskaya, V.; Ok, S.; Sousa, A.; Libera, M.; Sukhishvili, S. A. *Macromolecules* **2003**, *36*, 8590–8592. (c) Lee, D.; Rubner, M. F.; Cohen, R. E. *Chem. Mater.* **2005**, *17*, 1099–1105. (d) Yang, S. Y.; Lee, D.; Cohen, R. E. *Langmuir* **2004**, *20*, 5978–6981.

12. (a) Such, G. K.; Quinn, J. F.; Quinn, A.; Tjipto, E.; Caruso, F. *J. Am. Chem. Soc.* **2006**, *128*, 9318–9319. (b) Such, G. K.; Tjipto, E.; Postma, A.; Johnston, A. P. R.; Caruso, F. *Nano Lett.* **2007**, *7*, 1706–1710. (c) Ochs, C. J.; Such, G. K.; Staedler, B.; Caruso, F. *Biomacromolecules* **2008**, *9*, 3389–3396. (d) Connal, L. A.; Kinnane, C. R.; Zelikin, A. N.; Caruso, F. *Chem. Mater.* **2009**, *21*, 576–678. (e) Kinnane, C. R.; Such, G. K.; Antequera‐Garcia, G.; Yan, Y.; Dodds, S. J.; Liz‐Marzan, L. M.; Caruso, F. *Biomacromolecules* **2009**, *10*, 2839–2846. (f) Kinnane, C. R.; Wark, K.; Such, G. K.; Johnston, A. P. R.; Caruso, F. *Small* **2009**, *5*, 444–448.

13. (a) Kolb, H. C.; Finn, M. G.; Sharpless, K. B. *Angew. Chem., Int. Ed.* **2001**, *40*, 2004–2021. (b) Kolb, H. C.; Sharpless, K. B. *Drug Discovery Today* **2003**, *8*, 1128–1137. (c) Lewis, W. G.; Green, L. G.; Grynszpan, F.; Radic, Z.; Carlier, P. R.; Taylor, P.; Finn, M. G.; Sharpless, K. B. *Angew. Chem., Int. Ed.* **2002**, *41*, 1053–1057.

14. Huang, C.-J.; Chang, F.-C. *Macromolecules* **2009**, *42*, 5155–5166.

15. Discher, D. E.; Eisenberg, A. *Science* **2002**, *297*, 967–973.

16. (a) Discher, B. M.; Won, Y. Y.; Ege, D. S.; Lee, J. C.; Bates, F. S.; Discher, D. E.; Hammer, D. A. *Science* **1999**, *284*, 1143–1146.

17. (a) Zhang, L.; Yu, K.; Einsenberg, A. *Science* **1996**, *272*, 1777–1779. (b) Lomas, H.; Canton, I.; MacNeil, S. ; Du, J.; Armes, S. P.; Ryan, A. J.; Lewis, A. L. ; Battaglia, G. *Adv.*

Mater. **2007**, *19*, 4238–4243. (c) Du, J.; Tang, Y.; Lewis, A. L.; Armes, A. P. *J. Am. Chem. Soc.* **2005**, *127*, 17982–17983. (d) Du, J.; Armes, S. P. *J. Am. Chem. Soc.* **2005**, *127*, 12800–12801.

18. (a) Liu, X.; Jiang, M. *Angew. Chem. Int. Ed.* **2006**, *45*, 3846–3850. (b) Ikeda, T.; Mamiya, J.-I.; Yu, Y. *Angew. Chem. Int. Ed*, **2007**, *46*, 506–528. (c) Wang, G.; Tong, X.; Zhao, Y. *Macromolecules* **2004**, *37*, 8911–8917. (c) Konak, C.; Rathi, R. C.; Kopeckova, P.; Kopecek, J. *Macromolecules* **1997**, *30*, 5553–5556.
19. (a) Li, Y.; Lotiz, B.; McCormick, C. L. *Angew. Chem. Int. Ed.*, **2006**, *45*, 5792–5795. (b) Li, Y.; Smith, A. E.; Lokitz, B. S.; McCormick, C. L. *Macromolecules*, **2007**, *40*, 8524–8526.
20. (a) Discher, B. M.; Bermudez, H.; Hammer, D. A.; Discher, D. E.; Won, Y.–Y.; Bates, F. S. *J. Phys. Chem. B* **2002**, 106, 2848–2854. (b) Kros, A.; Linhardt, J. G.; Bowman, H. K.; Tirrell, D. A. *Adv. Mater.* **2004**, 16, 723–727.
21. (a) Thibault, R. J.; Uzun, O.; Hong, R.; Rotello, V. M. *Adv. Mater.* **2006**, 18, 2179–2183. (b) Ding, J.; Liu, G. *J. Phys. Chem. B* **1998**, 102, 6107–6113. (c) Zheng, R.; Liu, G. *Macromolecules* **2007**, 40, 5116–5121. (d) Walther, A.; Goldmann, A. S.; Yelamanchili, R. S.; Drechsler, M.; Schmalz, H.; Eisenberg, A.; Müller, A. H. E. *Macromolecules* **2008**, 41, 3254–3260.
22. (a) Du, J.; Armes, S. P. *J. Am. Chem. Soc.* **2005**, *127*, 12800–12801. (b) Du, J.; Chen, Y.; Zhang, Y.; Han, C. C.; Fischer, K.; Schmidt, M. *J. Am. Chem. Soc.* **2003**, *125*, 14710–14711.
23. Zhu, H.; Liu, Q.; Chen, Y. *Langmuir* **2007**, *23*, 790–794.
24. (a) Tsarevsky, N. V.; Matyjaszewski, K. *Chem. Rev.* **2007**, *107,* 2270–2299. (b) Braunecker, W. A.; Matyjaszewski, K. *Prog. Polym. Sci.* **2007**, *32*, 93–146.
25. Quinn, J. F.; Caruso, F. *Langmuir*, **2004**, *20*, 20–21.

26. Kozlovskaya, V.; Kharlampieva, E.; Mansfield, M. L.; Sukhishvili, S. A. *Chem. Mater.* **2006**, *18*, 328–326.

27. Donath, E.; Sukhorukov, G. B.; Caruso, F.; Davis, S. A.; Mohwald, H. *Angew. Chem. Int. Ed.* **1998**, *37*, 2201–2204.

28. Feil, H.; Bae, Y. H.; Feijen, J.; Kim, S. W. *Macromolecules* **1993**, *26*, 2496–2500.

29. (a) Chen, G.; Hoffman, A. S. *Macromol. Chem. Phys.* **1995**, *196*, 1251–1259. (b) Kuckling, D.; Adler, H.-J.; Arndt, K.-F.; Ling, L.; Habicher, W. D. *Macromol. Symp.* **1999**, 145, 65–74. (c) Kunugi, S.; Yamazaki, Y.; Takano, K.; Tanaka, N. *Langmuir* **1999**, *15*, 4056–4061. (d) Deng, Y.; Pelton, R. *Macromolecules* **1995**, *28*, 4617–4621.

Scheme 4-1: Synthesis of the *N*-(2-(2-(2-azidoethoxy)ethoxy)ethyl)acrylamide monomer, (1).

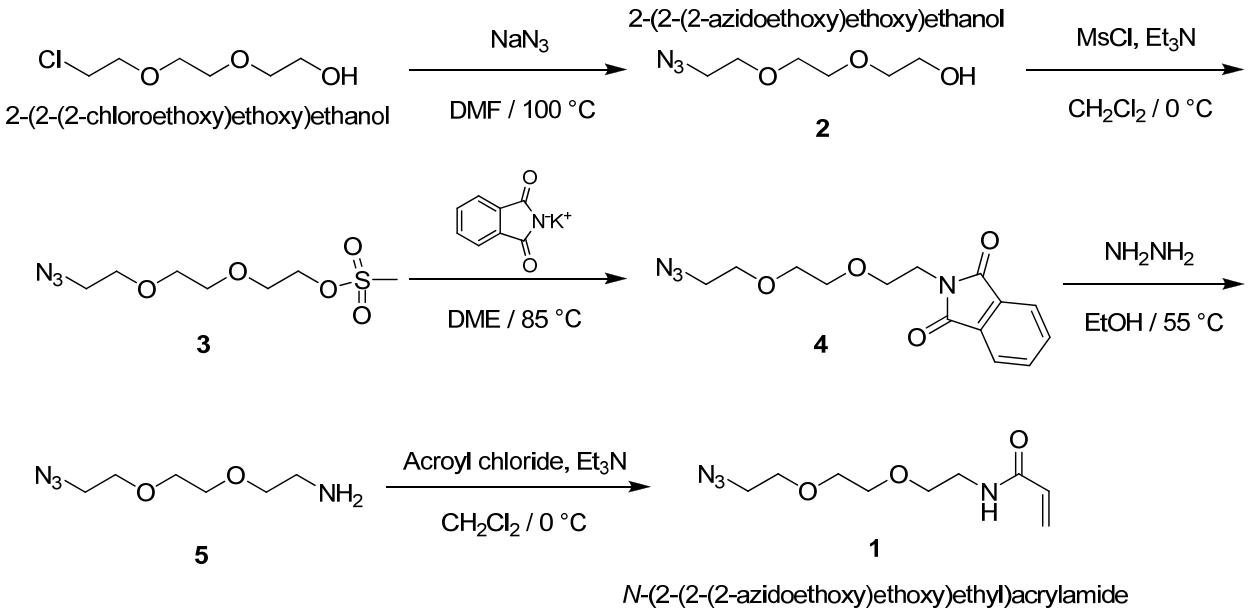

Scheme 4-2: Synthetic Pathway for Preparation of Alkyne- and Azido-Functionalized Poly(*N*-isopropylacrylamide) Random Copolymers via Atom Transfer Reversible Polymerization (ATRP).

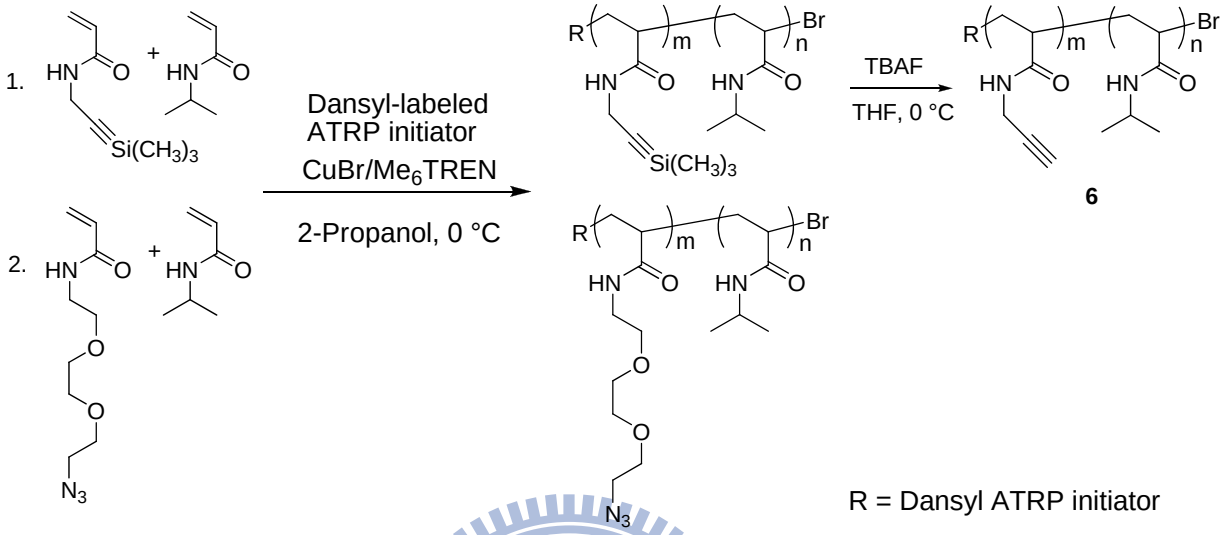

Scheme 4-3: Synthetic Pathway for the Aqueous Reversible Addition Fragmentation Chain Transfer (RAFT) Polymerization of Alkyne- and Azido-functionalized Poly(*N*-acryloylalanine) Random Copolymer with and 4,4-Azobis(4-cyanopentanoic acid) V-501 as the Free Radical Initiator.

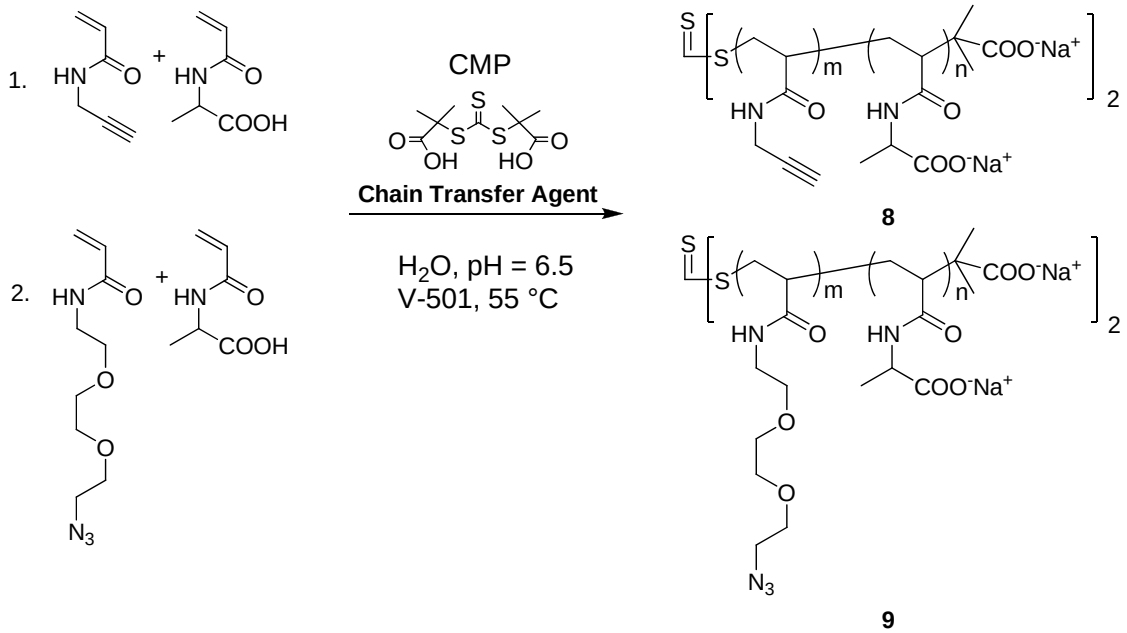

Scheme 4-4: Schematic Representation of the Preparation of Covalently Stabilized Dual Responsive Polymer Capsules through LbL Assembly Using Click Chemistry.

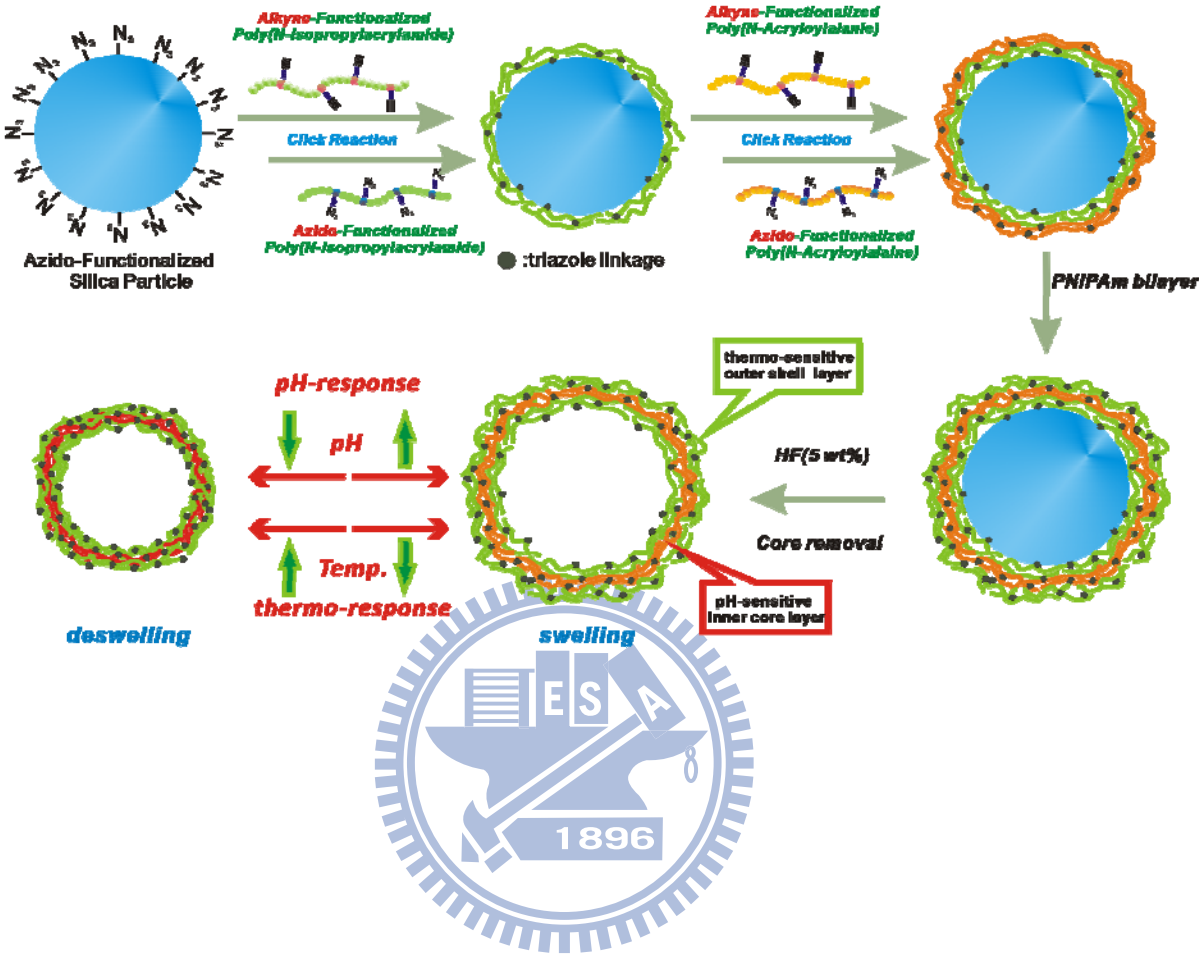

Table 4-1: Summary of Alkyne- and Azido-Functionalized Random Copolymers Characterization.

entry	Click-functionalized Copolymer Samples	$M_{n,\,GPC,\,PEO}$ (kg/mol)	$M_{n,\,NMR}$ (kg/mol)	M_w/M_n	F_{azide} [a]	F_{alkyne} [b]	Maximum of endothermic peak (°C)
1	$PNIPAm_{79}$-*r*-$PPAm_{15}$	7,100	10,500	1.08	—	16	32.7
2	$PNIPAm_{86}$-*r*- $PEOAm_{21}$	11,000	14,500	1.11	20	—	33.9
3	$PAAL_{45}$-*r*-$PPAAm_{9}$	8,650	7,700	1.60	—	17	—
4	$PAAL_{50}$-*r*- $PEOAm_{11}$	10,280	9,700	1.83	18	—	—

[a] F_{azide} = mole percentage of azide functionality; [b] $F_{acetylene}$ = mole fraction of alkyne functionality measured by ^1H NMR in D_2O at 20 °

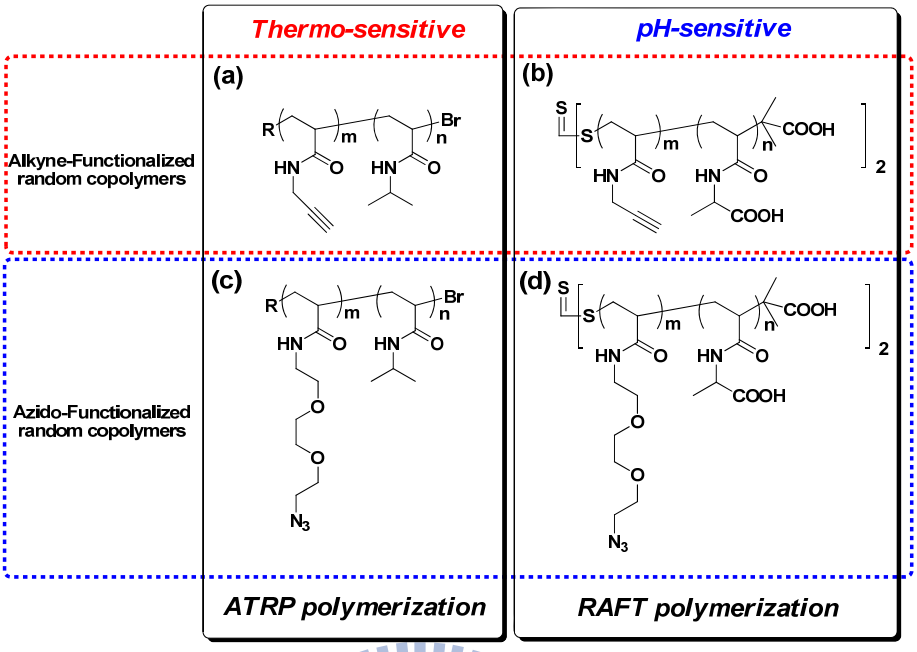

Figure 4-1: Chemical structures of the thermo and pH sensitive of (a, b) alkyne-functionalized and (c, d) azido-functionalized random copolymers prepared by ATRP and RAFT polymerization.

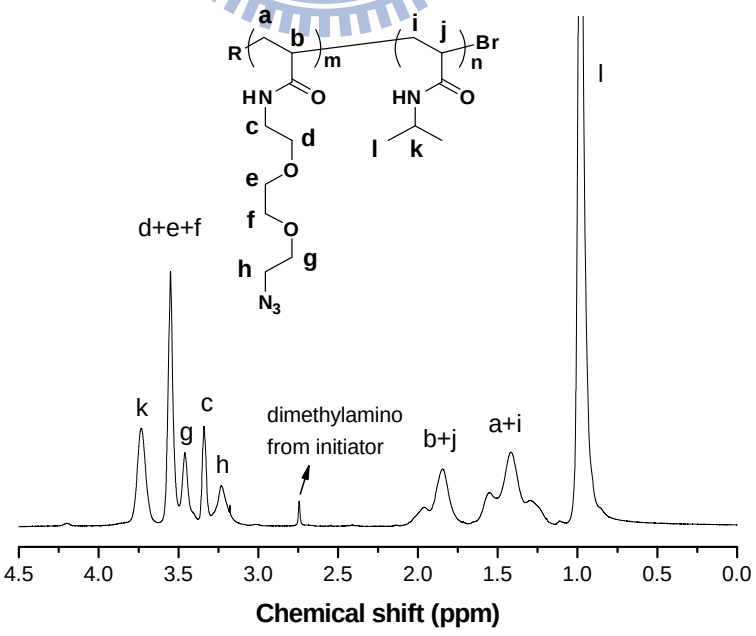

Figure 4-2: ^{1}H NMR (500 MHz, D_2O) spectrum of PNIPAm-*r*-PEOAm.

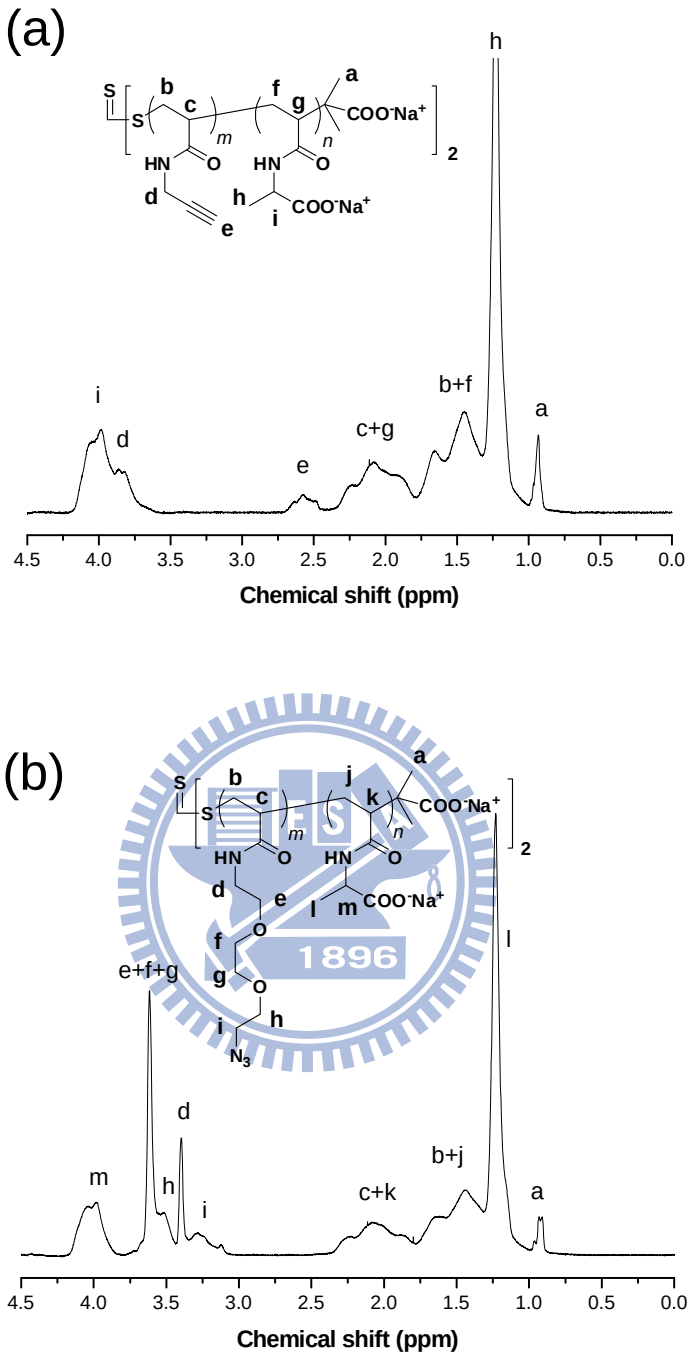

Figure 4-3: ^{1}H NMR (500 MHz, D_2O) spectra of (a) PAAL-*r*-PAAm and (b) PAAL-*r*-PEOAm.

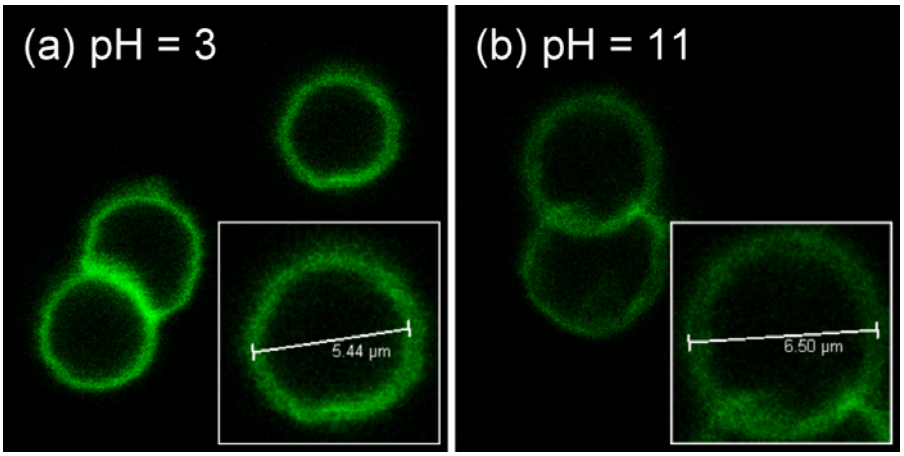

Figure 4-4: Confocal laser scanning microscopy (CLSM) images of PNIPAm/PLAA/PNIPAm click capsules obtained from 5 µm diameter silica particles at (a) pH 3 and (b) pH 11.

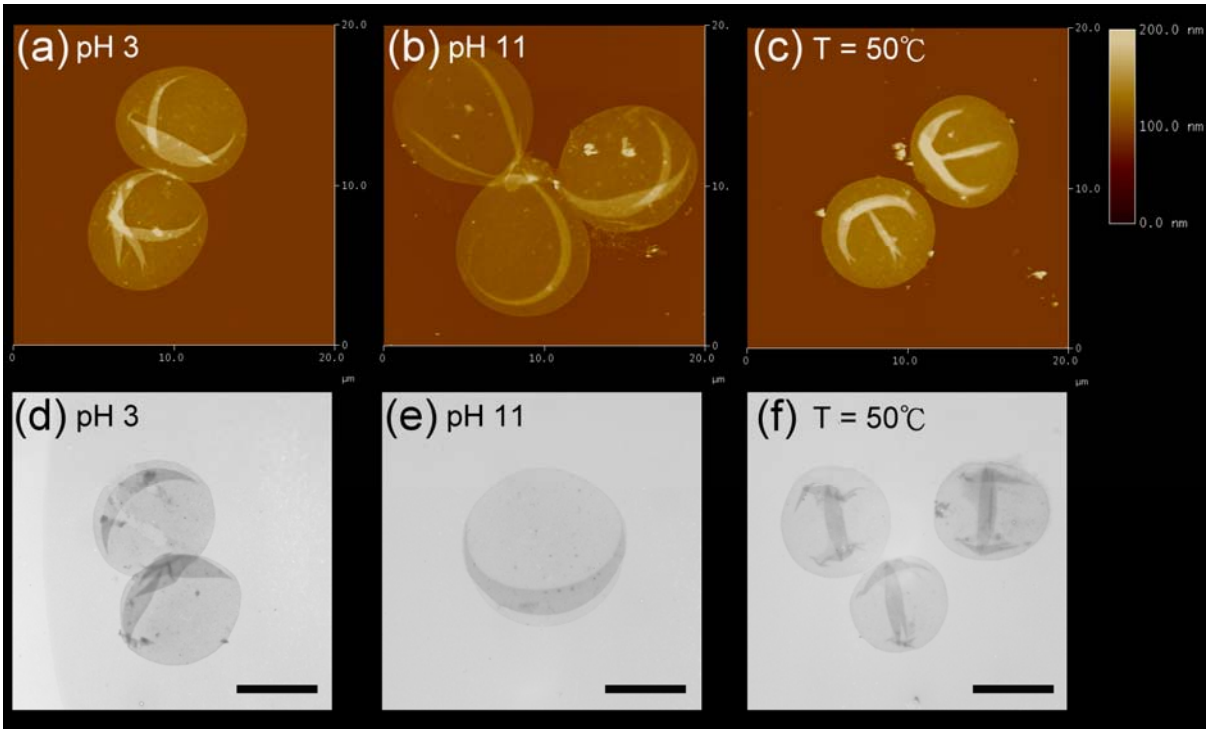

Figure 4-5: (a–c) AFM and (d–f) TEM images of the three-bilayer PNIPAm/PAAL/PNIPAm click capsules. Samples prepared at 25 °C (a, b, d, e) and at 50 °C (pH 3) (c, f). The AFM images for scanned areas of 20 × 20 μm^2. The scale bar in TEM images: 2µm.

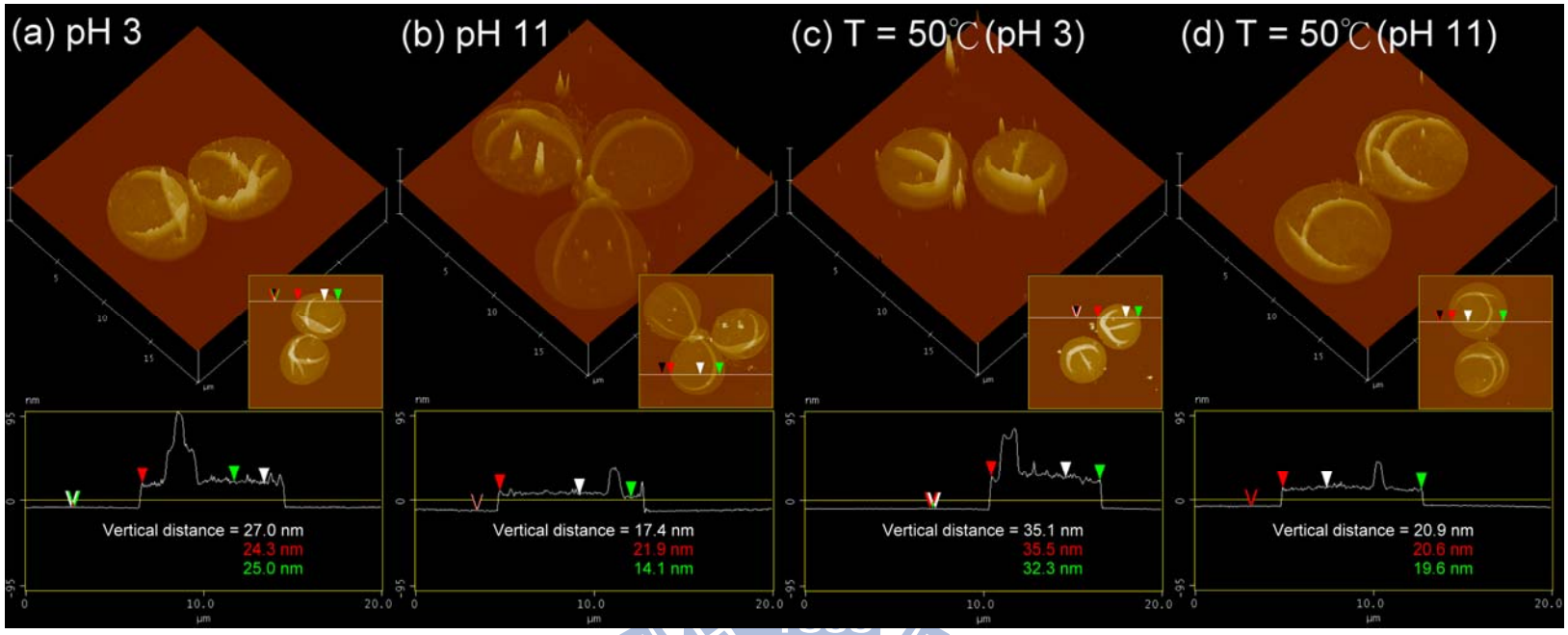

Figure 4-6: (a – d) AFM images and section analysis of the three-bilayer PNIPAm/PAAL/PNIPAm click capsules in (a) pH 3, (b) pH 11, (c) at 50 °C (pH 3), and (d) at 50 °C (pH 11).

Chapter 5

Conclusions

We have synthesized a series of stimuli-responsvie copolymers through atom transfer radical polymerization and ring-opening polymerization. The well-defined poly(*N*-isopropylacrylamide)-*b*-poly(Z-L-lysine) was obtained and the protective Cbz-group was successfully removed without cleavage of the block copolymer. We found that the amphiphilic hybrid rod-coil block copolymers were able to form various well-defined universal morphologies including micelles-spherical micelles, wormlike micelles, and vesicles by varying either the copolymer compositions on the helicogenic common solvents. We have confirmed the formation of the hierarchical lamellar-in-hexagonal self-assembly structure in $PNIPAm_{90}$-*b*-$PZLys_{71}$ at solid state by the synchrotron SAXS, WAXS, and TEM characterizations. The dual stimuli-responsive behaviors of the PNIPAm-*b*-PLys were also investigated by nuclear magnetic resonance spectroscopy in aqueous solution. Coil-to-helix and coil-globule transitions occur by changing the environmental conditions, by elevating the temperature or changing the pH value. This work has demonstrated the feasibility of using hetero-functional amide linkage initiator to synthesize hybrid block copolymers which both segments are able to response to environmental changes. In the effort to expand potential applications, these results provide a versatile method toward designing polymers to impart stimuli-responsive functionalities.

Futhermore, by using click chemistry, we have developed a novel approach to fabricate thermoresponsive PNIPAm microcapsules based on direct covalent bonding LbL assembly. This method not only provides a unique approach toward microcapsule construction with direct covalent bonding under mild reaction conditions but also opens a platform to better understand the effects of the degree of cross-linking on the thin film thickness and

morphology. The fabrication of these microcapsules can be tailored by adjusting the aqueous reaction temperature close to the LCST (30 °C), resulting in multilayer film materials exhibiting extremely low surface roughness and high thickness as a result of tighter packing of PNIPAm, a special characteristic of the LbL assembly of PNIPAm on the colloidal template. These microcapsules also undergo a thermo-reversible swelling/de-swelling transition upon changing the temperature of the medium. The surfaces of these multilayer thin films are easily modified using, for example, an azido-modified lissamine rhodamine dye, thereby allowing post-functionalization with a variety of small molecules or larger biomacromolecules. Permeability study reveals that the microcapsules with tighter packing wall are selectively permeable to molecules depending on molecular weight and show potential applications for the encapsulation of variety of materials.

Based on these results, we also developed a new and convenient method to fabricate a vesicle-like dual-responsive click capsules by LbL assembly via click chemistry. Consecutive layer-by-layer of these synthesized responsive clickable random copolymers was performed with a sequence of PNIPAm/PAAL/PNIPAm to fabricate the vesicle-like click capsule consisting of thermo-sensitive outer shell bilayers and pH-responsive inner core bilayer. The vesicle-like click capsules exhibited thermo and pH-responsive behaviors by elevating the solution temperature and incubating in acidic or basic solutions respectively. This combination of two widely employed techniques, layer-by-layer and copper-catalyzed 1,3-dipolar cycloaddition, is promising for introducing a broad range of new materials including different functional polymers with covalent stabilization. Furthermore, excess azide/alkyne groups that have not been utilized in the assembly can be used to postfunctionalize the outer multilayer films of the click capsules. The versatility and generality of this approach is expected to enable us to further design advanced and stimuli-responsive capsules.

List of Publications

Journal

1. SHIAO-WEI KUO, HSIN-FANG LEE, CHIH-FENG HUANG, **CHENG-JYUN HUANG**, FENG-CHIH CHANG **"Synthesis and Self-Assembly of Helical Polypeptide-Random Coil Amphiphilic Diblock Copolymer"** *J Polym Sci Part A: Polym Chem* **2008**, 46, 6296-6304.

2. **Cheng-Jyun Huang** and Feng-Chih Chang **"Polypeptide Diblock Copolymers: Syntheses and Properties of Poly(*N*-isopropylacrylamide-*b*-Polylysine)"** *Macromolecules* **2008**, 41, 7041-7051.

3. **Cheng-Jyun Huang** and Feng-Chih Chang **"Fabrication of Ultrathin Thermoresponsive Microcapsules by Directly Covalent Layer-by-Layer Assembly via Click Chemistry"** *Macromolecules* **2009**, *42*, 5155-5166. (Cover Story)

4. **Cheng-Jyun Huang,** Chia-Wei Hung and Feng-Chih Chang **"Fabrication of Vesicle-like Dual-responsive Click Capsules by Directly Covalent Layer-by-Layer Assembly"** submitted.

Introduction to the Author

English name: Jyun-Cheng Huang

Chinese name: 黃承鈞

Birthday: 1983/06/28

Address: 324 桃園縣平鎮市北勢里 8 鄰和平路 198 號

Education:

2001.09~2005.06 **B.S.,** Department of Chemical Engineering, National Taipei University, Taipei, Taiwan.

2005.09~2006.06 **M. S.,** Institute of Applied Chemistry, National Chiao Tung University, Hsin Chu, Taiwan.

2006.09~2010.06 **Ph. D.,** Institute of Applied Chemistry, National Chiao Tung University, Hsin Chu, Taiwan.